The Role of P-glycoprotein in Host-Pathogen Interactions

Dissertation

zur

Erlangung der naturwissenschaftlichen Doktorwürde
(Dr. sc. nat.)

vorgelegt der

Mathematisch-naturwissenschaftlichen Fakultät

der

Universität Zürich

von

Iveta Bottova

aus

der Slowakei

Promotionskomitee

Prof. Dr. Raimund Dutzler (Vorsitz)
Prof. Dr. Hanspeter Nägeli
PD Dr. Hubert Hilbi

Leitung der Dissertation
Prof. Dr. Adrian Hehl
Dr. Sabrina Sonda

Zürich, 2010

The Role of P-glycoprotein in Host-Pathogen Interactions

Faculty of Science

University of Zurich

PhD Thesis

Submitted by

Iveta Bottova

From Bratislava, Slovakia

Thesis advisors

Prof. Adrian B. Hehl
Dr. Sabrina Sonda
Institute of Parasitology
Veterinary Faculty of the University of Zurich

I	**Summary**	5
I	**Zusammenfassung**	7
II	**Introduction**	9
1	**P-glycoprotein**	9
1.1	Localization and function	9
1.2	Structure	9
1.3	P-glycoprotein and multidrug resistance	10
1.4	P-glycoprotein inhibition	10
1.5	Physiological function of P-glycoprotein	10
1.5.1	Cellular detoxification	10
1.5.2	Immunological functions	11
1.5.3	Ion transport activity	11
1.5.4	Lipid transport and intracellular cholesterol trafficking	11
1.6	P-gp in host-pathogen interaction	12
2	***Toxolpasma gondii***	12
2.1	Life cycle	13
2.2	Lytic cycle	13
2.2.1	Motility and Invasion	14
2.2.2	Vacuole formation and parasite replication	15
2.2.3	Parasite egress	16
2.3	Exploitation of the host cell	17
2.4	*T. gondii* P-gp	17
3	**The aim of the project**	18
4	**Additional project: Regulation of parasite stage conversion**	18
5	**References**	19
III	**Manuscripts**	23
Manuscript 1: Published	Host Cell P-glycoprotein Is Essential for Cholesterol Uptake and Replication of *Toxoplasma gondii*	23
Manuscript 2: Submitted	The P-glycoprotein Inhibitor GF120918 Modulates Ca^{2+}-Dependent Processes and Lipid Metabolism in *Toxoplasma gondii*	35
Manuscript 3: Submitted	Epigenetic mechanisms regulate stage differentiation in the minimized protozoan *Giardia lamblia*	60

IV	**Discussion**	91
1	**The role of P-glycoprotein in host-parasite interaction**	91
1.1	HOST P-gp	91
1.2	PARASITE P-gp	93
2	**Epigenetic regulation of stage conversion in *G. lamblia***	95
3	**References**	97
V	**Significance of research**	100
VI	**Perspectives**	101
VII	**Acknowledgements**	102
VIII	**Curriculum vitae**	103

Summary

P-glycoprotein (P-gp) is an exceptional membrane transporter because of its ability to carry a large variety of compounds across the plasma membrane. Thanks to this substrate promiscuity, P-gp over-expression is responsible for multidrug resistance (MDR) in a variety of cells from microorganisms to humans. The cellular MDR is responsible for failure of treatment in over 90% of patients with metastatic cancer, as well as in yeast and bacteria infections and in life-threatening human parasites such as *Plasmodium* causing malaria. P-gp is not only expressed in multidrug resistant cells but also in non-resistant cells at basal levels, but its physiological functions in the absence of drug pressure are not well understood. So far P-gp was proposed to be involved in several important cellular processes ranging from immunological functions to membrane lipid remodelling. Given the importance of P-gp in human and microbial MDR, there was an important need to identify the substrates and transport activities of this protein and to understand its physiological functions as a basis for the rational design of new drugs and MDR inhibitors. P-gp is localized mainly in the plasma membrane. Because the plasma membrane is the first barrier that intracellular pathogens need to cross to infect the host cell, we wanted to investigate whether P-gp plays a role in this first line host-pathogen interaction. As a model pathogen we used the human parasite *Toxoplasma gondii*, which causes toxoplasmosis, a potentially life-threatening disease in individuals with immunodeficiency. As both host cell and parasite have a P-gp localized in the plasma membrane, we hypothesised that both P-gps could be involved in events during parasite infection and replication. Our project had two goals: i) to characterize the physiological functions of host cell P-gp and its contribution to host-parasite interactions and ii) to characterize the *T. gondii* P-gp and its function in host-parasite interactions.

To investigate the physiological functions of host cell P-gp and its contribution to host-parasite interactions, we compared three mouse embryonic fibroblast cell lines with different P-gp expression: wild type cells (WT) and P-gp knockout (P-gp KO) cells, as well as P-gp complemented P-gp KO (P-gp KO/P-gp) cells. We used these cell lines to analyse the role of host P-gp in parasite invasion, replication and cholesterol transport, processes that are crucial for successful *T. gondii* propagation and survival. We showed that host P-gp is essential for normal *T. gondii* replication and specifically required for cholesterol transport from host endo-lysosomes to the parasite. Importantly, using cholesterol auxotrophic *T. gondii* replication as a bio-indicator of cholesterol homeostasis in the host cell, we found that P-gp is involved in host cholesterol trafficking from endo-lysosomes to the plasma membrane.

To characterize the *T. gondii* P-gp and its function in host-parasite interactions, we pharmacologically inhibited parasite P-gp (TgP-gp) with the P-gp specific inhibitor GF120918 (GF) and we used P-gp KO host cells to avoid the contribution of host P-gp to the observed phenotype. We analysed the role of parasite P-gp in invasion, replication and lipid metabolism. We showed that *T. gondii* P-gp is crucial for parasite Ca^{2+}-depended attachment and invasion. Moreover, we propose that TgP-gp is involved in Ca^{2+} signalling which is important for the regulation of these processes and essential for *T. gondii* survival. Importantly, TgP-gp functionality is required for successful *T. gondii* replication and involved in the parasite lipid synthesis and transport. In summary, in this study we showed for the first time that both host cell and parasite P-gp have an important role in host-parasite interactions.

I was also involved in a joint project focusing on the epigenetic regulation of stage conversion of *Giardia lamblia*. *G. lamblia* is an intestinal pathogen which infects millions of people all over the world causing the disease giardiasis. *G. lamblia* resides in the upper small intestine of humans and other vertebrates which become infected by ingestion of cysts from contaminated water or food. *Giardia* is characterized by two different developmental stages: the motile, proliferating trophozoites responsible for the clinical manifestation of the disease such as diarrhoea and malabsorption, and the cyst forms, the infective stage of the parasite. Infectious cysts are environmentally resistant and protected by a rigid extracellular matrix, the cyst wall. Stage conversion of *G. lamblia* is essential for transmission and survival of this human pathogen, but the understanding of the molecular mechanism which regulates this fundamental process still remains poorly understood. In this project we aimed to analyse the effect of histone deacetylase inhibitor FR235222 on gene regulation of stage conversion in *G. lamblia*. We showed for the first time that inhibition of a histone deacetylase activity in Giardia with FR235222 induced transcriptional changes in proliferating and differentiating stages and potently blocked formation of cysts. We propose that *G. lamblia* stage conversion is under the control of epigenetic regulation and dependent on the acetylation state of histones. In addition, histone deacetylase activity could be a promising target for developing new anti-Giardia drugs since the inhibition of histone deacetylase activity is blocking *G. lamblia* cyst formation and thus has potential to reduce disease transmission.

Zusammenfassung

Das P-Glykoprotein (P-gp) ist ein außergewöhnlicher Membrantransporter, vor allem wegen seiner Eigenschaft, eine Vielzahl verschiedener Stoffe über die Plasmamembran befördern zu können. Aufgrund der geringen Substratpräferenz führt das Überexprimieren von P-gp zu einer gesteigerten Antibiotikaresistenz in einer Vielzahl von Zellen sowohl in Mikroorganismen als auch beim Menschen. Diese zelluläre Antibiotikaresistenz, auch „multidrug resistance“ (MDR) genannt, ist verantwortlich für einen Misserfolg bei mehr als 90% der klinischen Behandlungen von Patienten mit metastatischem Krebs aber auch bei der Behandlung von pathogenen Pilzen oder Bakterien und lebensbedrohlichen menschlichen Parasiten wie dem Malariaerreger *Plasmodium.* Da P-gp nicht nur in Antibiotika-resistenten, sondern auch in nicht-resistenten Zellen exprimiert wird, ist es von großem Interesse die allgemeine physiologische Funktion dieses Proteins zu verstehen. Nach dem heutigen Wissensstand wird vermutet, dass P-gp in mehreren wichtigen zellulären Prozessen involviert ist und sowohl immunologische Funktionen übernimmt als auch bei der Modellierung von Membranlipiden mitwirkt. Aufgrund der Bedeutung von P-gp bei der mikrobiellen und humanen MDR ist es von großer Wichtigkeit, die Substratspezifität, Transportaktivität und physiologische Funktion des Proteins zu verstehen – letztlich, um bei der Entwicklung von neuen Antibiotka- oder MDR-Inhibitoren zu helfen. P-gp ist vor allem in der Plasmamembran lokalisiert. Da die Plasmamembran für pathogene Organismen die erste Barriere darstellt, die für die Infektion der Wirtszelle überwunden werden muss, untersuchten wir zunächst, ob P-gp eine Funktion bei der Interaktion zwischen Wirt und Pathogen übernimmt. Dabei diente der den Menschen infizierende Parasit *Toxoplasma gondii*, der in immunsupprimierten Individuen eine lebensbedrohliche Toxoplasmose hervorrufen kann, als Modellorganismus. Unser Projekt besaß zwei Zielsetzungen: i) die Erforschung der physiologischen Funktion von Wirtszellen P-gp und dessen Beitrag zur Wirt-Parasit-Interaktion und ii) die Charakterisierung von *T. gondii* P-gp und dessen Aufgabe bei der Wirt-Parasit-Interaktion.

Zur Bestimmung der physiologischen Funktion von Wirtszellen P-gp und dessen Interaktion mit dem Parasiten verglichen wir drei Zelllinien mit verschiedener P-gp Expression: embryonale Mausfibroblasten vom Wildtyp (WT), P-gp „knockout“ (P-gp KO) und P-gp komplementierten (P-gp KO/P-gp) Zellen. Wir untersuchten die Rolle von P-gp bei der Parasiteninvasion, der Replikation und des Cholesteroltransports, entscheidende Prozesse für die erfolgreiche Prolongation und das Bestehen von *T. gondii*. Wir konnten zeigen, dass P-gp essentiell für die reguläre Replikation in *T. gondii* ist, da das Protein für den Cholesterintransport vom Endolysosomen des Wirtes in *T. gondii* gebraucht wird. Bei der Analyse einer Cholesterol-auxotrophen Replikation in *T. gondii*, ein Bioindikator für die Cholesterol-Homeostase in der Wirtszelle, zeigten wir insbesondere, dass P-gp eingebunden ist in den Cholesteroltransport des Wirtes vom Endolysosomen zur Plasmamembran.

Zur Charakterisierung des *T. gondii* P-gp und dessen Funktion bei der Wirt-Parasit-Interaktion inhibierten wir pharmakologisch das P-gp des Parasiten (TgPgp) mit dem P-gp spezifischen Inhibitor GF120918 (GF). Dabei nutzen wir P-gp KO Wirtszellen, um einen Einfluss vom P-gp des Wirtes auf den Phänotyp auszuschließen. Wir analysierten die Funktion von P-gp bei der Invasion, der Replikation und beim Lipidmetabolismus des Parasiten. Es gelang aufzuzeigen, dass das Vorhandensein von P-gp in *T. gondii* ausschlaggebend für die Ca^{2+}-abhängige

Anheftung sowie die Invasion des Parasiten ist. Des Weiteren vermuten wir, dass TgPgp involviert ist in eine Ca^{2+}-abhängige Signalkaskade, die wichtige Prozesse für das Überleben von *T. gondii* steuert. Interessanterweise ist die Funktionalität von TgPgp erforderlich für die Replikation von *T. gondii* und beeinflusst zudem die Lipidsynthese und den Transport des Parasiten.

Zusammenfassend konnten wir in dieser Arbeit zum ersten Mal zeigen, dass sowohl das P-gp der Wirtszelle als auch das P-gp des Parasiten einen wesentlichen Einfluss auf die Wirt-Parasit-Interaktion ausübt.

Der Schwerpunkt des zweiten Teils meiner Arbeit beinhaltete Untersuchungen zur epigenetischen Regulation der Entwicklungsstadien von *Giardia lamblia*. *G. lamblia* ist ein Darmparasit, der in tausenden von Menschen weltweit das Krankheitsbild der Giardiasis hervorruft. *G. lamblia* besiedelt den oberen Dünndarm im Menschen und anderen Vertebraten, die im Allgemeinen durch die Aufnahme von kontaminiertem Trinkwasser oder verunreinigter Nahrung mit Zysten infiziert werden. *Giardia* durchläuft zwei charakteristische Entwicklungsstadien: eine Lebensphase mit beweglichen, begeißelten Trophozoiten, welche für die Proliferation und die klinische Manifestation der Krankheit, wie einer Diarrhoe oder Malabsorption, entscheidend sind. Die Zysten, die infektiösen Stadien des Parasiten, bestehen aus den Trophozoiten, welche umgeben sind von einer rigiden, schützenden Zystenwand, die das Überleben und die Übertragung des Parasiten auf neue Empfänger bei externen Umweltbedingungen sichert. Die Umwandlung in verschiedene Entwicklungsstadien ist essentiell für die Übertragung und das Überleben dieses menschlichen Pathogens, dennoch wirft der molekulare Mechanismus, der diesen fundamentalen Prozess regelt, bis heute viele Fragen auf. In diesem Projekt untersuchten wir den Einfluss des Histon-Deacetylase-Inhibitors FR235222 auf die Genregulation der Stadienumwandlung im extrazellulären *G. lamblia*-Parasiten. Zum ersten Mal konnten wir zeigen, dass die die Inhibition der Histon-Deacetylase mit FR235222 transkriptionelle Veränderungen in beiden Entwicklungsstadien von *G. lamblia* induzierte und interessanterweise auch die Zystenbildung blockierte. Wir vermuten, dass die Stadienumwandlung in *G. lamblia* unter Kontrolle der epigenetischen Regulation und der Histon-Acetylierung steht. Hinzukommend scheint die Aktivität der Histon-Deacetylase ein hoffnungsvoller Ansatz für die Entwicklung neuer Anti-Gardia-Wirkstoffe, da die Inhibierung der Histon-Deacetylase-Aktivität die Zystenbildung in *G. lamblia* blockiert und daher Potential besitzt, die Übertragung der Krankheit zu reduzieren.

1 P-glycoprotein (P-gp, ABCB1, MDR)

1.1 Localization and function

P-glycoprotein is an ATP-driven efflux pump which is a member of one of the largest families of proteins found in both prokaryotes and eukaryotes, so called ATP-Binding Cassette (ABC) transporters. ABC transporters use energy from ATP hydrolysis to transport a wide range of substrates across membranes of organisms from bacteria to humans (6). P-gp is one of the most extensively studied ABC transporters because of its central role in the development of multidrug resistance (MDR) in cancers and pathogenic microorganisms.

P-gp is predominantly localized in the plasma membrane of cells with barrier function, including epithelia of the liver, kidney, small and large intestine and capillary endothelial cells in brain, ovary and testis. Moreover, P-gp was found to be partially localized in intracellular compartments such as the Golgi apparatus (8,9), early endosomes and lysosomes (10).

P-gp is known to bind and to transport a large variety of hydrophobic and cationic organic compounds across the plasma membrane. P-gp substrates include many of the commonly used anticancer drugs and other pharmaceuticals ranging from antiarrhythmics and antihistamines to cholesterol-lowering statins (11) and HIV protease inhibitors (12). Moreover, P-gp also transports hydrophobic peptides (13), cytokines (14) and some lipids, such as steroid metabolites and phospholipids (15,16). The complete understanding of P-pg transport mechanism is important for the rational design of anticancer drugs and MDR inhibitors.

1.2 Structure

P-gp consists of 2 nucleotide-binding domains (NBD) and 12 transmembrane domains (TM 1-12) which form an inner channel in the plasma membrane (Figure 1A). Importantly, the structural composition of transmembrane helices results in the formation of substrate-binding internal cavity which is opened to the cytoplasm and the inner leaflet of the plasma membrane lipid bilayer (7). The P-gp substrates incorporate from outside of the cell into the plasma membrane inner leaflet and enter the internal substrate-binding pocket through an open cavity. Binding of the substrate is subsequently followed by activation of one of the ATP-binding domains, and the hydrolysis of ATP causes a large conformational change of P-gp, which results in the release of the substrate into the outer leaflet and the extracellular space (17). Hydrolysis of a second molecule of ATP is needed to restore the transporter to its original state so that it can repeat the cycle of substrate binding and release (18,19) (Figure 1B). The NBD are located on the cytoplasmic face of the protein and are characterized by Walker A and Walker B motifs, also found in many other nucleotide-binding proteins, and by a signature C motif unique to the ABC superfamily. The internal substrate-binding cavity contains 73 solvent-accessible residues, 15 are polar and only two are charged or potentially charged (7). The volume of the internal cavity within the lipid bilayer is extensive and could accommodate at least two transported compounds simultaneously (20). This detailed description of protein structure has helped to understand P-gp substrate promiscuity.

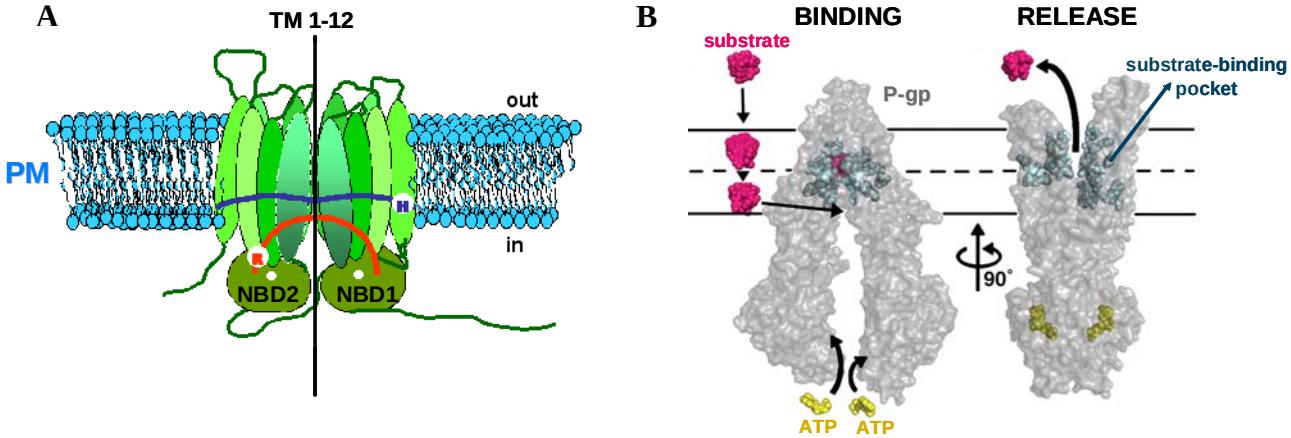

Figure 1: A) P-gp structure (4) B) Model of P-gp ATP-driven efflux (7)

1.3 P-glycoprotein and multidrug resistance

Ordinarily, drug resistance is specific to a single class of compounds. Cancer cells as well as microorganisms may also exhibit a cross-resistant phenotype against several unrelated drugs. This phenomenon has been termed multidrug resistance (MDR) and it is the major reason for failure of chemotherapeutical and pharmacological treatment. The principal mechanism of MDR is the active transport of drugs out of the cell which is responsible for failure of treatment in over 90% of patients with metastatic cancer (21). The P-gp efflux pump plays an important role in the multidrug export and this transporter is highly over-expressed in drug resistant tumour cells (22,23). The over-expression of P-gp is also responsible for drug resistance in the pathogenic yeast and bacteria and in the important human parasites *Plasmodium*, *Leishmania* and *Trypanosoma* (24).

P-gp is intensively studied in the human parasite *Plasmodium faciparum*. This parasite causes malaria and is responsible for over one million deaths each year also because traditional antimalarial drugs have recently become ineffective in many parts of the world due to the development of drug resistance. The *P. falciparum* P-gp homologue PfABCB1 (Pgh1, PfMDR1) is constitutively expressed and its over-expression and/or mutations have been implicated in decreased susceptibility to several antimalarial drugs (25,26).

Given the importance of P-gp in human and microbial MDR, it became urgent to identify the substrates and transport activities of this protein and its physiological function for the rational design of new drugs and MDR inhibitors.

1.4 P-glycoprotein inhibition

P-gp inhibition as a way of reversing MDR has been extensively studied for more than two decades. Many drugs have been investigated which modulate P-gp transport including calcium channel blocker such as verapamil, immunosuppressant such as cyclosporine A and the antisteroid tamoxifen (27). These compounds were not specifically developed to block P-gp, however, have low affinity for P-gp. Because many of them are substrates for other transporters and enzymes, their off-label use as MDR inhibitors entails a significant potential for side effects (28). To overcome the limitations of these first-generation inhibitors, several novel analogues of these P-gp modulators were developed with the aim of finding P-gp modulators with less toxicity and greater potency (29). These second-generation P-gp modulators include dexverapamil, valspodar (PSC 833) and biricodar (VX-710). They have an improved pharmacological profile, but they also retain some characteristics that limit their clinical usefulness. They also function as inhibitors for other transporters, particularly those of the ABC transporter family, whose inhibition reduces the ability of normal cells and tissues to protect themselves against cytotoxic agents (29). Recently, a new generation of inhibitors has reached clinical testing. These third-generation inhibitors are nontoxic, more specific, and more potent than the earlier inhibitors used in trials of P-gp modulation. These compounds include tariquidar, R101933, LY335979 and GF120918 which we used in our study. These modulators inhibit the ATPase activity of P-gp (30).

1.5 Physiological function of P-glycoprotein

It is well-established that P-gp mediates efflux of chemotherapeutic agents out of cancer cells and thereby its over-expression contributes to drug resistance. However, P-gp is also expressed at basal levels in non-malignant cells. The physiological function and the substrates of this protein in normal cells remain poorly characterized, however, there have been several attempts to define the physiological function of P-gp and so far a number of different roles have been proposed for P-gp:

1.5.1 Cellular detoxification

P-gp is present in a range of classical pharmacological barriers and excretory tissues like liver, intestine, kidney and blood-tissue barriers. Since the tissue distribution of a protein can yield

important clues to its function, it was hypothesised that this protein might be involved in protecting the organism against naturally occurring xenotoxins.

The analyses of the knockout mice lacking P-gp support the proposed role of P-gp in the protection against xenotoxins exposure. P-gp knockout mice do not show reduced viability, nor haematological parameters compared with the wild type in the absence of drug pressure (31). Importantly, in the presence of drug pressure the lack of P-gp significantly increased the uptake of these toxic compounds from the gastrointestinal tract and made the blood-brain barrier and other blood-tissue barriers strongly susceptible to the exposure of toxins that have entered the bloodstream compared with the wild type mice (31).

1.5.2 Immunological functions

P-gp was shown to be present in several sub-classes of bone marrow, peripheral leukocytes and also in human hematopoietic stem cells, which are precursors of all the blood cell types (32). This observation raised the hypothesis that P-gp might be involved in the hematopoietic development or function.

It has been shown that inhibition of P-gp efflux function using either specific monoclonal antibodies or pharmacological inhibitors reduced cytolytic activity of natural killer cells and CD8+ T-cells, possibly by mediating the release of the cytolytic protein perforin (33,34). Moreover, blocking P-gp inhibited the migration of antigen-presenting dendritic cells and T-cells during an immune response (35). P-gp is capable to transport peptides (13), thus it was proposed that this protein transports the polypeptide cytokine interleukin 2 and possibly other cytokines required for the migration of dendritic cells and T-cells (14,36).

1.5.3 Ion transport activity

P-gp is structurally similar to cAMP-activated chloride channels such as cystic fibrosis transmembrane conductance regulator (CFTR) (37). Thus it was speculated that P-gp might also function as an ion channel. It was shown that P-gp does not have basic ion channel activity but it can regulate a thus far unidentified endogenous chloride channel and like this it indirectly modulates channel activity (38,39). Recently, it was suggested that P-gp mediates H^+- Na^+- Cl^- symport as was shown using P-gp analogue LmrA from bacterium *Lactococcus lactis* (40). This protein can functionally substitute for P-gp function in human lung fibroblasts, and exhibits a substrate specificity similar to that of the human protein (41).

1.5.4 Lipid transport and intracellular cholesterol trafficking

Several ABC transporters act as flippases which transport lipids from the inner to the outer leaflet of plasma membrane (Figure 2) (42). Lipids are the main structural component of biological membranes and the key factors in variety of cellular processes including signalling. Therefore there has been a strong interest to define the role of ABC proteins in the lipid transport. One of the ABC transporters involved in lipid transport is ABCB4 which functions as a phosphatidylcholine (PC)-specific transporter (43). Given that P-gp is closely related to this PC-transporter (78% sequence similarity), it has been proposed that P-gp plays a role in the lipid transport by acting as a lipid flippase.

In support to this hypothesis, P-gp has been reported to act as a flippase for short-chain fluorescent analogs of plasma membrane lipids of very different structure such as PC, phosphatidylethanolamine (PE) (16), glucosylceramide (GlcCer) and sphingomyelin (SM) from the inner to the outer leaflet of the plasma membrane (15). In addition, it was shown that pharmacological inhibition of P-gp could limit SM movement from the inner to the outer leaflet of the plasma membrane, leading to an increase of hydrolysable SM pool (hydrolysis: SM→Ceramide) (44). The role of P-gp in lipid flipping has been also suggested in connection with cholesterol transport from the inner to the outer leaflet of plasma membrane using native membrane vesicles model (45). Moreover, some studies using second-generation of P-gp inhibitors have demonstrated that P-gp can modulate esterification of plasma membrane cholesterol (46,47). This observation was

confirmed in P-gp deficient mice where the lack of P-gp decreased hepatic accumulation and enhanced esterification of cholesterol (48). Recently, P-gp have been proposed to have a role in the secretion of lipid-based signalling molecules: platelet-activating factors (PAFs) from the inner to the outer membrane leaflet, from which they may diffuse into the extracellular environment (49). So far PAFs are the only natural lipids that have been shown to be transported by P-gp. Thus, the main question, whether natural unlabelled membrane lipids with two long acyl chains are transported by P-gp acting as plasma membrane lipid flippase, still remains open.

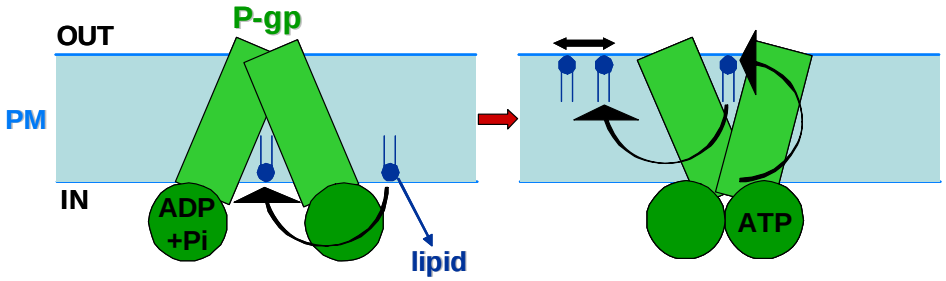

Figure 2: Model of P-gp acting as lipid flippase; PM-plasma membrane

1.6 P-gp in host-pathogen interaction

The interactions between a pathogen and its host are complex and dynamic. The outcome of such interactions is a manifestation of the pathogen capability to exploit its host and the ability of the host to respond to the infection. This outcome may range from disease to asymptomatic transmission or even pathogen elimination. The understanding of the mechanisms of such interactions is essential for the targeted development of effective prevention and control strategies.

P-gp seems to be involved in several important metabolic processes including membrane lipid remodelling and transport of signalling molecules. It is localized in the plasma membrane of a number of human cells types and since the plasma membrane is the first barrier that an intracellular pathogen has to cross for entry into the host cell, it is conceivable that P-gp plays role in host-pathogen interaction.

P-gp was proposed to be involved in essential biological processes of the medically relevant human parasite *Toxoplasma gondii* (50). It was shown that fundamental processes of this parasite such as intracellular replication and host cell invasion could be inhibited by second-generation P-gp modulators (50). These investigations have pointed out for the first time a possible role of P-gp in host-parasite interaction, and raised the major question about the physiological role of P-gp in the biology of *T. gondii*.

2 *Toxolpasma gondii*

Toxoplasma belongs to the phylum Apicomplexa, which consists of protozoan parasites that have a characteristically polarized cell structure and a complex cytoskeletal and organellar arrangement at their apical end (51) (Figure 3A). Other members of this phylum are the human and animal pathogens *Plasmodium* and *Cryptosporidium*, *Neospora* and *Sarcocystis*. *T. gondii* is an obligate intracellular parasite, which infects a broad range of vertebrate hosts, including humans. *T. gondii* causes toxoplasmosis, a potentially life-threatening disease in immunocompomised individuals such as AIDS patients and organ transplant recipients, and in congenitally infected foetuses. Currently existing chemotherapeutic regimens, while effective at controlling the proliferating parasite, cause severe side effects during the treatment and therefore there is a need for developing new improved drugs against toxoplasmosis.

Importantly, *T. gondii* is the most experimentally tractable of the Apicomplexa because of its feasible genetic and cell culture manipulations allowing easy *in vitro* propagation of the parasite

pathogenic stages and well-established mouse model. Thus, *T. gondii* has emerged as a major model for the study of apicomplexan biology (52), intracellular parasitism and host-parasite interactions.

2.1 Life cycle

The life cycle of *T. gondii* has two phases: a sexual and an asexual (Figure 3B). The sexual part of the life cycle takes place exclusively in members of the Felidae family, the definitive *T. gondii* host. The production of gametes and fertilized zygotes occur within feline intestinal enterocytes, giving rise to diploid oocysts, which undergo meiosis (53). Excreted oocysts undergo sporulation and can survive in soil for several months. The asexual part of the life cycle can take place in any warm-blooded animal like mammals and birds, the intermediate *T. gondii* host. Interestingly, *T. gondii* are less infective and less pathogenic in the definitive host compared with intermediate hosts (54).

Our study focuses on asexual life cycle. Asexual life cycle is composed of three stages: the rapidly replicating tachyzoites, the slowly replicating bradyzoites contained in tissue cysts, and the sporozoites formed in oocysts during the sexual phase of the cycle. The two major ways of human infection with the parasite are by ingestion of tissue cysts in under-cooked meat or by ingestion of food or water contaminated with oocysts. After ingestion, both bradyzoites from tissue cysts and sporozoites from oocysts infect the intestinal epithelium and convert to tachyzoites, observed during the acute stage of infection. Tachyzoites invade a variety of cell types, where they rapidly multiply. Tachyzoite replication eventually leads to lysis of host cells and release of parasites, which then start a new cycle of the infection by invading a new host cell. In the chronic stage of toxoplasmosis, tachyzoites convert to the slowly replicating bradyzoites, which form cysts in several tissues, including the brain. Since bradyzoite cysts are not detected by the host immune system, they persist in the tissues for the life span of the host (54).

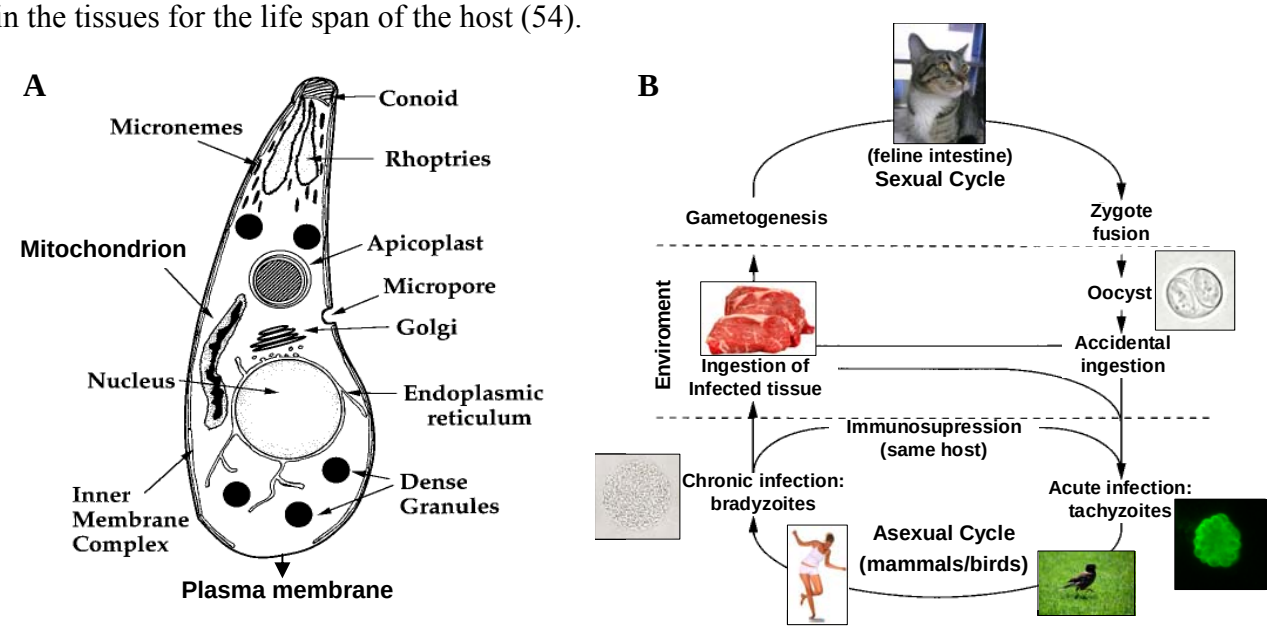

Figure 3: A) *T. gondii* tachyzoite structure with the major organelles. B) *T. gondii* life cycle (1)

2.2 Lytic cycle

The lytic cycle of toxoplasmosis starts with invasion of the host cell. The tachyzoite first attaches via its apical pole to the host cell (55,56), and by using contractile proteins, including actin and myosin, the parasite penetrates the host cell (57,58). This active process of parasite invasion leads to the formation of a specialized parasitophorous vacuole (PV). The PV is derived from the host cell membrane and modified by the parasite to avoid fusion with host cell lysosomes (59). The

PV segregation from the host vesicular traffic provides the parasite with a unique niche where parasites successfully replicate and then egress to infect neighbouring cells (60) (Figure 4).

T. gondii has a number of secretory organelles that include the apical micronemes, rhoptries and dense granules (Figure 3A). Each compartment contains its own pool of proteins whose function is consistent with the timing of their release during the lytic cycle (61): micronemes release their contents (adhesins) early during the attachment-invasion process to initiate apical attachment and penetration of the host cell. Rhoptry proteins are released as invasion proceeds to assists in the formation of the developing PV and its interaction with host organelles. Finally dense granules discharge their contents when invasion is essentially completed to prepare the PV for intracellular replication and for survival of the parasite. *T. gondii* has been extensively studied and crucial factors involved in invasion, PV formation and replication have been identified, but relatively few have been thoroughly characterised yet.

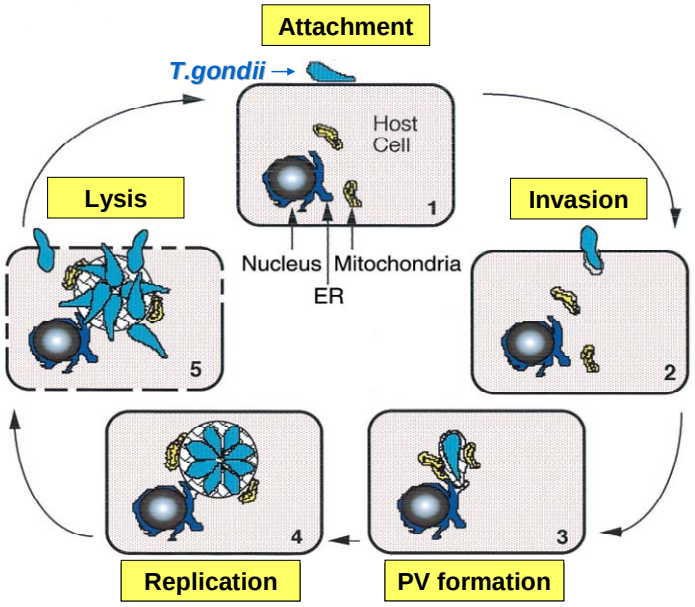

Figure 4: *T. gondii* tachyzoite lytic cycle (1); 1) Attachment of tachyzoite to its host cell, 2) The tachyzoite reorientates to its apical end and initiates invasion, 3) The newly formed parasitophorous vacuole (PV) recruits host mitochondria and ER, 4) The tachyzoite undergoes several rounds of replication 5) which results in host cell lysis and parasite exit.

2.2.1 Motility and Invasion

T. gondii motility and cell invasion are essential elements of the infection process ensuring the propagation and survival of the parasite, and therefore they are an important focus of research investigations. It is expected that a detailed understanding of these processes will help with the identification of novel therapeutic targets.

To gain the entry into a host cell, the parasite must first make a direct contact with the plasma membrane of the host cell. Subsequently, *T. gondii* uses a substrate-dependent locomotion termed gliding motility for tissue migration and cell invasion (2,62). The gliding motility relies on a complicated linear motor system sandwiched between the parasite's plasma membrane and the inner membrane complex (IMC) of the parasite (Figure 3A). Motive force is generated by the myosin that is anchored to the inner membrane complex by two gliding-associated proteins (GAP) (63), and short actin microfilaments. The actin microfilaments associate with the enzyme aldolase (64), which links the complex to the transmembrane adhesive proteins (microneme proteins) that bridge over the parasite's plasma membrane (Figure 5A). The secretion of transmembrane adhesion proteins from the apical end, and a unidirectional orientation of the actin microfilaments support forward motion with the apical pole leading the way.

The actino-myosin motor that drives the motility is intracellular, thus at least one transmembrane bridge is required for the parasite to link it to an extracellular host cell ligand for locomotion. Consistent with the model for motility *T. gondii* invasion is highly polarized, with the parasite exclusively using its apical end and conoid extrusion (56) to initiate penetration into the target cell.

Several adhesins are released from apical secretory organelles called micronemes to allow parasite attachment to the host cell. For example, microneme proteins MIC1 contains two adhesive sequences related to a domain of thrombospondin (involved in blood colagulation), and it is capable of binding host cells *in vitro* (65). Similarly, MIC2 includes several thrombospondin-like repeat sequences and an integrin- like adhesive domain (66) and recently it was demonstrated that this microneme protein is responsible for the parasite host cell binding activity later forming a tight connection between the parasite and host plasma membrane: MIC2-host receptor conjugates known as the moving junction (61,67) (Figure 5A, B).

The process of invasion involves two Ca^{2+}-dependent events: extrusion of the apical conoid and the induction of secretion of MIC proteins from the micronemes. It has been shown that addition of calcium ionophores, such as ionomycin and A23187 activated both conoid extrusion and microneme secretion (68-70).Conversely, loading of *T. gondii* tachyzoites with the intracellular Ca^{2+}-chelator BAPTA-AM prevented calcium ionophore-induced conoid extrusion, MIC secretion and inhibited invasion (68-70). Furthermore, the gliding motility of *T. gondii* is also activated by elevated cytosolic Ca^{2+} levels (68). The largest store of Ca^{2+} in apicomplexan protozoa is found in the acidocalcisomes (71), acidic organelles which are present in a diverse range of microorganisms, but absent in mammalian cells (72,73). These studies revealed the importance of the intracellular Ca^{2+} in the process of parasite–host cell interaction, but the stimulus for these Ca^{2+} changes remains unknown.

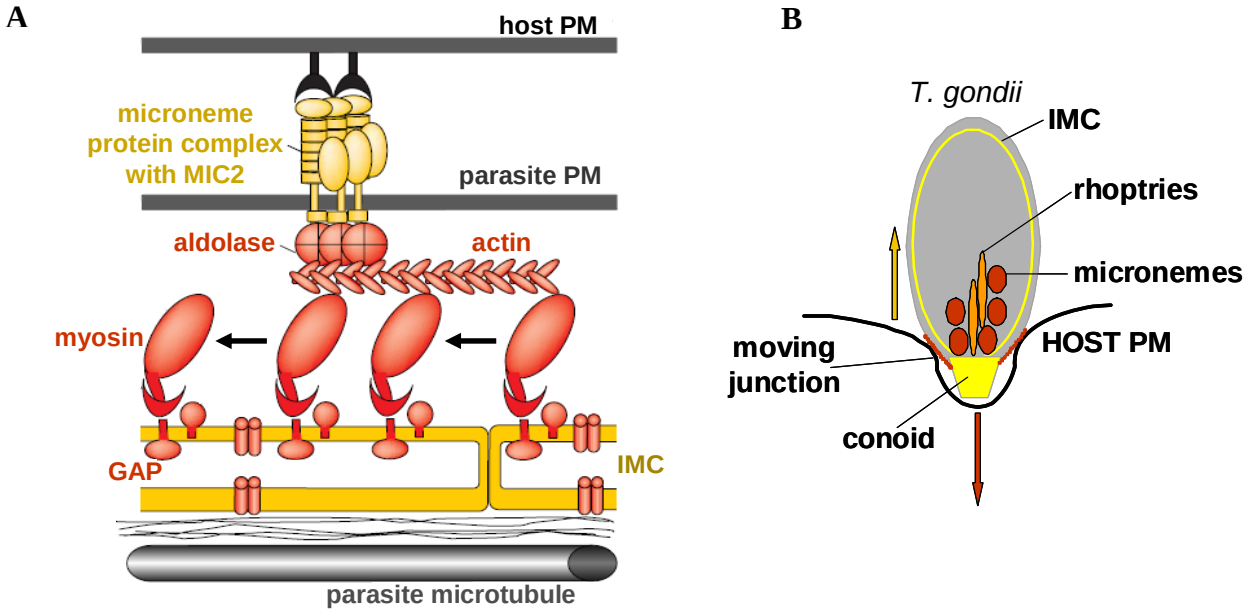

Figure 5: A) *T. gondii* gliding motility sandwich (modified from (2)). Plasma membrane (PM), gliding-associated proteins (GAP), microneme protein (MIC2), inner membrane complex (IMC); B) *T. gondii* model of invasion (modified from (2)).

2.2.2 Vacuole formation and parasite replication

The vacuole formed by the parasite after invasion is atypical because it does not acidify (74) and does not fuse with any vesicles of the endocytic pathway including lysosome (75,76). To prevent parasitophorous vacuole (PV) acidification and endocytic processing, the PV must either exclude or rapidly eliminate surface proteins which guarantee vesicular fusion. Such displacement of host membrane proteins from PV membrane was demonstrated for Na^+/K^+ ATPase, β1-integrin and CD44 and was proposed to be accomplished by the moving junction (77), however the complete mechanism of this sorting remains undefined.

After the PV is formed, a third set of secretory organelles, called dense granules, release their contents from both the anterior and posterior poles of the parasite (61). Dense granule proteins are

responsible for the construction of the tubulovesicular network that extends from the *T. gondii* cell surface into the lumen of the PV (78) (Figure 6A). The PV recruits host mitochondria and endoplasmic reticulum (ER) immediately following invasion (79). These organelles form a close interaction with the PV membrane and they are suggested to provide lipids for the PV (80) which could be transported to intra-vacuolar parasites through a tubulovesicular network established within the PV (79).

Following entry, *T. gondii* rapidly divides by a special manner termed endodyogeny, where two daughter cells are formed within a mother cell. Once the resources of the host cell cytoplasm are exhausted, the parasites actively exit the dying cell to find another host. This lytic cycle involved tissue damage and one round of invasion and lysis typically takes 24–48 h and results in production of 16 to 128 tachyzoites that originate from a single invaded parasite.

The investigation of *T. gondii*-infected cells demonstrated that the PV imports Ca^{2+} from the host cytoplasm and after 48 h of intracellular replication, a significant decrease in the level of host cytosolic Ca^{2+} was observed compared to that in uninfected cells. This could suggest that the increase of $[Ca^{2+}]_i$ in the PV may act as a signal that triggers the egress of the parasite (81).

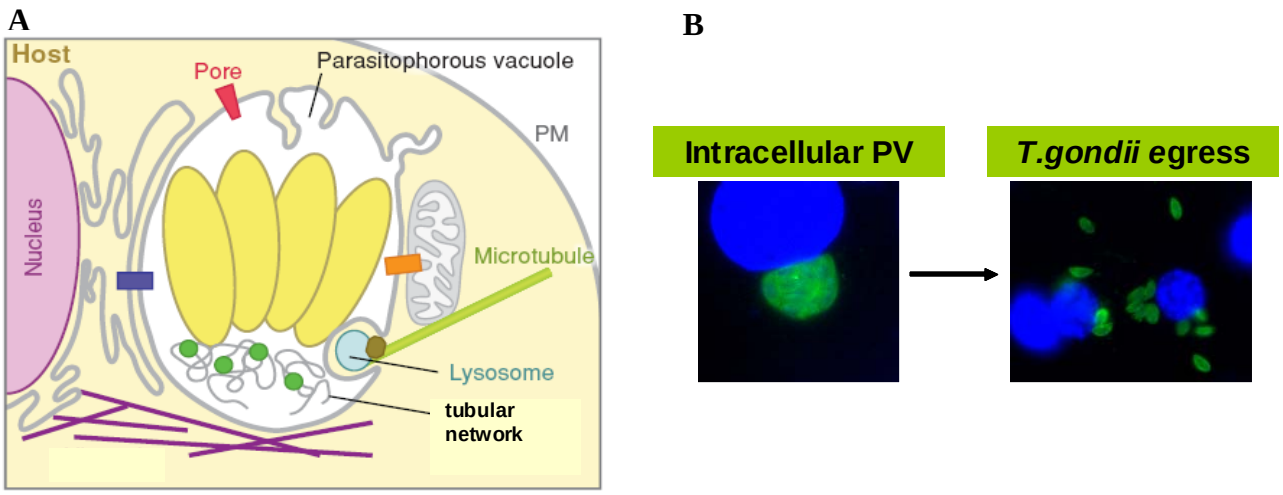

Figure 6: A) *T. gondii* intracellular parasitophorus vacuole (PV) (modified from (3)); B) Calcium ionophore induced egress (5).

2.2.3 Parasite egress

As with the process of invasion, intracellular parasites have evolved a mechanism for egress and transmission to neighbouring cells. The *T. gondii* egress is a rapid process and results in the lyses of the host cell and release of motile parasites (Figure 6B). The mechanism of this event remains poorly understood.

During natural egress *T. gondii* mechanically ruptures the host cell with escalating tension on the host cell membrane due to increased parasite burden (82,83). However the exact mechanism by which the parasites rupture the membrane is not completely understood. Recently, it was shown that micronemal perforin-like protein 1 facilitates parasite egress by compromising the integrity of the PV (84). Determination of factors required during natural egress is difficult to asses because of the fact that natural egress is highly variable in the timing and it is asynchronous between parasites in different host cells (82). Conversely, the egress induced by the artificial host cell permeabilization or by Ca^{2+} ionophore such as A23187 (85) allows easy manipulation of the timing and synchronization (85-87). Consequently, induced egress has become an important model for the study how the egress may occur under natural conditions (88).

Similar to invasion, *T. gondii* egress from host cells is affected by Ca^{2+} flux. The Ca^{2+} ionophore-stimulated egress can occur even when extraparasitic (vacuolar and host cell) Ca^{2+} has been removed with Ca^{2+}chelators (85-87), indicating that the parasite uses its own Ca^{2+} stores.

These observations suggest that activation of motility and induction of calcium fluxes are sufficient to cause egress in the intracellular parasites. Consistent with this concept, chelation of $[Ca^{2+}]_i$ in intracellular parasites using BAPTA-AM severely inhibited natural egress (86).

2.3 Exploitation of the host cell

T. gondii resides and replicates inside a nonfusogenic PV during the entire intracellular cycle. Such a safe niche guarantees resistance to host cell defences but significantly limits the access of parasites to host metabolites. The intracellular parasite adopted the strategy to remodel the PV membrane (PVM) to make it accessible to nutrients. The newly formed PVM of *T. gondii* is immediately modified and contains the pore that allows free diffusion of small molecules such as simple sugars, amino acids, nucleobases and cofactors (89). The pore allows the passage of small molecules into the PV in the absence of transporters, while their subsequent uptake by the parasite is mediated via substrate-specific transporters or endocytosis. This molecular filter plays a critical role in the context of the multiple parasite auxotrophies.

T. gondii depends on host-derived glucose for energy and as a carbon source for fatty acid biosynthesis (90), and it is auxotrophic for amino acids such as arginine (91) and tryptophan (92). *T. gondii* salvages purines and pyrimidines (93,94) despite its ability to synthesize pyrimidines *de novo* (95). Because *T. gondii* lacks the mitochondrial genes required for de novo synthesis of lipoic acid, a cofactor for many biosynthetic pathways, the host mitochondria are likely the source of this compound for the parasite (96).

Importantly, the segregation of the PV from host cell vesicular transport pathways limits also the possibility of the acquisition of exogenous lipids whose trafficking is restricted to those pathways. The acquisition of essential lipids is fundamental for membrane biogenesis to support successful parasite replication. *T. gondii* has the autonomous capacity to synthesize phospholipids, but it also readily scavenges precursors from its environment for the construction of more complex lipids (97,98). Conversely, *T. gondii* lacks enzymes to synthesize steryl molecules and needs to acquire these lipids intact from the host cell (99). A recent study has proposed a novel mechanism established by the parasite to acquire low density lipoprotein (LDL)-derived cholesterol from the host cell. It was suggested that *T. gondii* sequesters host lysosomes to the PV lumen by recruiting host microtubules and forming H.O.S.T (host organelle sequestering tubulo-structures) (Figure 6A) (100). However, the exact molecular mechanism of cholesterol delivery to the parasite is still unknown. Since cholesterol is required for parasite membrane biogenesis and cholesterol import is necessary for *T. gondii* replication (99), it is essential to define the mechanism of cholesterol transport from the host to the PV. The elucidation of the cholesterol import mechanism would improve our understanding of host-parasite interaction and could lead to the identification of new drug targets in *T. gondii*.

2.4 *T. gondii* P-gp

Recently, it was demonstrated that efflux of xenobiotics could be modulated in extracellular *T. gondii* using the first generation of P-gp inhibitors: verapamil and cyclosporine A, thus providing indirect evidence for the existence of *T. gondii* P-gp homologue (101). Subsequently, it was shown that *T. gondii* contains two P-gp homologues termed TgABCB1 (TgP-gp) and TgABCB2, which share about 50% amino acid identity and sequence similarity with the *P. falciparum* PfABCB1 and human HuABCB4, respectively. TgP-gp is constitutively expressed in the three major *T. gondii* genotypes and the intracellular localization analysis revealed a plasma membrane-association of this protein. The highest TgP-gp expression was demonstrated in the most virulent *T. gondii* RH strain, at both the transcriptional and translational levels (102,103). The role of *T. gondii* P-gp homologue in parasite biological processes remains unsolved.

3 The aim of the project

It has been already well established that P-gp over-expression is responsible for multidrug resistance in a variety of cells, but the physiological functions of P-gp in absence of drug pressure are still not completely understood, neither in human cells nor in parasitic protozoa. The aim of our project was to characterize the role of P-gp in host-pathogen interaction using *T. gondii* as a model parasite. Specifically, our aims were:

1) To define the precise role of host P-gp in the host cells and in biological processes of the parasite. To perform this study we used mouse embryonic fibroblasts (MEF) lacking P-gp (mouse double knockout in *mdr*1a and *mdr*1b genes; DKO; P-gp KO) as model system but also P-gp complemented P-gp knockout MEF (DKO/P-gp) and the wild type MEF (WT) as well.

2) To characterize the P-gp homologue in *T. gondii* and its function. To study *T. gondii* P-gp, we used specific pharmacological inhibition of the parasite protein by third-generation P-gp modulators: GF120918 in a host cell background of DKO cells to study the function of the parasite protein in isolation to avoid contribution of host cell P-gp to the final effect.

4 Additional project: Regulation of the parasite stage conversion

During infection in mammals, intracellular *T. gondii* undergoes stage conversion between the rapidly replicating tachyzoites that are responsible for acute toxoplasmosis and the dormant non-replicating bradyzoites that cause the chronic infection (Figure 3B). The bradyzoites survive within a cyst limited by a cyst-wall in several tissues such as brain and muscle during the lifetime of the host. Stage conversion is an important step for parasite transmission because bradyzoites within tissue cysts act as a source of infection for transmission via carnivorism. Moreover, in immunocompromised individuals, the majority of cases of fatal toxoplasmosis is the result of reactivation of encysted bradyzoites into actively replicating tachyzoites (104).

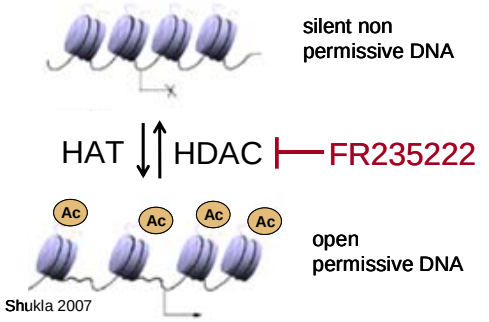

Figure 7: Histone acetylation. histone acetylase (HAT), histone deacetylase (HDAC) inhibited by FR235222.

Recently, it has been proposed that histone modifications, particularly acetylation, could be the key epigenetic regulators of parasite stage conversion. Histone acetylation regulates DNA packaging, and therefore influences gene expression (Figure 7). Histone hyperacetylation is usually linked with chromatin decondensation, because it neutralizes the basic charge of target lysine residues on histones (105). It was shown, using histone deacetylase inhibitor FR235222, that a histone deacetylase (HDAC3) plays a role in expression of stage-specific genes, stage conversion, and cell-cycle control of *T. gondii*. Moreover, FR235222 strongly inhibits *T. gondii* and *Plasmodium* replication (106).

In the project that I contributed to, we analysed the effect of histone deacetylase inhibitor FR235222 on the epigenetic regulation of the stage conversion in extracellular parasite *Giardia lamblia*.

G. lamblia (also called *G. intestinalis* or *G. duodenalis*), is a simple eukaryote causing the disease giardiasis. *G. lamblia* resides in the upper small intestine of humans and several other vertebrates usually infected by ingestion of cysts from contaminated water or food (107). The parasite is non-invasive, and neither toxins nor virulence factors have been clearly defined (107). *Giardia* is characterized by two different developmental stages: the motile, flagellate trophozoites that are responsible for the proliferation and the clinical manifestation of the disease such as diarrhoea and malabsorption, and the cyst forms which are shed into the environment (Figure 8). The cysts are the infective stage of the parasite, in which trophozoites are surrounded by a rigid, protective cyst wall that allows the parasite to survive in the environment and permits transmission

of the infection to susceptible hosts (108). The stage conversion process of *G. lamblia* is essential for transmission and survival of this human pathogen, but the understanding of the molecular mechanism which regulates this fundamental process still remains poorly understood. Importantly for our study, the inhibitor FR235222 gave us the tool to investigate for the first time the role of histone deacetylase in the epigenetic regulation of the stage conversion of *G. lamblia*.

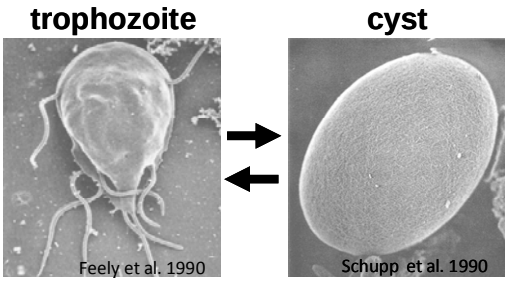

Figure 8: *G. lamblia* developmental stages.

5 References

1. Black, M. W., and Boothroyd, J. C. (2000) *Microbiol Mol Biol Rev* **64**(3), 607-623
2. Keeley, A., and Soldati, D. (2004) *Trends in cell biology* **14**(10), 528-532
3. Plattner, F., and Soldati-Favre, D. (2008) *Annual review of microbiology* **62**, 471-487
4. Sharom, F. J. (2006) *Biochemistry and cell biology = Biochimie et biologie cellulaire* **84**(6), 979-992
5. Bottova, I., Sauder, U., Olivieri, V., Hehl, A.B., and Sonda S. (2009)
6. Higgins, C. F. (1992) *Annual review of cell biology* **8**, 67-113
7. Aller, S. G., Yu, J., Ward, A., Weng, Y., Chittaboina, S., Zhuo, R., Harrell, P. M., Trinh, Y. T., Zhang, Q., Urbatsch, I. L., and Chang, G. (2009) *Science (New York, N.Y* **323**(5922), 1718-1722
8. Willingham, M. C., Richert, N. D., Cornwell, M. M., Tsuruo, T., Hamada, H., Gottesman, M. M., and Pastan, I. H. (1987) *J Histochem Cytochem* **35**(12), 1451-1456
9. Molinari, A., Cianfriglia, M., Meschini, S., Calcabrini, A., and Arancia, G. (1994) *International journal of cancer* **59**(6), 789-795
10. Fu, D., and Roufogalis, B. D. (2007) *American journal of physiology* **292**(4), C1543-1552
11. Bogman, K., Peyer, A. K., Torok, M., Kusters, E., and Drewe, J. (2001) *British journal of pharmacology* **132**(6), 1183-1192
12. Lee, C. G., and Gottesman, M. M. (1998) *The Journal of clinical investigation* **101**(2), 287-288
13. Sarkadi, B., Muller, M., Homolya, L., Hollo, Z., Seprodi, J., Germann, U. A., Gottesman, M. M., Price, E. M., and Boucher, R. C. (1994) *Faseb J* **8**(10), 766-770
14. Drach, J., Gsur, A., Hamilton, G., Zhao, S., Angerler, J., Fiegl, M., Zojer, N., Raderer, M., Haberl, I., Andreeff, M., and Huber, H. (1996) *Blood* **88**(5), 1747-1754
15. van Helvoort, A., Smith, A. J., Sprong, H., Fritzsche, I., Schinkel, A. H., Borst, P., and van Meer, G. (1996) *Cell* **87**(3), 507-517
16. Bosch, I., Dunussi-Joannopoulos, K., Wu, R. L., Furlong, S. T., and Croop, J. (1997) *Biochemistry* **36**(19), 5685-5694
17. Ramachandra, M., Ambudkar, S. V., Chen, D., Hrycyna, C. A., Dey, S., Gottesman, M. M., and Pastan, I. (1998) *Biochemistry* **37**(14), 5010-5019
18. Sauna, Z. E., and Ambudkar, S. V. (2001) *The Journal of biological chemistry* **276**(15), 11653-11661
19. Sauna, Z. E., and Ambudkar, S. V. (2000) *Proceedings of the National Academy of Sciences of the United States of America* **97**(6), 2515-2520
20. Loo, T. W., Bartlett, M. C., and Clarke, D. M. (2003) *The Journal of biological chemistry* **278**(41), 39706-39710
21. Longley, D. B., and Johnston, P. G. (2005) *The Journal of pathology* **205**(2), 275-292
22. Ueda, K., Cardarelli, C., Gottesman, M. M., and Pastan, I. (1987) *Proceedings of the National Academy of Sciences of the United States of America* **84**(9), 3004-3008
23. Juliano, R. L., and Ling, V. (1976) *Biochimica et biophysica acta* **455**(1), 152-162

24. Klokouzas, A., Shahi, S., Hladky, S. B., Barrand, M. A., and van Veen, H. W. (2003) *International journal of antimicrobial agents* **22**(3), 301-317
25. Wilson, C. M., Serrano, A. E., Wasley, A., Bogenschutz, M. P., Shankar, A. H., and Wirth, D. F. (1989) *Science (New York, N.Y* **244**(4909), 1184-1186
26. Foote, S. J., Thompson, J. K., Cowman, A. F., and Kemp, D. J. (1989) *Cell* **57**(6), 921-930
27. Robert, J. (1998) *Expert opinion on investigational drugs* **7**(6), 929-939
28. Thomas, H., and Coley, H. M. (2003) *Cancer Control* **10**(2), 159-165
29. Krishna, R., and Mayer, L. D. (2000) *Eur J Pharm Sci* **11**(4), 265-283
30. Martin, C., Berridge, G., Mistry, P., Higgins, C., Charlton, P., and Callaghan, R. (1999) *British journal of pharmacology* **128**(2), 403-411
31. Schinkel, A. H. (1997) *Seminars in cancer biology* **8**(3), 161-170
32. Chaudhary, P. M., and Roninson, I. B. (1991) *Cell* **66**(1), 85-94
33. Gupta, S., Kim, C. H., Tsuruo, T., and Gollapudi, S. (1992) *Journal of clinical immunology* **12**(6), 451-458
34. Chong, A. S., Markham, P. N., Gebel, H. M., Bines, S. D., and Coon, J. S. (1993) *Cancer Immunol Immunother* **36**(2), 133-139
35. Randolph, G. J., Beaulieu, S., Pope, M., Sugawara, I., Hoffman, L., Steinman, R. M., and Muller, W. A. (1998) *Proceedings of the National Academy of Sciences of the United States of America* **95**(12), 6924-6929
36. Raghu, G., Park, S. W., Roninson, I. B., and Mechetner, E. B. (1996) *Experimental hematology* **24**(10), 1258-1264
37. Bear, C. E., Li, C. H., Kartner, N., Bridges, R. J., Jensen, T. J., Ramjeesingh, M., and Riordan, J. R. (1992) *Cell* **68**(4), 809-818
38. Valverde, M. A., Diaz, M., Sepulveda, F. V., Gill, D. R., Hyde, S. C., and Higgins, C. F. (1992) *Nature* **355**(6363), 830-833
39. Gill, D. R., Hyde, S. C., Higgins, C. F., Valverde, M. A., Mintenig, G. M., and Sepulveda, F. V. (1992) *Cell* **71**(1), 23-32
40. Velamakanni, S., Lau, C. H., Gutmann, D. A., Venter, H., Barrera, N. P., Seeger, M. A., Woebking, B., Matak-Vinkovic, D., Balakrishnan, L., Yao, Y., U, E. C., Shilling, R. A., Robinson, C. V., Thorn, P., and van Veen, H. W. (2009) *PloS one* **4**(7), e6137
41. van Veen, H. W., Callaghan, R., Soceneantu, L., Sardini, A., Konings, W. N., and Higgins, C. F. (1998) *Nature* **391**(6664), 291-295
42. Borst, P., Zelcer, N., and van Helvoort, A. (2000) *Biochimica et biophysica acta* **1486**(1), 128-144
43. Smith, A. J., Timmermans-Hereijgers, J. L., Roelofsen, B., Wirtz, K. W., van Blitterswijk, W. J., Smit, J. J., Schinkel, A. H., and Borst, P. (1994) *FEBS letters* **354**(3), 263-266
44. Bezombes, C., Maestre, N., Laurent, G., Levade, T., Bettaieb, A., and Jaffrezou, J. P. (1998) *Faseb J* **12**(1), 101-109
45. Garrigues, A., Escargueil, A. E., and Orlowski, S. (2002) *Proceedings of the National Academy of Sciences of the United States of America* **99**(16), 10347-10352
46. Luker, G. D., Nilsson, K. R., Covey, D. F., and Piwnica-Worms, D. (1999) *The Journal of biological chemistry* **274**(11), 6979-6991
47. Debry, P., Nash, E. A., Neklason, D. W., and Metherall, J. E. (1997) *The Journal of biological chemistry* **272**(2), 1026-1031
48. Luker, G. D., Dahlheimer, J. L., Ostlund, R. E., Jr., and Piwnica-Worms, D. (2001) *Journal of lipid research* **42**(9), 1389-1394
49. Eckford, P. D., and Sharom, F. J. (2006) *Biochemistry and cell biology = Biochimie et biologie cellulaire* **84**(6), 1022-1033
50. Silverman, J. A., Hayes, M. L., Luft, B. J., and Joiner, K. A. (1997) *Antimicrobial agents and chemotherapy* **41**(9), 1859-1866
51. Dubey, J. P., Lindsay, D. S., and Speer, C. A. (1998) *Clinical microbiology reviews* **11**(2), 267-299

52. Roos, D. S., Crawford, M. J., Donald, R. G., Fohl, L. M., Hager, K. M., Kissinger, J. C., Reynolds, M. G., Striepen, B., and Sullivan, W. J., Jr. (1999) *Novartis Foundation symposium* **226**, 176-195; discussion 195-178
53. Dubey, J. P., and Frenkel, J. K. (1972) *The Journal of protozoology* **19**(1), 155-177
54. Dubey, J. P. (1998) *International journal for parasitology* **28**(7), 1019-1024
55. Nichols, B. A., and O'Connor, G. R. (1981) *Laboratory investigation; a journal of technical methods and pathology* **44**(4), 324-335
56. Aikawa, M., Komata, Y., Asai, T., and Midorikawa, O. (1977) *The American journal of pathology* **87**(2), 285-296
57. Dobrowolski, J. M., and Sibley, L. D. (1996) *Cell* **84**(6), 933-939
58. Dobrowolski, J. M., Carruthers, V. B., and Sibley, L. D. (1997) *Molecular microbiology* **26**(1), 163-173
59. Joiner, K. A., Fuhrman, S. A., Miettinen, H. M., Kasper, L. H., and Mellman, I. (1990) *Science (New York, N.Y* **249**(4969), 641-646
60. Radke, J. R., and White, M. W. (1998) *Molecular and biochemical parasitology* **94**(2), 237-247
61. Carruthers, V. B., and Sibley, L. D. (1997) *European journal of cell biology* **73**(2), 114-123
62. Sibley, L. D. (2004) *Science (New York, N.Y* **304**(5668), 248-253
63. Gaskins, E., Gilk, S., DeVore, N., Mann, T., Ward, G., and Beckers, C. (2004) *The Journal of cell biology* **165**(3), 383-393
64. Jewett, T. J., and Sibley, L. D. (2003) *Molecular cell* **11**(4), 885-894
65. Fourmaux, M. N., Achbarou, A., Mercereau-Puijalon, O., Biderre, C., Briche, I., Loyens, A., Odberg-Ferragut, C., Camus, D., and Dubremetz, J. F. (1996) *Molecular and biochemical parasitology* **83**(2), 201-210
66. Wan, K. L., Carruthers, V. B., Sibley, L. D., and Ajioka, J. W. (1997) *Molecular and biochemical parasitology* **84**(2), 203-214
67. Carruthers, V. B., Giddings, O. K., and Sibley, L. D. (1999) *Cellular microbiology* **1**(3), 225-235
68. Mondragon, R., and Frixione, E. (1996) *The Journal of eukaryotic microbiology* **43**(2), 120-127
69. Carruthers, V. B., and Sibley, L. D. (1999) *Molecular microbiology* **31**(2), 421-428
70. Carruthers, V. B., Moreno, S. N., and Sibley, L. D. (1999) *The Biochemical journal* **342 (Pt 2)**, 379-386
71. Docampo, R., and Moreno, S. N. (2001) *Molecular and biochemical parasitology* **114**(2), 151-159
72. Ruiz, F. A., Marchesini, N., Seufferheld, M., Govindjee, and Docampo, R. (2001) *The Journal of biological chemistry* **276**(49), 46196-46203
73. Marchesini, N., Ruiz, F. A., Vieira, M., and Docampo, R. (2002) *The Journal of biological chemistry* **277**(10), 8146-8153
74. Sibley, L. D., Weidner, E., and Krahenbuhl, J. L. (1985) *Nature* **315**(6018), 416-419
75. Sibley, L. D., Krahenbuhl, J. L., and Weidner, E. (1985) *Infection and immunity* **49**(3), 760-764
76. Jones, T. C., Yeh, S., and Hirsch, J. G. (1972) *The Journal of experimental medicine* **136**(5), 1157-1172
77. Mordue, D. G., Desai, N., Dustin, M., and Sibley, L. D. (1999) *The Journal of experimental medicine* **190**(12), 1783-1792
78. Sibley, L. D., Krahenbuhl, J. L., Adams, G. M., and Weidner, E. (1986) *The Journal of cell biology* **103**(3), 867-874
79. Sinai, A. P., Webster, P., and Joiner, K. A. (1997) *Journal of cell science* **110 (Pt 17)**, 2117-2128
80. Trotter, P. J., and Voelker, D. R. (1994) *Biochimica et biophysica acta* **1213**(3), 241-262

81. Pingret, L., Millot, J. M., Sharonov, S., Bonhomme, A., Manfait, M., and Pinon, J. M. (1996) *J Histochem Cytochem* **44**(10), 1123-1129
82. Lund, E., Lycke, E., and Sourander, P. (1961) *British journal of experimental pathology* **42**, 357-362
83. Lavine, M. D., and Arrizabalaga, G. (2008) *Eukaryotic cell* **7**(1), 131-140
84. Kafsack, B. F., Pena, J. D., Coppens, I., Ravindran, S., Boothroyd, J. C., and Carruthers, V. B. (2009) *Science (New York, N.Y* **323**(5913), 530-533
85. Endo, T., Sethi, K. K., and Piekarski, G. (1982) *Experimental parasitology* **53**(2), 179-188
86. Moudy, R., Manning, T. J., and Beckers, C. J. (2001) *The Journal of biological chemistry* **276**(44), 41492-41501
87. Black, M. W., Arrizabalaga, G., and Boothroyd, J. C. (2000) *Molecular and cellular biology* **20**(24), 9399-9408
88. Hoff, E. F., and Carruthers, V. B. (2002) *Trends in parasitology* **18**(6), 251-255
89. Schwab, J. C., Beckers, C. J., and Joiner, K. A. (1994) *Proceedings of the National Academy of Sciences of the United States of America* **91**(2), 509-513
90. Blume, M., Rodriguez-Contreras, D., Landfear, S., Fleige, T., Soldati-Favre, D., Lucius, R., and Gupta, N. (2009) *Proceedings of the National Academy of Sciences of the United States of America* **106**(31), 12998-13003
91. Fox, B. A., Gigley, J. P., and Bzik, D. J. (2004) *International journal for parasitology* **34**(3), 323-331
92. Pfefferkorn, E. R., Eckel, M., and Rebhun, S. (1986) *Molecular and biochemical parasitology* **20**(3), 215-224
93. Schwartzman, J. D., and Pfefferkorn, E. R. (1982) *Experimental parasitology* **53**(1), 77-86
94. Krug, E. C., Marr, J. J., and Berens, R. L. (1989) *The Journal of biological chemistry* **264**(18), 10601-10607
95. Fox, B. A., and Bzik, D. J. (2002) *Nature* **415**(6874), 926-929
96. Crawford, M. J., Thomsen-Zieger, N., Ray, M., Schachtner, J., Roos, D. S., and Seeber, F. (2006) *The EMBO journal* **25**(13), 3214-3222
97. Charron, A. J., and Sibley, L. D. (2002) *Journal of cell science* **115**(Pt 15), 3049-3059
98. Gupta, N., Zahn, M. M., Coppens, I., Joiner, K. A., and Voelker, D. R. (2005) *The Journal of biological chemistry* **280**(16), 16345-16353
99. Coppens, I., Sinai, A. P., and Joiner, K. A. (2000) *The Journal of cell biology* **149**(1), 167-180
100. Coppens, I., Dunn, J. D., Romano, J. D., Pypaert, M., Zhang, H., Boothroyd, J. C., and Joiner, K. A. (2006) *Cell* **125**(2), 261-274
101. Sauvage, V., Aubert, D., Bonhomme, A., Pinon, J. M., and Millot, J. M. (2004) *Molecular and biochemical parasitology* **134**(1), 89-95
102. Schmid, A., Sauvage, V., Escotte-Binet, S., Aubert, D., Terryn, C., Garnotel, R., and Villena, I. (2009) *Molecular and biochemical parasitology* **163**(1), 54-60
103. Sauvage, V., Millot, J. M., Aubert, D., Visneux, V., Marle-Plistat, M., Pinon, J. M., and Villena, I. (2006) *Molecular and biochemical parasitology* **147**(2), 177-192
104. Luft, B. J., Hafner, R., Korzun, A. H., Leport, C., Antoniskis, D., Bosler, E. M., Bourland, D. D., 3rd, Uttamchandani, R., Fuhrer, J., Jacobson, J., and et al. (1993) *The New England journal of medicine* **329**(14), 995-1000
105. Kouzarides, T. (2007) *Cell* **128**(4), 693-705
106. Bougdour, A., Maubon, D., Baldacci, P., Ortet, P., Bastien, O., Bouillon, A., Barale, J. C., Pelloux, H., Menard, R., and Hakimi, M. A. (2009) *The Journal of experimental medicine* **206**(4), 953-966
107. Adam, R. D. (2001) *Clinical microbiology reviews* **14**(3), 447-475
108. Lujan, H. D., Mowatt, M. R., and Nash, T. E. (1997) *Microbiol Mol Biol Rev* **61**(3), 294-304

Manuscript 1

Host Cell P-glycoprotein Is Essential for Cholesterol Uptake and Replication of *Toxoplasma gondii*

THE JOURNAL OF BIOLOGICAL CHEMISTRY VOL. 284, NO. 26, pp. 17438–17448, June 26, 2009

Host Cell P-glycoprotein Is Essential for Cholesterol Uptake and Replication of *Toxoplasma gondii*[*][S]

Received for publication, December 15, 2008, and in revised form, March 27, 2009 Published, JBC Papers in Press, April 22, 2009, DOI 10.1074/jbc.M809420200

Iveta Bottova[‡], Adrian B. Hehl[‡], Saša Štefanić[‡], Gemma Fabriàs[§], Josefina Casas[§], Elisabeth Schraner[¶], Jean Pieters[‖], and Sabrina Sonda[‡1]

From the Institutes of [‡]Parasitology and [¶]Veterinary Anatomy, University of Zurich, 8057 Zurich, Switzerland, the [§]Institut de Química Avançada de Catalunya, Consejo Superior de Investigaciones Científicas, 08034 Barcelona, Spain, and [‖]Biozentrum, University of Basel, 4056 Basel, Switzerland

P-glycoprotein (P-gp) is a membrane-bound efflux pump that actively exports a wide range of compounds from the cell and is associated with the phenomenon of multidrug resistance. However, the role of P-gp in normal physiological processes remains elusive. Using P-gp-deficient fibroblasts, we showed that P-gp was critical for the replication of the intracellular parasite *Toxoplasma gondii* but was not involved in invasion of host cells by the parasite. Importantly, we found that the protein participated in the transport of host-derived cholesterol to the intracellular parasite. *T. gondii* replication in P-gp-deficient host cells not only resulted in reduced cholesterol content in the parasite but also altered its sphingolipid metabolism. In addition, we found that different levels of P-gp expression modified the cholesterol metabolism in uninfected fibroblasts. Collectively our findings reveal a key and previously undocumented role of P-gp in host-parasite interaction and suggest a physiological role for P-gp in cholesterol trafficking in mammalian cells.

P-glycoprotein (P-gp, ABCB1, MDR1)[2] is one of the most intensively studied members of the ABC transporter superfamily. With remarkably broad substrate recognition, P-gp drives the ATP-dependent efflux of toxic metabolites and xenobiotics from the cell (1) and is thus a central mediator of drug bioavailability. Importantly, P-gp overexpression following drug treatment is responsible for the multidrug resistance (MDR) phenotype, a major reason for chemotherapy failure not only in cancer cells (2) but also in pathogenic microorganisms (3, 4). Aside from its well known role in drug efflux, P-gp is also expressed at basal levels in many different tissues, yet the normal physiological functions of the protein remain poorly understood.

* This work was supported by grants from the Marie Heim-Vögtlin Foundation, Fondation Pierre Mercier pour la Science, Roche and Novartis (to S. S.), Bundesamt für Bildung and Wissenschaft C03.0007 COST Action 857 (to A. B. H.), and the Swiss National Foundation (to J. P.).

[S] The on-line version of this article (available at http://www.jbc.org) contains supplemental Figs. S1–S6.

[1] To whom correspondence should be addressed: Institute of Parasitology, University of Zurich, Winterthurerstrasse 266a, 8057 Zurich, Switzerland. Tel.: 41-44-6358514; Fax: 41-44-6358907; E-mail: sabrina.sonda@vetparas.uzh.ch.

[2] The abbreviations used are: P-gp, P-glycoprotein; MDR, multidrug resistance; PV, parasitophorous vacuole; WT, wild type; DKO, double knock-out; PBS, phosphate-buffered saline; CD, methyl-β-cyclodextrin; HDL, high density lipoprotein(s); p.i., post-infection; H.O.S.T., host organelle-sequestering tubulo-structures; apoA-I, apolipoprotein A-I.

The possibility that physiological levels of host P-gp play a role in host-pathogen interaction, other than mediating drug resistance, has not been investigated so far. We addressed this question using *Toxoplasma gondii* as a model pathogenic parasite. *T. gondii* is the causative agent of toxoplasmosis, a potentially fatal disease not only for immunocompromised patients and fetuses but according to recent insights also emerging as a life threatening infection in immunocompetent individuals (5). *T. gondii* infects virtually all nucleated host cells and resides in a highly specialized vacuole, called the parasitophorous vacuole (PV), which is formed by invaginating the host cell membrane at the time of invasion. The PV is not competent for lysosome fusion, thus avoiding acidification (6), but it is closely associated with host organelles, including lysosomes, mitochondria, and endoplasmic reticulum (reviewed in Ref. 7). Even though the PV does not intersect directly with host vesicular traffic, *T. gondii* remains dependent on host cells for a number of critical nutrients. Significant progress has been made in our understanding of the mechanisms *T. gondii* uses to scavenge nutrients from its host, especially in the case of lipid molecules. An important recent example was the identification of H.O.S.T. (host organelle-sequestering tubulo-structures), a unique system of tubular structures formed by the parasite to sequester cholesterol-containing endolysosomes from the host cytoplasm into the PV (8). However, the molecular mechanisms of the traffic from the host cell to the PV are not completely elucidated, and the existence of transporters has been proposed frequently.

To analyze whether the P-gp transporter plays a role in *T. gondii* biology we compared parasite replication in wild type (WT) mouse embryonic fibroblasts with double knock-out (DKO) fibroblasts in which neither of the two murine P-gp isoforms are expressed (9). In parallel, we also analyzed DKO cells complemented with the human P-gp homologue (DKO/P-gp) (10), which restored P-gp functionality to DKO cells and allowed P-gp expression levels higher than those found in WT cells (supplemental Fig. S1). In this way, our model did not depend on either drug-selected P-gp-overexpressing cells, which may acquire adaptation mechanisms different from P-gp overexpression during the development of the MDR phenotype, or P-gp inhibitors, several of which are known to have side effects on host metabolism.

EXPERIMENTAL PROCEDURES

Biochemical Reagents—Unless otherwise stated, all chemicals were purchased from Sigma, cell culture reagents were

Supplemental Material can be found at:
http://www.jbc.org/content/suppl/2009/04/23/M809420200.DC1.html

from Invitrogen, and radiolabeled lipids were from Amersham Biosciences. Anti-P-gp monoclonal antibody C219 was purchased from Alexis Biochemicals; anti-Lamp1 1D4B antibody was obtained through the Developmental Studies Hybridoma Bank (University of Iowa, Iowa City, IA); anti-giantin and anti-tubulin were a kind gift from J. Rohrer and M. A. Hakimi, respectively. Conjugated secondary antibodies were from Invitrogen. Reconstituted high density lipoproteins and apolipoprotein A-I (apoA-I) were a kind gift from P. Lerch (CSL Behring, Bern, Switzerland). NDB-cholesterol was from Avanti Polar Lipids.

Mammalian Cell and Parasite Culture—Mouse embryonic fibroblasts double knocked out for P-gp (77.1, Mdr1a$^{-/-}$/Mdr1b$^{-/-}$) (9), triple knocked out for P-gp and MRP1 (3.8, Mdr1a$^{-/-}$/Mdr1b$^{-/-}$/Mrp1$^{-/-}$) (11) and parental cells were kindly provided by A. Schinkel (The Netherlands Cancer Institute, Amsterdam, The Netherlands). Mdr1 transfected 77.1 (10) and G185 NIH 3T3 fibroblasts (12) were a generous gift from M. M. Gottesman (National Cancer Institute, National Institutes of Health, Bethesda, MD).

The cells were routinely cultured in Dulbecco's modified Eagle's medium supplemented with 10% fetal calf serum, 2 mM glutamine, 50 units of penicillin/ml, and 50 μg of streptomycin/ml at 37 °C with 5% CO_2. Mdr1 transfected 77.1 and G185 cells were maintained in 20 and 60 ng/ml colchicine, respectively. Colchicine was removed from the culture medium during parasite infection.

β-Galactosidase expressing *T. gondii* and *Neospora caninum* were a kind gift from J. Boothroyd and D. Sibley, respectively. The parasites were maintained by serial passages in mouse embryonic fibroblasts, harvested from infected host cells by passage through a 26-gauge needle, and purified by separation on Sephadex-G25 columns (Amersham Biosciences) as described (13). Purified parasites were counted in a hemocytometer chamber and used for a new cycle of host cell invasion at the multiplicity of infection of 1. Parasite burden was quantified after 24 h by direct parasite counting or after 48 or 72 h by colorimetric detection of parasite β-galactosidase using chlorophenol red-β-D-galactopyranoside as substrate, as described (14). In some experiments, parasite quantification in infected host cells was performed by flow cytometry analysis on a FACSCalibur flow cytometer (Becton Dickinson), after staining permeabilized cells with a rabbit polyclonal anti-*T. gondii* tachyzoite antiserum (15) at 1:2000 dilution, followed by fluorescein-conjugated anti-rabbit secondary antibody at 1:300 dilution. Parasite invasion was determined by dual color immunostaining with the described anti-*T. gondii* antiserum to differentiate intracellular and extracellular parasites, as described (16).

Lipid Analyses—For cholesterol transport to intracellular *T. gondii*, infected host cells were labeled with 0.5 μCi/ml [^{3}H]cholesterol for 5 h. After extensive washing with PBS and 0.05% fat-free bovine serum albumin in PBS, parasites were isolated as previously described and counted, and the associated radioactivity was measured by liquid scintillation. Background radioactivity resulting from host cell debris was determined using similarly processed uninfected host cells and subtracted from parasite samples.

For cholesterol uptake analysis, host cells were incubated with 0.5 μCi/ml [^{3}H]cholesterol for 5 h and extensively washed, and cell-associated radioactivity was measured by liquid scintillation. Steady state cholesterol mass was assessed using the Amplex Red kit (Invitrogen) or by lipid extraction according to Bligh and Dyer (17) and high performance thin layer chromatography separation of aliquots corresponding to equal protein content on Silica Gel 60 plates in benzene/2-propanol/water (100:10:0.25). The bands were visualized with 10% $CuSO_4$ in 8% aqueous phosphoric acid and quantified by densitometry.

Liquid chromatography-mass spectrometry analysis of lipids from *T. gondii* grown in WT or DKO host cells was performed as described (18) in a Waters Aquity UPLC system connected to a Waters LCT Premier orthogonal accelerated time of flight mass spectrometer (Waters, Millford, MA), operated in positive electrospray ionization mode.

For analysis of sphingolipid synthesis in *T. gondii*, purified parasites were labeled with 0.5 μCi/ml [^{3}H]palmitic acid for 3 h, lipids were extracted as before and aliquots corresponding to equal protein content were separated by high performance thin layer chromatography using chloroform/methanol/25% NH_4OH (65:25:4.5). Radiolabeled bands were visualized by use of a tritium-sensitive screen (PerkinElmer Life Sciences) in a Personal Molecular PhosphoImager FX (Bio-Rad), identified according to co-migrating standards visualized by iodine vapors and quantified using ImageQuant software (Amersham Biosciences).

For kinetic of cholesterol esterification, host cells were labeled with 0.5 μCi/ml [^{3}H]cholesterol for 5, 24, and 48 h, and lipids were extracted as before and separated by high performance thin layer chromatography using benzene/2-propanol/water (100:10:0.25) as a solvent system. After iodine vapor visualization, bands co-migrating with cholesterol and cholesteryl ester standards were cut out of the plates, and the associated radioactivity was measured by liquid scintillation. The data for cholesterol esterification are reported as a percentage of [^{3}H]cholesteryl esters from total cellular [^{3}H]cholesterol.

For cholesterol extraction with methyl-β-cyclodextrin (CD) and efflux to reconstituted high density lipoproteins (HDL) or apoA-I, the cells were labeled with 0.5 μCi/ml [^{3}H]cholesterol for 24 h, extensively washed, and incubated with 2 mM CD, 20 μg/ml reconstituted HDL, or 10 μg/ml apoA-I in medium without fetal calf serum. Medium aliquots were measured by liquid scintillation at the time points indicated in the figures. Residual cell radioactivity was measured after cell solubilization in 0.1 N NaOH. Total radioactivity was calculated as medium + cell-associated radioactivity. Background efflux to medium alone was measured at the same time points and subtracted from the values obtained with the cholesterol acceptors CD, reconstituted HDL, and apoA-I.

Cholesterol Visualization and Immunofluorescence Analysis—To visualize intracellular transport of fluorescent cholesterol, host cells were seeded on glass slides and infected with *T. gondii* for 24 h. The cells were incubated with 5 μM NBD-cholesterol in Dulbecco's modified Eagle's medium without fetal calf serum for 1 h at 37 °C, fixed in 3% formaldehyde, mounted in Vectashield antifade agent (Vector Laboratories, Inc., Burlingame, CA), and imaged employing an excitation filter of 450–500 nm.

For visualization of unesterified cholesterol, the cells were seeded as before, fixed, and incubated with 0.05 mg/ml filipin in PBS, 10% fetal calf serum for 1 h at room temperature. The images were collected using an excitation filter of 350–410 nm. For visualization of esterified cholesterol in intracellular lipid droplets, the cells were fixed with 3% formaldehyde, blocked, and stained with Nile red at a concentration of 0.5 μg/ml in PBS for 20 min. The cells were extensively washed in PBS and mounted, and lipid fluorescence was analyzed employing an excitation filter of 450–500 nm.

For P-gp localization, DKO/Pgp host cells grown on glass slides were infected with *T. gondii* for 24 h, prior to fixation in acetone at −20 °C for 10 min. Anti-P-gp monoclonal antibody C219 was used at 1:10 dilution according to the manufacturer's instruction, followed by fluorescein-conjugated secondary antibody at 1: 200 dilution. *T. gondii* was stained with a rabbit polyclonal anti-*T. gondii* tachyzoite antiserum (15) at 1:2000 dilution, followed by Texas Red-conjugated anti-rabbit secondary antibody at 1:300 dilution. The nuclei were visualized with 4′,6-diamidino-2-phenylindole.

For endo-lysosome localization, host cells grown on glass slides were infected with *T. gondii* or *N. caninum* for 24 h, incubated with 6 μg/ml fluorescein-conjugated cholera toxin B subunit for 60 min at 37 °C, and analyzed after fixation. For lysosome and Golgi localization, cells were seeded as before, fixed, and stained with anti-Lamp1 (1:50) or anti-giantin (1:750) antibodies followed by fluorescein-conjugated secondary antibody.

Microscopy analyses were performed on a Leica DM IRBE fluorescence microscope or on a Leica SP2 AOBS confocal laser-scanning microscope (Leica Microsystems, Wetzlar, Germany), using the appropriate settings. Image stacks of optical sections were further processed using the Huygens deconvolution software package version 2.7 (Scientific Volume Imaging, Hilversum, NL).

Transmission Electron Microscopy Analysis—Host cells grown on sapphire disks were infected with *T. gondii* and incubated at 37 °C for 24 h, prior to fixation with 0.25% glutaraldehyde and freezing in a high pressure freezing machine (HPM 010, BAL-TEC) as described by Monaghan *et al.* (19). Frozen cells were transferred into a freeze substitution unit (FS 7500, Boeckeler Instruments, Tucson, AZ) precooled to −88 °C for substitution with acetone and subsequent fixation with 0.25% glutaraldehyde and 0.5% osmium tetraoxide at temperatures between −30 °C and +2 °C as described in detail (20) and embedded in Epon. 50–60-nm-thick sections were stained with uranyl-acetate and lead-citrate and analyzed in a transmission electron microscope (CM12; Philips, Eindhoven, The Netherlands) equipped with a CCD camera (Ultrascan 1000; Gatan, Pleasanton, CA) at an acceleration voltage of 100 kV.

Cell Viability Following Cholesterol Loading—Host cells were loaded with cyclodextrin-cholesterol complexes (Sigma) for 24 h at the concentrations indicated in the figure legend, washed in medium, and incubated at 37 °C for additional 24 h. Cell viability was tested by using the AlamarBlue® assay (BIOSOURCE, Camarillo, CA), according to the manufacturer's instructions.

P-glycoprotein Functional Assay—P-gp activity was assessed by cellular retention of the P-gp substrate rhodamine 123 (Rho). Briefly, the cells were incubated with 0.5 μg/ml Rho in PBS for 30 min at 37 °C, washed in PBS, and incubated in medium at 37 °C for the time points indicated in the figure legend. The kinetic of rhodamine retention was quantified by flow cytometry.

Western Blot Analysis—Cell lysates for immunoblots were prepared by sonicating cells at 10^7/ml in 50 mM Tris-HCl (pH 6.8), 10% glycerol, 2% SDS, 5 mM dithiothreitol, 0.5 mM phenylmethylsulfonyl fluoride, and complete protease inhibitor mixture (Calbiochem). Samples corresponding to 40 μg proteins were mixed with SDS-PAGE loading buffer and incubated 10 min at room temperature to prevent P-gp aggregation. The samples were separated on 7.5% SDS-PAGE gels, transferred to nitrocellulose membranes, and probed using anti-P-gp C219 (1:50) and anti-tubulin (1:2000) monoclonal antibodies. Immunoreactive bands were visualized with horseradish peroxidase-conjugated secondary antibodies and ECL.

Determination of Protein Concentration—Protein content was determined using the Bio-Rad Protein Assay according to the instructions provided by the manufacturer. Bovine serum albumin was used for the standard curve.

Statistical Analyses—The data are expressed as the means ± S.E. One-way analysis of variance was performed (GraphPad Prism 4.0c; GraphPad Software, Inc.), and a probability value $<$ 0.05 was considered statistically significant. When the overall probability value was $<$ 0.05, the Dunnett multiple-comparisons test was used as a post-test to determine whether there was a significant difference between values of control (reference sample) and samples of interest.

RESULTS

Host Cell P-gp Is Essential for Normal Parasite Replication—To determine whether the activity of host P-gp plays a role in parasite replication, host cells expressing different levels of the protein (supplemental Fig. S1) were infected with *T. gondii* expressing β-galactosidase, which allows parasite quantification by colorimetric reaction (21). Direct parasite count at 24 h post-infection (p.i.) revealed the presence of smaller vacuoles containing fewer parasites in P-gp-deficient host cells (Fig. 1*A*). Importantly, complementation of P-gp-deficient cells with the human P-gp homologue fully restored parasite replication. Analysis of parasite burden by visualization of parasite vacuoles at 48 h p.i. (Fig. 1*B*) and colorimetric reaction at 48 and 72 h p.i. (Fig. 1*C*) confirmed that *T. gondii* replication was strongly inhibited in the absence of host P-gp. In addition, P-gp-complemented host cells generated a higher *T. gondii* burden than that found in WT cells. To further confirm that P-gp activity confers a replication advantage for the parasite, we used WT 3T3 fibroblasts transfected to overexpress P-gp as host cells (12). Parasite quantification was performed either at the level of single host cells using flow cytometry or as parasite burden of the whole host cell monolayer by colorimetric reaction (supplemental Fig. S2). Both analyses indicated a positive correlation between P-gp expression levels and parasite replication. Absence of the multidrug transporter MRP1, in addition to the two P-gp isoforms (triple KO cells) (11), did not further

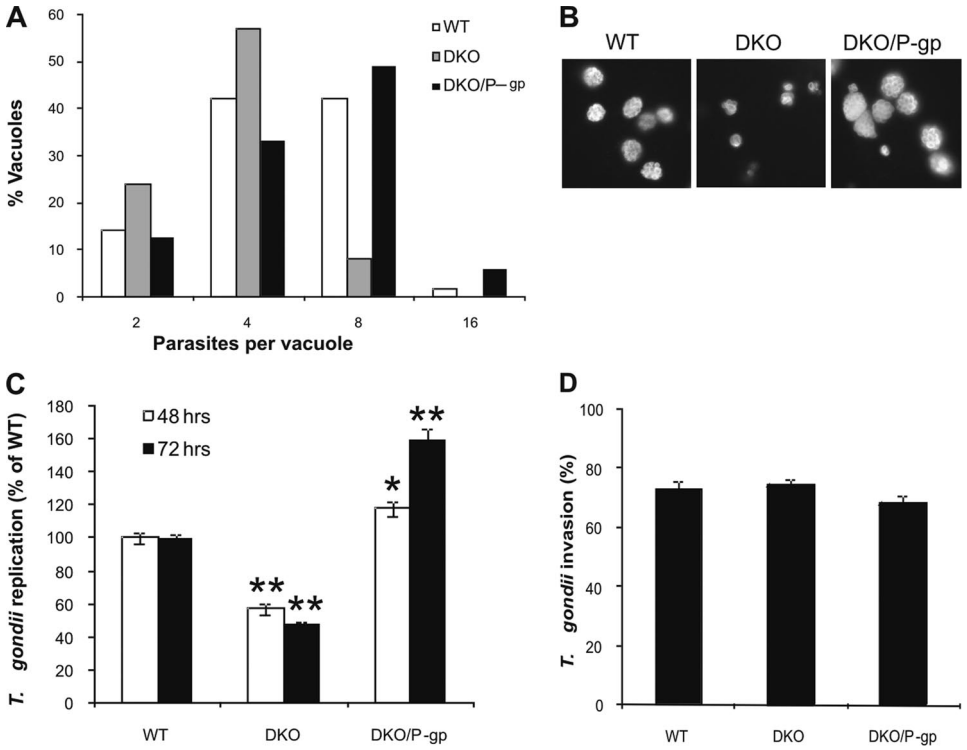

FIGURE 1. **Host cell P-gp modulates parasite replication.** *A*, WT, P-gp-deficient (DKO) and P-gp-complemented (DKO/P-gp) host cells were infected with *T. gondii* at multiplicity of infection 1. After 24 h p.i., intracellular parasites were quantified by direct counting. The distribution of the parasite number in single vacuoles is expressed as percentage of total vacuoles examined ($n > 30$). *B*, immunofluorescence analysis of intracellular vacuoles containing parasites at 48 h p.i. using anti-*T. gondii* serum, followed by fluorescein-conjugated secondary antibodies. *C*, quantification of parasite burden at 48 and 72 h p.i. by a colorimetric assay measuring the amount of parasite-expressed β-galactosidase. The results are expressed as percentages of parasite number in WT host cells ± S.E. ($n = 6$). *, $p < 0.05$; **, $p < 0.01$. *D*, host cell monolayers were incubated with *T. gondii* at a multiplicity of infection of 1. After 2 h of incubation, 20 fields of infected cells were examined, and the number of intracellular invaded parasites was determined as described under "Experimental Procedures." The data are expressed as percentages of total parasite number ± S.E. ($n = 20$).

decrease parasite replication (data not shown). Collectively, these data unambiguously show that the presence of an active P-gp in the host is directly involved in a process controlling *T. gondii* replication.

Host Cell P-gp Is Not Involved in Parasite Invasion—The reduction in parasite number seen in P-gp-deficient cells could have resulted from either decreased parasite replication or decreased invasion efficiency. To assess whether the absence of P-gp on the host plasma membrane compromises the ability of *T. gondii* to enter host cells, an invasion assay was performed using parasites harvested from WT host cells and allowed to infect cells expressing different levels of P-gp. The number of intracellular parasites was comparable in all tested cell lines at 2 h post-infection (Fig. 1*D*), indicating that host P-gp is not required for parasite invasion and that the reduced parasite burden observed in DKO cells is not due to a defect in host cell entry.

Host Cell P-gp Deficiency Inhibits Cholesterol Transport to T. gondii—The reduced parasite replication observed in P-gp-deficient host cells led us to hypothesize that the absence of P-gp may disturb the supply of lipid components necessary for assembly of new parasite membranes. To test this hypothesis, we evaluated cholesterol trafficking and metabolism in the parasite, because *T. gondii* is auxotrophic for cholesterol and depends solely on the host for its supply (22). When we tested the transport of exogenous radiolabeled cholesterol to the parasite, we found that in the absence of host P-gp, cholesterol delivery was strongly reduced (Fig. 2*A*). Importantly, P-gp DKO cells showed normal uptake of exogenous cholesterol (supplemental Fig. S3), indicating that the reduced cholesterol transport to the parasite is not caused by a compromised uptake of this lipid by the host cells. In addition, the increased *T. gondii* replication in P-gp-complemented host cells coincided with enhanced cholesterol delivery to the parasites, suggesting that the level of cholesterol transport was regulating parasite replication rate.

In addition, we monitored the cholesterol transport *in vivo* by using the fluorescently labeled analogue NBD-cholesterol (Fig. 2*B*). Similar to the observations during the radiolabeled cholesterol incubation, transport of NBD-cholesterol to parasites grown in DKO cells was reduced compared with WT cells and a pattern of punctuated structures, reminiscent of endocytic vesicles, accumulated around the parasite vacuoles. Conversely, parasites infecting P-gp-complemented cells showed high level of fluorescence, indicating a robust trafficking of cholesterol to the vacuole.

To test whether decreased cholesterol availability in the absence of host P-gp was directly responsible for the reduced *T. gondii* replication, we evaluated the parasite burden in DKO cells loaded with exogenous cholesterol following infection. This treatment improved parasite replication in a dose-dependent manner (Fig. 2*C*), confirming that insufficient cholesterol availability was indeed the limiting factor for parasite replication.

To investigate the mechanism of P-gp involvement in the cholesterol trafficking to *T. gondii*, we inhibited the vesicular transport of host cholesterol from lysosomes to both plasma membrane and endoplasmic reticulum with the class 2 amphiphile U-18666A (23). Treatment with U-18666A has been shown to decrease the cholesterol delivery to intracellular parasites (22). This broad inhibition of cholesterol trafficking severely affected *T. gondii* replication in WT host cells, with higher levels of inhibition than the ones observed in P-gp defective cells (Fig. 2*D*). On the other hand, parasite replication in DKO cells was further inhibited by only 10% upon U-18666A treatment. The absence of a significant cumulative effect between the lack of P-gp and inhibitor treatment indicates that P-gp may operate, directly or indirectly, on a similar pathway of cholesterol trafficking that is essential for parasite replication.

Supplemental Material can be found at:
http://www.jbc.org/content/suppl/2009/04/23/M809420200.DC1.html

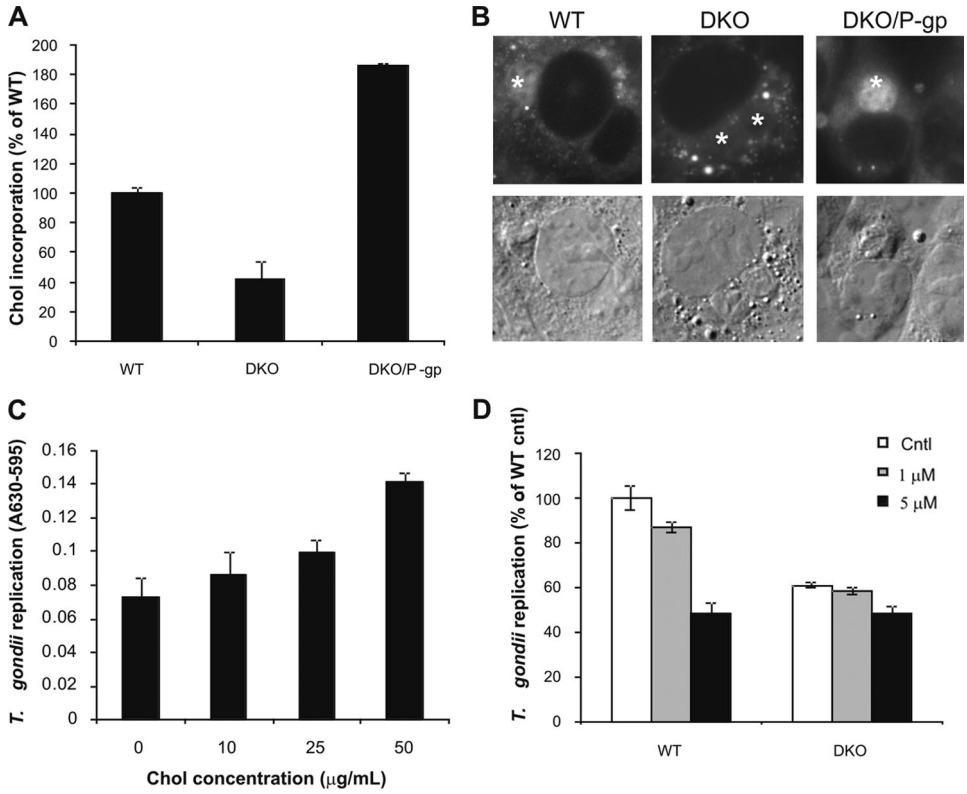

FIGURE 2. **Host cell P-gp deficiency inhibits cholesterol transport to *T. gondii*.** *A*, *T. gondii*-infected host cells were labeled for 5 h with 0.5 μCi/ml [^{3}H]cholesterol. The parasites were isolated, and [^{3}H]cholesterol incorporation was measured by liquid scintillation. The data are expressed as percentages of cholesterol in parasites (dpm/10^6 parasites) isolated from WT host cells $\pm$ S.E. ($n = 6$). *B*, host cell monolayers were infected with *T. gondii* for 24 h followed by incubation with NBD-cholesterol and observed by fluorescence microscopy. The *asterisks* indicate parasite vacuoles. *C*, after *T. gondii* invasion, DKO host cells were loaded with the indicated concentrations of cyclodextrin-cholesterol complexes, and parasite replication was monitored at 48 h p.i. as described in the legend to Fig. 1. The data are averages $\pm$ S.E. ($n = 3$). *D*, after *T. gondii* infection, WT and DKO host cells were treated with the class 2 amphiphile U-18666A at the indicated concentrations, and parasite replication was quantified at 48 h p.i. The results are expressed as percentages of parasite number in untreated (*Cntl*) WT cells. The data are averages $\pm$ S.E. ($n = 6$).

P-gp Associates with the Parasite Vacuole—Our previous results suggest that P-gp may be involved in the cholesterol trafficking to the parasite via the endocytic pathway. To investigate this possibility, we localized host P-gp in infected cells. P-gp is mainly present in the plasma membrane of the cells, but a minority also localizes in intracellular compartments, including endo-lysosomes (24, 25). Because endo-lysosomes have been shown to be recruited to the PV in *T. gondii* infected cells (8), we reasoned that P-gp also associates with the parasite vacuole. To test this hypothesis, we infected P-gp-complemented host cells, whose level of P-gp expression allows analysis by immunofluorescence using the P-gp specific monoclonal antibody C219 (supplemental Fig. S1). This analysis showed that P-gp was predominantly present on the host plasma membrane as expected. In addition, P-gp was also found closely associated with the PV (Fig. 3, *A* and *B*).

Host Organelles Are Recruited to the PV in the Absence of Host P-gp—*T. gondii* scavenges cholesterol from host endo-lysosomal compartments (22), and these organelles are actively recruited by the parasite to the PV in a time-dependent manner after infection (8). To test whether the decreased cholesterol delivery to the parasite in P-gp-deficient cells was due to a failure in recruiting the cholesterol rich endo-lysosomes, we probed the localization of these organelles in infected cells (Fig. 3*C*). First we analyzed the labeling of endocytic vesicles using cholera toxin B-subunit, which binds to the raft-associated sphingolipid GM1 and enters the cell by retrograde transport in the secretory pathway (26). Cholera toxin-positive structures were equally found around the PV of parasites infecting WT, DKO, and P-gp-complemented host cells. Moreover, Lamp1 (lysosome-associated membrane protein 1) staining further confirmed that lysosomes are recruited to the PV in DKO cells. Finally, host Golgi, which was previously shown to redistribute at the PV (8), was also found close to the PV surface in all tested cell lines. Collectively, our results show that the absence of host P-gp does not inhibit the parasite-mediated recruitment of host organelles to the PV.

Cholesterol Accumulates outside the PV in the Absence of Host P-gp—Despite the normal recruitment of lysosomes around the PV in DKO host cells, the accumulation of NBD-cholesterol observed in this cell type (Fig. 2*B*) prompted us to analyze whether the intracellular distribution of endogenous cholesterol is altered in absence of host P-gp. Staining of unesterified cholesterol with the poliene antibiotic filipin (27) in infected WT cells showed labeling of parasite membranes and perinuclear vesicular structures, previously reported to be endo-lysosomal compartments (Fig. 4*A*). On the contrary, in DKO cells the filipin-positive vesicular structures were bigger and more intensely labeled and accumulated outside the PV. Importantly, P-gp complementation prevented the cholesterol accumulation, indicating that the cholesterol accumulation is P-gp-dependent.

Inhibition of Cholesterol Transport to the Parasite Vacuole Does Not Depend on H.O.S.T. Formation—Next we assessed whether the defective transport of cholesterol to the parasite resulted from a faulty formation of the H.O.S.T. system, a recently described structure that can supply the parasite with cholesterol contained in host endo-lysosomes (8). Analysis by electron microscopy found normal recruitment of host organelles to the PV, including mitochondria, both in WT and DKO host cells (Fig. 4*B*, *arrowheads*). Importantly, parasites grown in DKO host cells were able to form H.O.S.T. structures with clearly visible tubules and vesicles (Fig. 4*B*, *arrows* and *magnified images*). Thus, host P-gp is not required for the formation of structurally normal parasite vacuoles. In this respect, the observed inhibition of cholesterol transport despite the for-

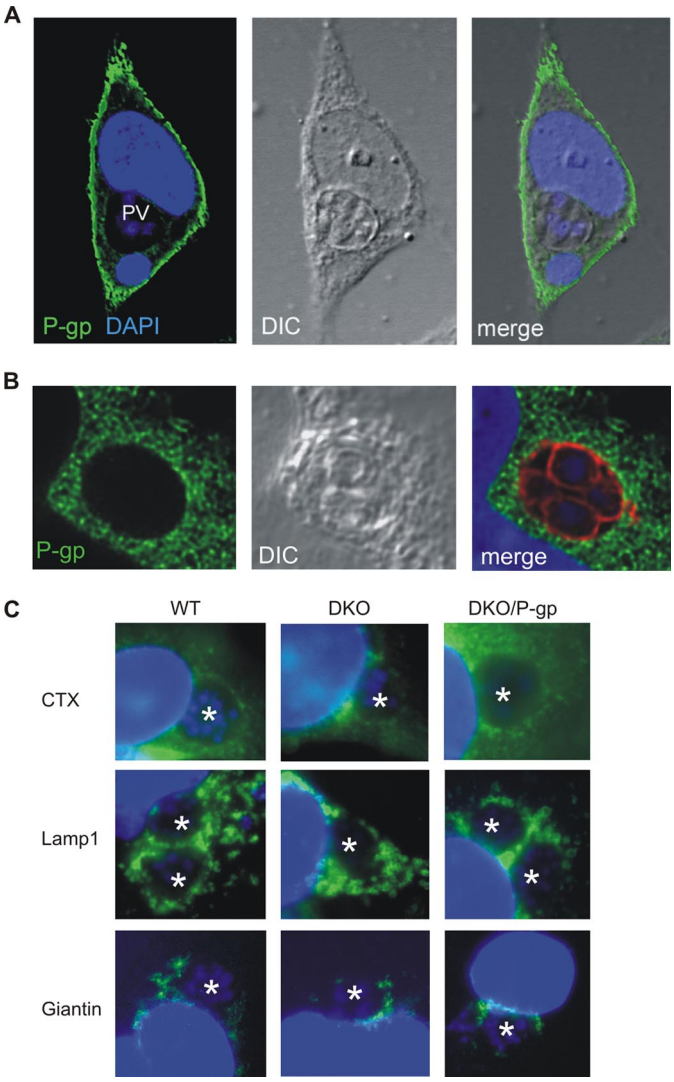

FIGURE 3. **Host P-gp associates with the parasite vacuole.** *A*, confocal microscopy of P-gp localization in P-gp-complemented (DKO/Pgp) cells infected for 24 h with *T. gondii*. Nuclear DNA was stained with 4′,6-diamidino-2-phenylindole (*DAPI*). PV, parasitophorous vacuole. *DIC*, differential interference contrast image. *B*, confocal microscopy of infected cells as described for *A*, showing P-gp (*green*) and parasite (*red*) staining. *C*, fluorescence microscopy of infected WT, P-gp-deficient (DKO) and P-gp-complemented (DKO/P-gp) host cells showing that *T. gondii* PV associated with labeled host endo-lysosomes (cholera toxin (*CTX*)), lysosomes (Lamp1), and Golgi (giantin). The *asterisks* indicate parasite vacuoles.

mation of H.O.S.T. suggests that either P-gp acts at a later stage than the development of these structures, or it affects a H.O.S.T.-independent mechanism of cholesterol delivery. To test the latter hypothesis, we analyzed the replication of *N. caninum*, an apicomplexan parasite related to *T. gondii* whose intracellular vacuoles recruit host endo-lysosomes (supplemental Fig. S4) but are devoid of H.O.S.T (8). As with *T. gondii*, *N. caninum* replication was inhibited in absence of host P-gp and could be rescued by P-gp complementation (Fig. 4*C*). In addition, *N. caninum* growth in DKO host cells resulted in decreased free cholesterol content and cholesteryl ester storage in lipid droplets (Fig. 4*D*), suggesting that P-gp-mediated cholesterol supply to the parasite operates via a mechanism independent of the H.O.S.T. system found in the PV.

Host Cell P-gp Deficiency Affects T. gondii Sphingolipid Metabolism—Our previous results showed that cholesterol transport to the parasite is defective in P-gp-deficient host cells. We then investigated whether this impaired transport affected the lipid content of the parasite. Lipid analyses of *T. gondii* maintained in DKO host cells revealed that the steady state of cholesterol content was comparable with WT after one lysis passage (23 ± 1.6 μg/mg protein) but decreased after prolonged growth in these cells (four lysis passages) (Fig. 5*A*). Similar to the observations in *N. caninum*, a marked decrease in cholesteryl esters stored in lipid droplets was observed in parasites isolated from DKO cells (supplemental Fig. S5).

Because cholesterol is an important regulator of membrane fluidity, membrane domains and signaling processes (reviewed in Ref. 28), we investigated whether the reduced cholesterol content observed in *T. gondii* grown in DKO host cells affected the lipid profile of the parasite membranes. Unexpectedly, liquid chromatography-mass spectrometry analysis of parasite sphingolipids revealed a considerably higher amount of ceramide, ceramide phosphatidylethanolamine, sphingomyelin, and lactosylceramide, whereas the levels of glucosylceramide did not change (Fig. 5*B*). Given the crucial role of ceramide in cell physiology both as a precursor of complex sphingolipids and as a second messenger regulating a variety of cellular processes (reviewed in Ref. 29), we analyzed whether neosynthesis of this lipid was up-regulated in *T. gondii* grown in DKO host cells. Metabolic labeling of extracellular parasites revealed that ceramide synthesis was higher in *T. gondii* isolated from DKO host cells after four lysis passages than in WT cells (Fig. 5*C*), supporting the hypothesis that the higher ceramide levels observed are indeed an active response of the parasite. These results suggest that reduced cholesterol availability triggers compensatory mechanisms in *T. gondii*, presumably to adapt to the intracellular environment of DKO cells and/or to adjust the lipid composition of its membranes.

Absence of P-gp Alters Normal Cholesterol Metabolism in Uninfected Fibroblasts—The observed inhibition of cholesterol transport to the parasite and the accumulation of cholesterol-loaded organelles around the PV in P-gp-deficient host cells prompted us to analyze whether P-gp is also involved in cholesterol trafficking in uninfected host cells. To test this hypothesis, we investigated whether P-gp expression levels correlated with alterations in cholesterol metabolism in fibroblasts. Analysis of intracellular cholesterol distribution visualized with filipin revealed that P-gp DKO cells accumulated cholesterol in perinuclear vesicles compared with WT and P-gp-complemented cells (Fig. 6*A*). In addition, despite comparable uptake of radiolabeled cholesterol (supplemental Fig. S3), DKO cells showed a time-dependent increase in cholesterol esterification compared with WT cells (Fig. 6*B*). On the other hand, P-gp complementation of DKO cells lowered the levels of cholesterol esterification. This correlation between the absence of P-gp and increased cholesterol esterification was evident not only in the kinetics of the process, but also in the steady state cholesteryl ester content (supplemental Fig. S6). Next we evaluated cholesterol levels in the plasma membrane by extraction with CD or efflux to the extracellular acceptors

reconstituted HDL (30) and apoA-I. We found that less cholesterol could be extracted with CD from the plasma membrane of DKO cells and that P-gp complementation increased the level of cholesterol extraction (Fig. 6*C*). Furthermore, P-gp complementation also enhanced the ABCA1-mediated efflux of cholesterol to its natural acceptor HDL (Fig. 6*D*) and apoA-I (Fig. 6*E*). These data reveal that cells deficient in P-gp accumulated free and esterified cholesterol in perinuclear vesicular structures and cytosolic lipid droplets, respectively. On the other hand, cells expressing high levels of P-gp showed increased amounts of cholesterol in the plasma membrane, which then resulted in increased efflux to extracellular acceptors. To further test whether WT cells were more prone to accumulate free cholesterol in the plasma membrane than DKO cells, we exploited the toxicity induced by destabilizing the plasma membrane via exogenous cholesterol loading. Analysis of cell viability showed that DKO cells were minimally affected by exogenous cholesterol loading, whereas viability decreased with increasing levels of P-gp expression in WT and P-gp-complemented cells (Fig. 6*F*). As previously reported in cholesterol-loaded macrophages (31), blocking cholesterol transport from lysosomes to the plasma membrane using the hydrophobic amine U-18666A (23) prevented the cholesterol toxicity in P-gp-expressing cells but did not alter the viability of DKO cells (data not shown). Thus, these data suggest that inhibition of intracellular cholesterol transport mimics the increased survival of DKO cells during cholesterol loading.

DISCUSSION

P-gp is a unique transporter because of its broad substrate specificity, and its expression constitutes a major obstacle in the fight against multidrug-resistant tumor cells and pathogens. Yet P-gp also plays a key

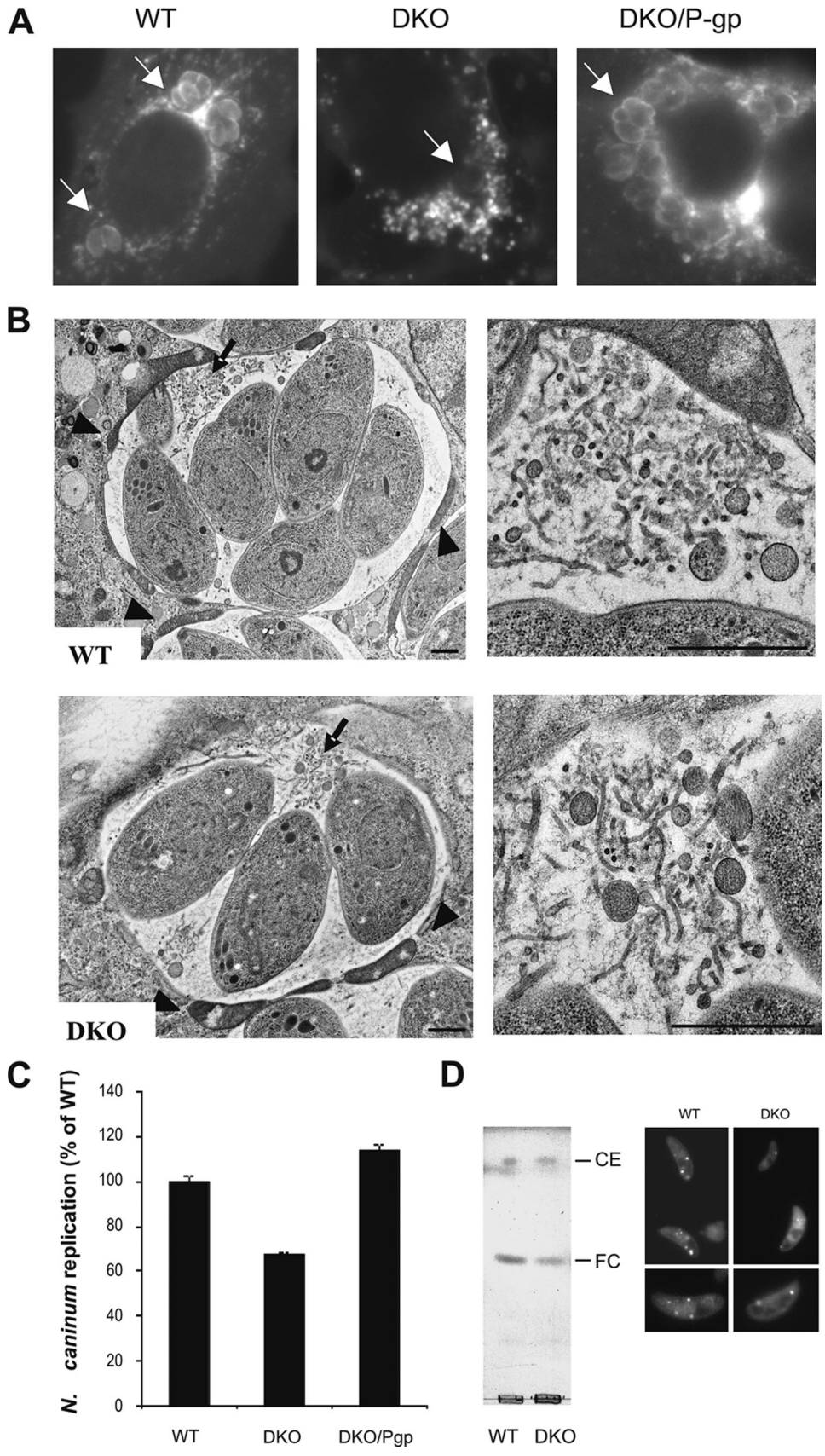

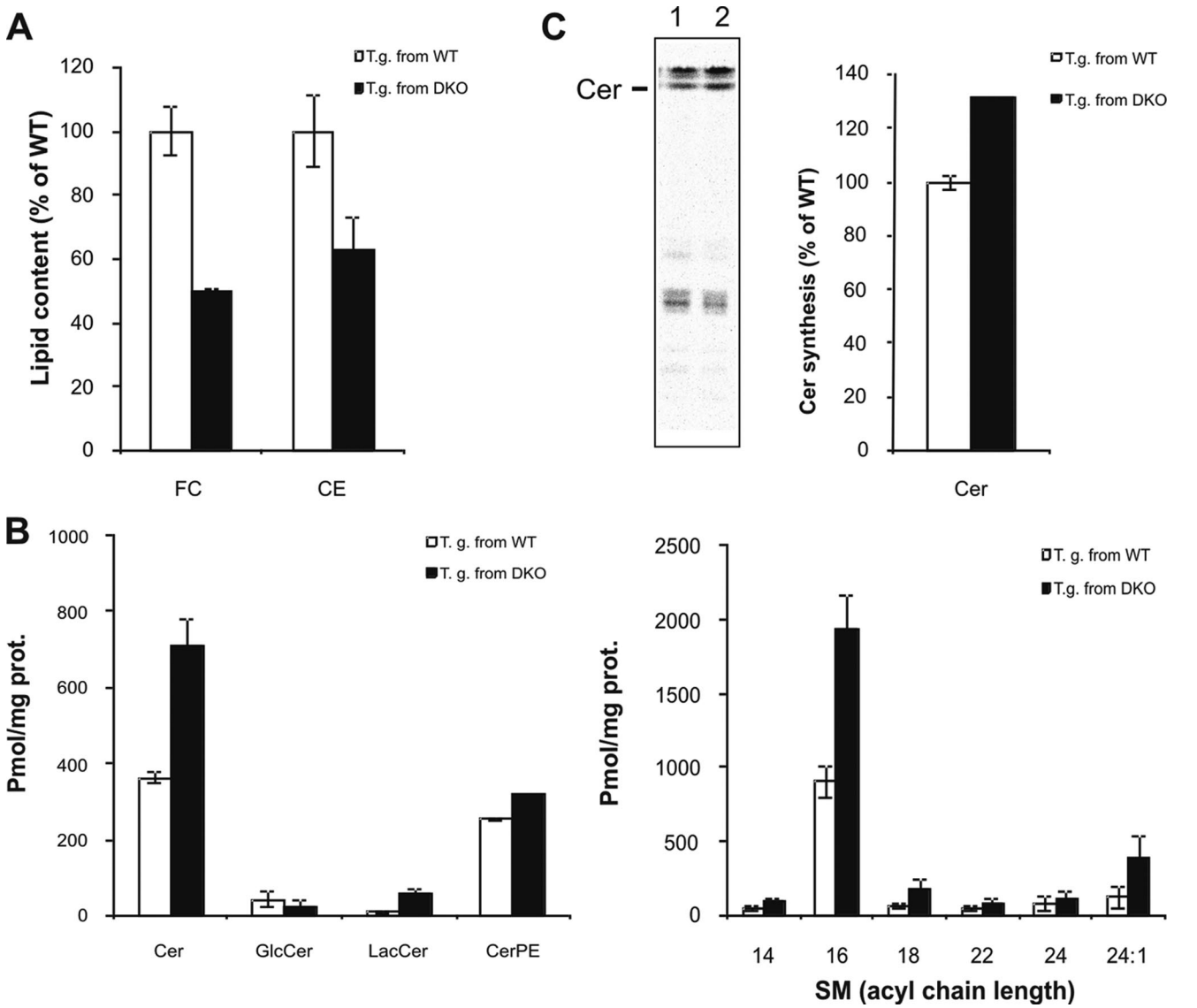

FIGURE 5. **Host cell P-gp deficiency affects *T. gondii* lipid metabolism.** *A*, quantification of free cholesterol (*FC*) and cholesteryl esters (*CE*) by enzymatic reaction (Amplex red®) in *T. gondii* isolated from WT or DKO host cells after four lysis passages. The data are expressed as percentages of lipid content in *T. gondii* from WT cells ± S.E. ($n = 5$). *B*, liquid chromatography-mass spectrometry analysis of sphingolipids of *T. gondii* isolated from WT or DKO host cells after four lysis passages. The data are averages ± S.E. ($n = 3$) of a representative from two experiments done in triplicate. *Cer*, ceramide; *GlcCer*, glucosylceramide; *LacCer*, lactosylceramide; *CerPE*, ceramide phosphoethanolamine. The predominantly detected C16 species are plotted. *SM*, sphingomyelin. *C*, *left panel*, TLC separation of *de novo* synthesized lipids labeled with [^{3}H]palmitic acid in *T. gondii* isolated from WT (1) or DKO (2) cells. *Right panel*, newly synthesized ceramide is expressed as a percentage of ceramide in *T. gondii* isolated from WT host cells. The data are averages ± S.E. ($n = 3$).

role in normal physiological processes, including preventing cellular toxicity at the blood brain barrier, as shown *in vivo* by the extremely high sensitivity of P-gp KO mice to toxic compounds (32).

Our aim was to investigate whether host P-gp plays a role in host-pathogen interaction that is distinct from multidrug resistance. Previous studies using P-gp inhibitors suggested that *T. gondii* may require a functional P-gp to survive in the host cell (33). In the present work more detailed investigation found that host P-gp is in fact a crucial modulator of *T. gondii* and *N. caninum* replication. In addition, we found that host P-gp is not a receptor for the parasite, and its absence does not affect parasite invasion or the formation of structurally normal parasite vacuoles. Importantly, we found that transport of cholesterol from the host cell to the parasites, a process on which *T. gondii* is completely dependent, was impaired in absence of

FIGURE 4. **Cholesterol accumulates outside the parasite vacuole in absence of host P-gp.** *A*, WT, P-gp-deficient (DKO), and P-gp-complemented (DKO/P-gp) host cell monolayers were infected with *T. gondii* for 24 h. After fixation, the intracellular distribution of unesterified cholesterol was visualized with filipin and observed by fluorescence microscopy. The *arrows* indicate parasite vacuoles. *B*, electron microscopy of *T. gondii* infected WT and P-gp-deficient (DKO) host cells at 24 h p.i., showing PV-associated mitochondria (*arrowheads*) and H.O.S.T. structures (*arrows*). *Right panels*, magnification of H.O.S.T. structures. *Scale bars*, 2 μm. *C*, host cells monolayers were infected with *N. caninum* and parasite replication quantified at 72 h p.i., as described. The results are expressed as percentages of parasite number in WT host cells ± S.E. ($n = 3$). *D*, lipids were extracted from *N. caninum* isolated from WT or DKO host cells after four lysis passages. A representative TLC of lipids corresponding to equal protein amount is shown. Free cholesterol (*FC*) and cholesteryl esters (*CE*) were visualized with $CuSO_4$. *Inset*, Nile red staining of cholesteryl esters-containing lipid droplets in parasites isolated from WT or DKO host cells after four lysis passages.

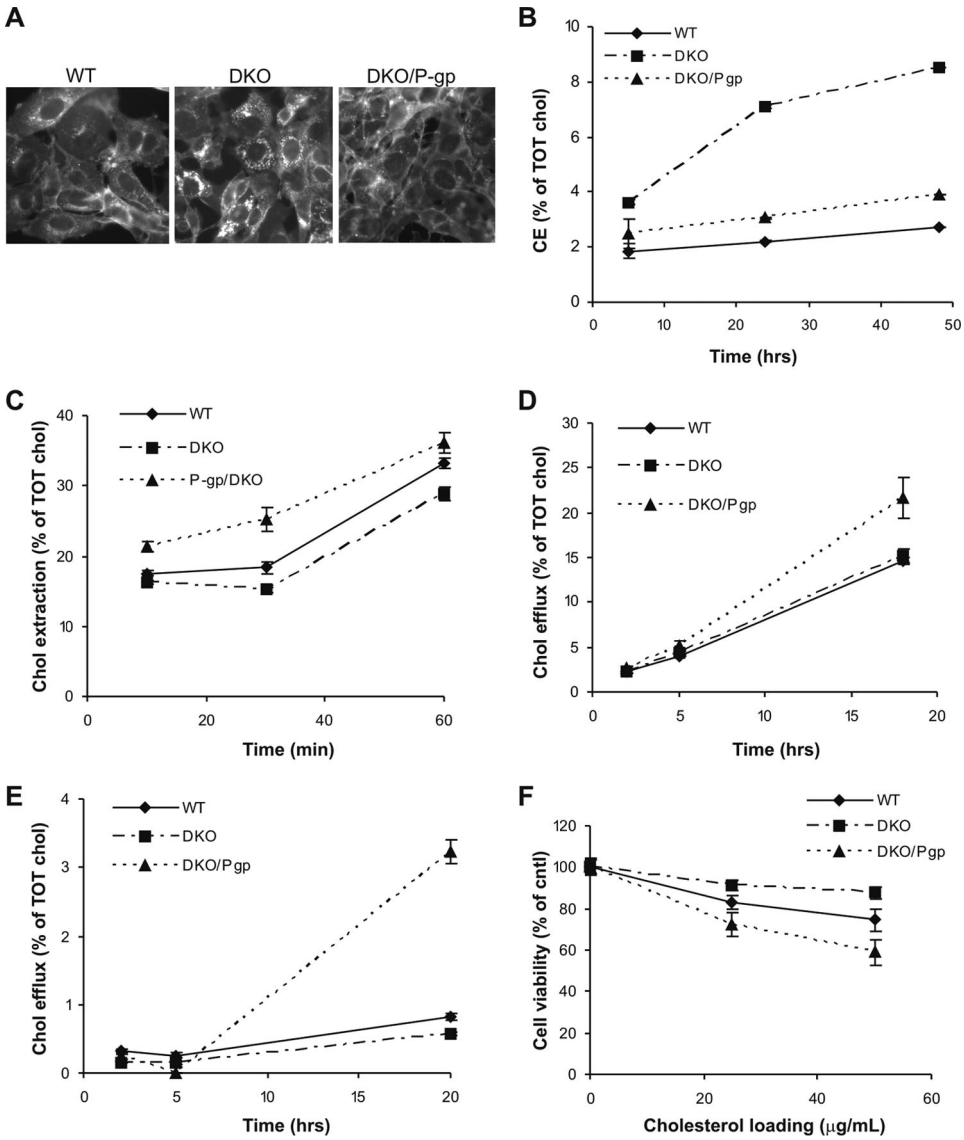

FIGURE 6. **P-gp expression alters cholesterol metabolism in fibroblasts.** *A*, filipin labeling of WT, P-gp-deficient (DKO), and P-gp-complemented (DKO/P-gp) host cells monolayers to visualize the intracellular distribution of unesterified cholesterol. *B*, host cells were labeled with [^{3}H]cholesterol, and the time course of [^{3}H]cholesterol esterification was measured at the indicated time points. The data are percentages of [^{3}H]cholesteryl esters (*CE*) of total cellular [^{3}H]cholesterol. *C*, cells were labeled with [^{3}H]cholesterol for 24 h, washed, and incubated with 2 mM methyl-β-cyclodextrin. Medium aliquots were taken at the indicated time points, and extracted [^{3}H]cholesterol was measured by liquid scintillation. Extracted cholesterol is expressed as a percentage of total [^{3}H]cholesterol (medium + cell associated radioactivity). *D* and *E*, the cells were similarly labeled and incubated with 20 μg/ml reconstituted HDL (*D*) or 10 μg/ml apoA-I (*E*). Cholesterol efflux is expressed as a percentage of total [^{3}H]cholesterol as before. *F*, cells were loaded with the indicated concentrations of cyclodextrin-cholesterol complexes for 24 h, and viability was measured by AlamarBlue® assay. Results are expressed as percentage of untreated (*cntl*) cell viability. All of the data are averages ± S.E. ($n = 3$).

host P-gp. Biochemical analyses revealed that the lipid composition of the parasite was altered when grown in P-gp-deficient host cells. Specifically, both free and esterified cholesterol levels were reduced, as expected from a decreased uptake of cholesterol from the host; interestingly, the content of selected sphingolipids also changed compared with *T. gondii* grown in WT cells. In particular, the level of sphingomyelin, a major structural sphingolipid mainly found on the plasma membrane, was increased 2-fold. Sphingomyelin has a high affinity for and closely associates with cholesterol and both lipids contribute to the ordered state of plasma membrane domains. Although it is well accepted that cholesterol homeostasis is modulated by sphingomyelin content, studies on the regulation of sphingomyelin metabolism by varying the cellular cholesterol levels produced contradictory results in different cell types analyzed (reviewed in Ref. 34). However, cholesterol depletion was shown to stimulate sphingomyelin synthesis in fibroblasts (35), and high levels of sphingolipids can retain the ordered state of model membranes (36), suggesting that in conditions of cholesterol depletion, increased sphingomyelin content could still contribute to the maintenance of an ordered plasma membrane structure. Thus, it is possible that the increased sphingomyelin content detected in parasites with limited cholesterol levels plays a role in conserving the structural properties of parasite membranes.

Also noteworthy was the increased ceramide content in parasites from P-gp-deficient host cells. It is tempting to speculate that this elevation is a compensatory mechanism for the decreased cholesterol in the membranes, because ceramide-cholesterol replacement has been shown to occur *in vitro* (37). However, the ceramide increase observed does not justify this hypothesis, because similarly for mammalian cells, ceramide in the parasite is about 10 times less abundant than cholesterol. On the other hand, ceramide plays a well known role of second messenger in a variety of cellular processes, including stress response (reviewed in Ref. 38); thus it seems more likely that the enlarged ceramide pool helps to fulfill the signaling needs of *T. gondii* in a host cell environment not optimal for parasite survival. The increased ceramide synthesis observed in labeled parasites isolated from P-gp-deficient host cells supports the idea that the content of this lipid is modulated at least in part by an active synthetic process in the parasite. Scavenging of sphingolipids from the host cell cannot be excluded at this stage, although it has not been demonstrated to date in this parasite.

Although our results clearly indicate that cholesterol transport from the host to the parasite is defective in absence of host P-gp, the data regarding the modality of this transport were quite surprising. So far, *T. gondii* has been shown to depend on

two forms of host-derived cholesterol: free cholesterol contained in endo-lysosomes (22) and esterified cholesterol present in cytosolic lipid bodies (14). The former requires functional host vesicular trafficking (22, 39) and relies on the recruitment of host endo-lysosomes around the PV and their diversion to the PV interior via the formation of H.O.S.T. structures (8). Our data show that P-gp-deficient cells were competent for cholesterol esterification, endo-lysosome recruitment to the PV, and H.O.S.T. formation; thus, the inhibition of cholesterol trafficking to the parasite cannot be attributed to lack of these processes. However, the observed accumulation of cholesterol in endo-lysosomes in P-gp-deficient cells raised the possibility that P-gp contributes to the cholesterol mobilization from lysosomes, a crucial process for cholesterol trafficking to the PV (8, 22). Thus, P-gp in endocytic compartments (25) could help to mobilize cholesterol from endo-lysosomes either juxtaposed to or internalized in the PV via the H.O.S.T. system. This scenario is also in agreement with the reduced cholesterol content in *N. caninum* when grown in P-gp-deficient cells, because the PV of this parasite does not contain H.O.S.T. but is in close proximity with host endo-lysosomes.

Collectively, these results show that host P-gp plays an important role in cholesterol transport to the parasite vacuole. However, there are several observations implying that P-gp does not control all cholesterol transport to the parasite and that P-gp-independent transport pathways must also exist, namely (i) the slight (10%) additional inhibition of parasite replication in DKO cells following U-18666A drug treatment, (ii) the increased parasite replication upon cholesterol loading of DKO cells, and (iii) the ability of the parasite to replicate in DKO cells for several lysis passages.

Considering these results, it seems that the mechanism underlying P-gp-mediated cholesterol transport to the parasite is most likely to fall within one of two general scenarios, namely (i) P-gp does not transport cholesterol directly but is critical in another yet unidentified cellular process essential for cholesterol transport and parasite replication or (ii) P-gp plays a direct but seemingly not exclusive role in cholesterol transport and/or metabolism. The role of P-gp as a transporter of cellular cholesterol has been the subject of considerable debate. Although the presence of cholesterol in the membrane surrounding P-gp is crucial for the ATPase activity of the protein (40), results of studies addressing the role of P-gp in cholesterol trafficking have been contradictory. P-gp has been proposed to translocate cholesterol between the plasma membrane leaflets *in vitro* (40). In addition, several reports using chemically selected cell lines or inhibitors associated P-gp overexpression with increased cholesterol transport to the endoplasmic reticulum and consequent esterification (reviewed in Ref. 41). However, from these studies it is not clear whether the enhanced cholesterol trafficking observed is due to a direct role of the protein or to an elevated turnover of the cholesterol-rich membranes where P-gp is located (42). Our understanding of P-gp-mediated cholesterol transport is further compromised by the contradictory results obtained through the use of P-gp inhibitors with potential side effects and cell type-specific outcome of P-gp expression (41). In our work using P-gp-deficient cells, we found that free cholesterol accumulated in vesicular structures located in the perinuclear region and that this accumulation was absent once P-gp activity was restored. In addition, contrary to previous reports using P-gp inhibitors (43, 44) or selected MDR cell lines (45), cholesteryl esters accumulated in the absence of P-gp. Interestingly, a similar increase in cholesterol esterification was observed *in vivo* in the liver of P-gp-deficient mice (46). Furthermore, we found a positive correlation between cholesterol extractability/efflux from the plasma membrane and P-gp expression. Taken together, our results suggest that P-gp does play a significant role in cholesterol transport in both host-parasite interaction and in normal metabolism of fibroblasts.

Thus, although an indirect effect on cholesterol transport in the absence of P-gp cannot be completely excluded, we observed a number of indications consistent with a model in which P-gp resident in the endo-lysosomes is involved in cholesterol mobilization from these compartments to the PV in case of parasite infection. These indications include: the endo-lysosome recruitment around the PV in infected cells, the cholesterol accumulation outside the PV, the reduced cholesterol supply to the parasite in the absence of host P-gp, and the observation that P-gp-mediated parasite inhibition depends on vesicular trafficking of cholesterol. In addition, several alterations in cholesterol metabolism observed in DKO host cells also suggest that P-gp plays a role in cholesterol trafficking from endo-lysosomes to the plasma membrane in uninfected cells. Such observations include the accumulation of free cholesterol in endo-lysosome like structures in the absence of P-gp, the decreased recycling of exogenous cholesterol to the plasma membrane, and the increase in cholesterol esterification. On the other hand, increased P-gp expression in host cells correlates with increased cholesterol content in the plasma membrane and efflux and increased sensitivity to cholesterol loading toxicity.

In summary, our studies using the intracellular parasites *T. gondii* and *N. caninum* provide evidence that host cell P-gp plays a previously unidentified role in host-parasite interaction. Our results reveal that host P-gp is required for cholesterol transport to the parasite vacuole via a mechanism independent of H.O.S.T. formation and is also involved in normal cholesterol metabolism in uninfected mammalian fibroblasts.

Acknowledgments—We thank Alfred Schinkel for kindly providing the P-gp-deficient murine embryonic fibroblasts, Michael M. Gottesman for the P-gp-complemented murine embryonic fibroblasts and P-gp overexpressing 3T3 fibroblasts, and Peter Lerch for the reconstituted HDL and apolipoprotein A-I. We are grateful to John Boothroyd and David Sibley for the β-galactosidase-expressing T. gondii and N. caninum, to Jack Rohrer and Mohamed-Ali Hakimi for providing anti-giantin and anti-tubulin antibodies, and to Therese Michel and Eva Dalmau for technical assistance. In particular, we thank Piet Borst and Gerrit van Meer for invaluable advice and discussion.

REFERENCES

1. Loo, T. W., and Clarke, D. M. (1999) *Biochem. Cell Biol.* **77,** 11–23
2. Gottesman, M. M., Hrycyna, C. A., Schoenlein, P. V., Germann, U. A., and Pastan, I. (1995) *Annu. Rev. Genet.* **29,** 607–649
3. van Veen, H. W., and Konings, W. N. (1998) *Biochim. Biophys. Acta* **1365,** 31–36

4. Blackmore, C. G., McNaughton, P. A., and van Veen, H. W. (2001) *Mol. Membr. Biol.* **18,** 97–103
5. Maubon, D., Ajzenberg, D., Brenier-Pinchart, M. P., Dardé, M. L., and Pelloux, H. (2008) *Trends Parasitol.* **24,** 299–303
6. Mordue, D. G., Håkansson, S., Niesman, I., and Sibley, L. D. (1999) *Exp. Parasitol.* **92,** 87–99
7. Martin, A. M., Liu, T., Lynn, B. C., and Sinai, A. P. (2007) *J. Eukaryot. Microbiol.* **54,** 25–28
8. Coppens, I., Dunn, J. D., Romano, J. D., Pypaert, M., Zhang, H., Boothroyd, J. C., and Joiner, K. A. (2006) *Cell* **125,** 261–274
9. Schinkel, A. H., Mayer, U., Wagenaar, E., Mol, C. A., van Deemter, L., Smit, J. J., van der Valk, M. A., Voordouw, A. C., Spits, H., van Tellingen, O., Zijlmans, J. M., Fibbe, W. E., and Borst, P. (1997) *Proc. Natl. Acad. Sci. U.S.A.* **94,** 4028–4033
10. Alemán, C., Annereau, J. P., Liang, X. J., Cardarelli, C. O., Taylor, B., Yin, J. J., Aszalos, A., and Gottesman, M. M. (2003) *Cancer Res.* **63,** 3084–3091
11. Wijnholds, J., deLange, E. C., Scheffer, G. L., van den Berg, D. J., Mol, C. A., van der Valk, M., Schinkel, A. H., Scheper, R. J., Breimer, D. D., and Borst, P. (2000) *J. Clin. Invest.* **105,** 279–285
12. Currier, S. J., Kane, S. E., Willingham, M. C., Cardarelli, C. O., Pastan, I., and Gottesman, M. M. (1992) *J. Biol. Chem.* **267,** 25153–25159
13. Hemphill, A., Gottstein, B., and Kaufmann, H. (1996) *Parasitology* **112,** 183–197
14. Sonda, S., Ting, L. M., Novak, S., Kim, K., Maher, J. J., Farese, R. V., Jr., and Ernst, J. D. (2001) *J. Biol. Chem.* **276,** 34434–34440
15. Fuchs, N., Sonda, S., Gottstein, B., and Hemphill, A. (1998) *J. Parasitol.* **84,** 753–758
16. Hemphill, A. (1996) *Infect. Immun.* **64,** 4279–4287
17. Bligh, E. G., and Dyer, W. J. (1959) *Can. J. Med. Sci.* **37,** 911–917
18. Munoz-Olaya, J. M., Matabosch, X., Bedia, C., Egido-Gabás, M., Casas, J., Llebaria, A., Delgado, A., and Fabriàs, G. (2008) *Chem. Med. Chem.* **3,** 946–953
19. Monaghan, P., Cook, H., Hawes, P., Simpson, J., and Tomley, F. (2003) *J. Microsc.* **212,** 62–70
20. Wild, P., Schraner, E. M., Adler, H., and Humbel, B. M. (2001) *Microsc. Res. Tech.* **53,** 313–321
21. McFadden, D. C., Seeber, F., and Boothroyd, J. C. (1997) *Antimicrob. Agents Chemother.* **41,** 1849–1853
22. Coppens, I., Sinai, A. P., and Joiner, K. A. (2000) *J. Cell Biol.* **149,** 167–180
23. Underwood, K. W., Andemariam, B., McWilliams, G. L., and Liscum, L. (1996) *J. Lipid Res.* **37,** 1556–1568
24. Kim, H., Barroso, M., Samanta, R., Greenberger, L., and Sztul, E. (1997) *Am. J. Physiol. Cell Physiol.* **273,** C687–702
25. Fu, D., and Roufogalis, B. D. (2007) *Am. J. Physiol. Cell Physiol.* **292,** C1543–1552
26. Lencer, W. I., and Saslowsky, D. (2005) *Biochim. Biophys. Acta* **1746,** 314–321
27. Zhang, M., Dwyer, N. K., Neufeld, E. B., Love, D. C., Cooney, A., Comly, M., Patel, S., Watari, H., Strauss, J. F., 3rd, Pentchev, P. G., Hanover, J. A., and Blanchette-Mackie, E. J. (2001) *J. Biol. Chem.* **276,** 3417–3425
28. Maxfield, F. R., and Tabas, I. (2005) *Nature* **438,** 612–621
29. Lahiri, S., and Futerman, A. H. (2007) *Cell Mol. Life Sci.* **64,** 2270–2284
30. Lerch, P. G., Förtsch, V., Hodler, G., and Bolli, R. (1996) *Vox Sang* **71,** 155–164
31. Warner, G. J., Stoudt, G., Bamberger, M., Johnson, W. J., and Rothblat, G. H. (1995) *J. Biol. Chem.* **270,** 5772–5778
32. Schinkel, A. H., Smit, J. J., van Tellingen, O., Beijnen, J. H., Wagenaar, E., van Deemter, L., Mol, C. A., van der Valk, M. A., Robanus-Maandag, E. C., te Riele, H. P., Berns, A. J., and Borst, P. (1994) *Cell* **77,** 491–502
33. Silverman, J. A., Hayes, M. L., Luft, B. J., and Joiner, K. A. (1997) *Antimicrob. Agents Chemother.* **41,** 1859–1866
34. Ridgway, N. D. (2000) *Biochim. Biophys. Acta* **1484,** 129–141
35. Leppimäki, P., Kronqvist, R., and Slotte, J. P. (1998) *Biochem. J.* **335,** 285–291
36. Brown, R. E. (1998) *J. Cell Sci.* **111,** 1–9
37. Megha, and London, E. (2004) *J. Biol. Chem.* **279,** 9997–10004
38. Hannun, Y. A., and Obeid, L. M. (2008) *Nat. Rev. Mol. Cell Biol.* **9,** 139–150
39. Sehgal, A., Bettiol, S., Pypaert, M., Wenk, M. R., Kaasch, A., Blader, I. J., Joiner, K. A., and Coppens, I. (2005) *Traffic* **6,** 1125–1141
40. Garrigues, A., Escargueil, A. E., and Orlowski, S. (2002) *Proc. Natl. Acad. Sci. U.S.A.* **99,** 10347–10352
41. Orlowski, S., Martin, S., and Escargueil, A. (2006) *Cell Mol. Life Sci.* **63,** 1038–1059
42. Liscovitch, M., and Lavie, Y. (2000) *Trends Biochem. Sci.* **25,** 530–534
43. Debry, P., Nash, E. A., Neklason, D. W., and Metherall, J. E. (1997) *J. Biol. Chem.* **272,** 1026–1031
44. Luker, G. D., Nilsson, K. R., Covey, D. F., and Piwnica-Worms, D. (1999) *J. Biol. Chem.* **274,** 6979–6991
45. Santini, M. T., Romano, R., Rainaldi, G., Filippini, P., Bravo, E., Porcu, L., Motta, A., Calcabrini, A., Meschini, S., Indovina, P. L., and Arancia, G. (2001) *Biochim. Biophys. Acta* **1531,** 111–131
46. Luker, G. D., Dahlheimer, J. L., Ostlund, R. E., Jr., and Piwnica-Worms, D. (2001) *J. Lipid Res.* **42,** 1389–1394

Manuscript 2

The P-glycoprotein Inhibitor GF120918 Modulates Ca^{2+}-Dependent Processes and Lipid Metabolism in *Toxoplasma gondii*

The P-glycoprotein Inhibitor GF120918 Modulates Ca^{2+}-Dependent Processes and Lipid Metabolism in *Toxoplasma gondii*

Iveta Bottova[1], Ursula Sauder[2], Vesna Olivieri[2], Adrian B. Hehl[1] and Sabrina Sonda[1]*

[1]Institute of Parasitology, University of Zurich, 8057 Zurich, Switzerland and [2] Biozentrum, University of Basel, 4056 Basel, Switzerland.

*Corresponding author

Abstract

Up-regulation of the membrane-bound efflux pump P-glycoprotein (P-gp) is associated with the phenomenon of multidrug-resistance in pathogenic organisms, including protozoan parasites. In addition, P-gp plays a role in normal physiological processes, however our understanding of these P-gp functions remains limited. In this study we investigated the effects of the P-gp inhibitor GF120918 in *Toxoplasma gondii*, a model apicomplexan parasite and an important human pathogen. We found that GF120918 treatment severely inhibited parasite invasion and replication. Further analyses of the molecular mechanisms involved revealed that the P-gp inhibitor modulated parasite motility, microneme secretion and egress from the host cell, all cellular processes known to depend on Ca^{2+} signaling in the parasite. In support of a potential role of P-gp in Ca^{2+}-mediated processes, immunoelectron and fluorescence microscopy showed that *T. gondii* P-gp was localized in acidocalcisomes, the major Ca^{2+} storage in the parasite, at the plasma membrane, and in the intravacuolar tubular network. In addition, metabolic labeling of extracellular parasites revealed that inhibition or down-regulation of *T. gondii* P-gp resulted in aberrant lipid synthesis. These results suggest a crucial role of *T. gondii* P-gp in essential processes of the parasite biology and further validate the potential of P-gp activity as a target for drug development.

Abbreviations

P-gp, P-glycoprotein; P-gp DKO, murine embryonic fibroblast knocked out for the two mouse P-gp isoforms; TLC, thin layer chromatography.

Introduction

The integral membrane protein P-glycoprotein (P-gp, MDR1, ABCB1) is one of the most studied cellular transporters of the ATP-binding cassette (ABC) transporter superfamily [1]. The clinical importance of P-gp derives from the fact that over-expression of this transporter is commonly associated with the phenomenon of multidrug resistance [2], a major public health problem associated with drug-resistant cancer cells and microbial pathogens. The main function of P-gp is the export of xenobiotics from the cell, as corroborated by the findings that P-gp deficient mice are viable but show strikingly altered pharmacokinetics and increased sensitivity to a variety of drugs [3]. In addition to this well known role, an increasing amount of evidence now suggests that P-gp also participates in normal physiological processes, including the transport of steroid hormones [4] and lipid translocation (rev. in [5]).

Here we investigated the effects of the potent P-gp inhibitor GF120918 in the biology of *Toxoplasma gondii*, a model intracellular parasite and an important human pathogen, causing toxoplasmosis. Previous studies

based on efflux analyses in the presence of P-gp inhibitors suggested that an active P-gp homologue is present in *T. gondii* [6,7]. Recently, two P-gp homologues with the typical P-gp structure have been identified in the genome of the parasite (TgABC.B1 and TgABC.B2) and found to be constitutively expressed in both the vegetative and quiescent stages of *T. gondii*'s life cycle [8]. Further molecular characterization revealed that TgABC.B1 is coded by a single copy gene, expressed as a membrane-associated protein of ~150 kDa, and constitutively present in different parasite strains [9]. Indications that *T. gondii* P-gp may be involved in key biological processes, such as replication and host cell invasion were provided by early works using P-gp inhibitors [6,10]. However, given that these studies used host cells containing P-gp, it was not possible to discriminate between the contribution of *T. gondii* and host cell P-gp. Indeed, we recently showed that host cell P-gp plays a crucial role in *T. gondii* replication by facilitating the transport of host cholesterol to the parasite vacuole [11]. In this study we used P-gp deficient host cells [3] in parallel with pharmacological inhibition of P-gp, thereby enabling more selective insights into the specific role of *T. gondii* P-gp. Inhibition of parasite P-gp was achieved with the acridonecarboxamide derivative GF120918, a potent competitive P-gp inhibitor of the latest generation [12,13], whose use has been

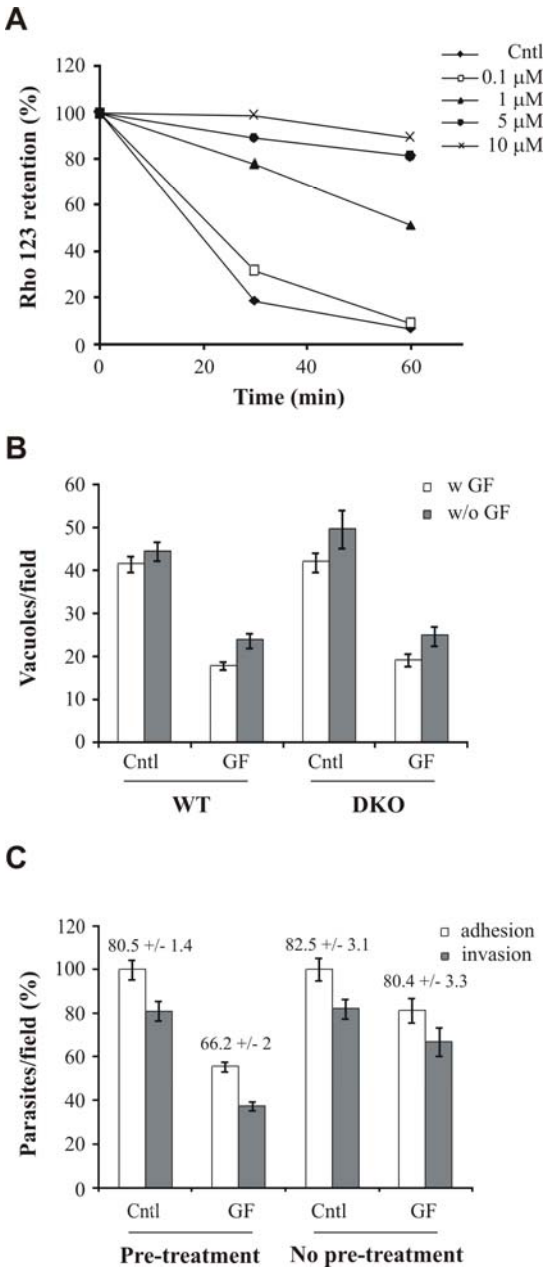

Figure 1: GF120918 treatment inhibits parasite invasion. A. Functionality assay of P-gp in isolated *T. gondii* treated with the indicated inhibitor concentrations as measured by time course analysis of intracellular rhodamine 123 (Rho 123) retention. Retention is expressed as percentage of mean fluorescence of intracellular Rho 123 at time 0. B. Invasion assay in presence of 10 μM GF120918 (GF) or solvent (cntl). *T. gondii* were pre-treated with GF120918 for 30 min and allowed to infect wild type (WT) or P-gp deficient (DKO) host cell monolayers in presence of GF120918 (pre-treatment and invasion, white bars). Alternatively, parasites were pre-treated with 10 μM GF120918 for 4 h, washed to remove the drug and incubated with host cells in absence of GF120918 (only pre-treatment, gray bars). Invasion was quantified by enumerating the parasite vacuoles at 24 h post infection. Data are average of vacuoles per field ± SE (n=15). C. Adhesion/invasion assay in presence of 10 μM GF120918 (GF) or solvent (cntl). Parasites were pre-treated with GF120918 for 30 min at 37°C and allowed to infect DKO host cell monolayers for 2 h in presence of the drug. Alternatively, drug pre-treatment was omitted and GF120918 added at the time of invasion. Adherent (intracellular + extracellular) and invaded (intracellular) parasites were counted after dual color immunostaining. Data are average of parasites per field ± SE (n=15) and expressed as percentage of cntl adhesion. Numbers above the bars represent the invasion index (percentage of intracellular parasites out of the total parasite number).

widely published both *in vitro* [14] and *in vivo* [15,16]. Importantly, GF120918 does not inhibit the P-gp-related multidrug transporters MRP1 and MRP2 [17] nor cytochrome P450 3A, a key enzyme in drug metabolism [18], and achieves adequate P-gp inhibition *in vivo* without significant side effects [13,19]

Results

GF120918 inhibits parasite invasion. As an obligate intracellular parasite, *T. gondii* depends completely on host cells for its survival and propagation; thus host cell invasion is an essential process in the parasite's biology. To block the function of *T. gondii* P-gp, isolated parasites were treated with GF120918, a potent P-gp inhibitor of the latest generation [13]. GF120918 was found to strongly hamper P-gp function in the parasite at low micromolar concentrations, as assessed by efflux analysis of the specific P-gp substrate rhodamine 123 (Fig. 1A). To analyze whether GF120918 inhibits parasite invasion, parasites were pre-treated for 30 min with the inhibitor, then allowed to infect host cells wild type (WT) or deficient in the two mouse P-gp isoforms (P-gp DKO) [3] for 4 h in presence of the inhibitor. The drug was then removed and the infection was determined by counting the parasite vacuoles after 24 h incubation. GF120918 treatment reduced the number of intracellular vacuoles by 50% in both host cell types, indicating that host P-gp is not involved in parasite invasion (Fig.1B, white bars). Importantly, the invasion inhibition was not caused by parasite lethality following compound treatment, as GF120918 did not significantly compromise parasite viability at the concentration inhibitory for invasion (data not shown). To analyse whether the presence of GF120918 at the time of infection was necessary for the inhibitory effect, parasites were pre-treated with GF120918, washed and incubated with host cells in absence of the drug. Also in these experimental conditions, parasite invasion was reduced by ~50% (Fig. 1B, grey bars), confirming that the drug inhibited parasite invasion by acting solely on the parasite. These results also showed that the invasion inhibition is not reversed by removal of the drug from the medium, suggesting that GF120918 stably inhibited the parasite target.
Having shown that GF120918 inhibited parasite invasion, we then further dissected the inhibitory effect using a sequential staining method, which allows discrimination between the processes of adhesion to a host cell and active invasion. GF120918 treatment reduced the number of both adherent and invaded parasites by ~ 50% compared with control cells (Fig. 1C, pre-treatment). This dual inhibition is indicative of an effect on parasite attachment, since attachment is required for invasion [20]. Consistently, we found that the invasion index, namely the percentage of invaded parasites calculated out of the total number of parasites present, decreased by less than 20% in presence of GF120918. Interestingly, in absence of parasite pre-treatment, the inhibitory effect of GF120918 on parasite adhesion and invasion was less pronounced and did not decrease the invasion index (Fig. 1C, no pre-treatment), suggesting that a time delay after adding the compound is necessary for the inhibitory effect to take place.

GF120918 treatment increases T. gondii motility. From the above experiments we established that GF120918 inhibited parasite invasion. As parasite invasion is an active process which depends on parasite motility (reviewed in [21]), we next examined whether the GF120918-mediated inhibition of invasion was a consequence of defective *T. gondii* motility. Parasite motility was analyzed by allowing parasites to glide on a substratum in presence or absence of GF120918 whilst visualizing the trails

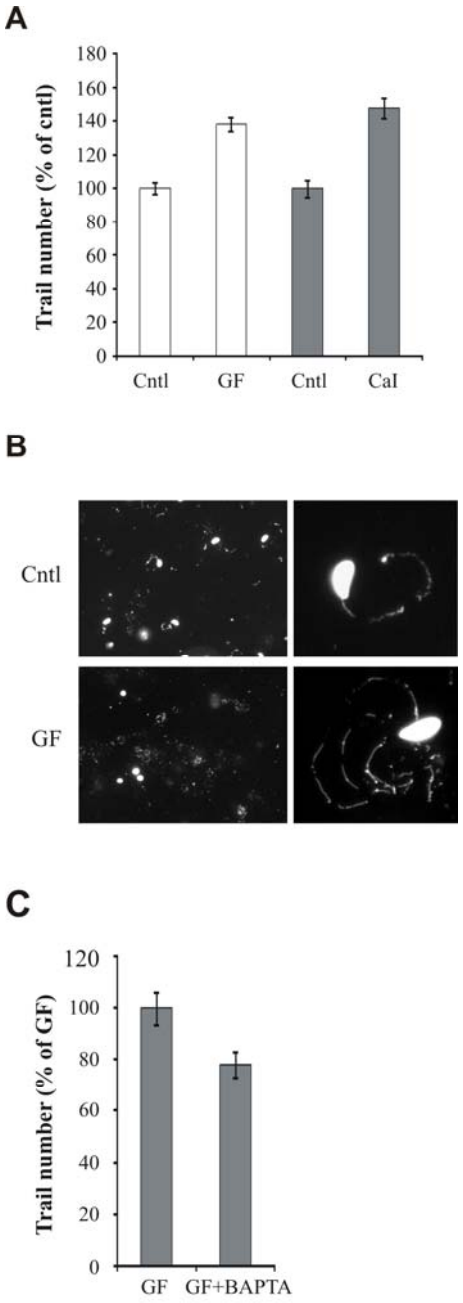

produced by parasite movement by immunofluorescence [22]. Surprisingly, GF120918 treatment did not reduce parasite motility, as assessed by the number of trails generated. On the contrary, the trails produced by GF120918-treated cells were more numerous (Fig. 2A, white bars) and longer (Fig. 2B) compared with control cells. Parasite motility is known to be regulated by intracellular Ca^{2+} fluxes [23,24]. To test whether the alteration of parasite motility induced by GF120918 treatment correlates with the effects of Ca^{2+} deregulation, we increased intracellular calcium levels using the Ca^{2+} ionophore A23187. In our experimental conditions, both P-gp inhibitor and A23187 incubations increased parasite motility in a comparable manner (Fig. 2A, gray bars). Similarly to what was observed during GF120918 treatment, incubation with A23187 reduced parasite adhesion and invasion as well (Fig. 2C). In addition, when parasites were co-treated with GF120918 together with the Ca^{2+} chelator BAPTA, the increase in motility was reduced compared with parasites solely treated with GF120918 (Fig. 2D). Collectively, these findings indicated that GF120918 treatment increases parasite motility and that this increase is likely to depend on alterations in parasite's Ca^{2+} fluxes.

GF120918 treatment induces microneme secretion. Secretion of micronemes, secretory organelles located at the apical end of the parasite, depends on Ca^{2+} fluxes in the parasite and it is essential for *T. gondii*

Figure 2: GF120918 treatment increases parasite motility. A. Parasites were treated with 10 µM GF120918 (GF, white bars), 1 µM Ca^{2+} ionophore A23187 (CaI, gray bars) or the respective solvents (cntl) and the trails deposited during gliding enumerated. Data are average of trail number per field ± SE (n=10) and expressed as percentage of cntl. B. Indirect immunofluorescence microscopy demonstrating that the average length of trails increased with GF120918 (GF) treatment. C. Adhesion/invasion assay in presence of 1 µM of the Ca^{2+} ionophore A23187 (CaI) or solvent (cntl). Adherent and invaded parasites were counted after dual color immunostaining. Data are average of parasites per field ± SE (n=10) and expressed as percentage of cntl adhesion. D. Parasites were treated with 10 µM GF120918 (GF) in presence or absence of 100 µM BAPTA and trail deposition was quantified as before. Data are average of trail number per field ± SE (n=10) and expressed as percentage of GF120918-treated parasites.

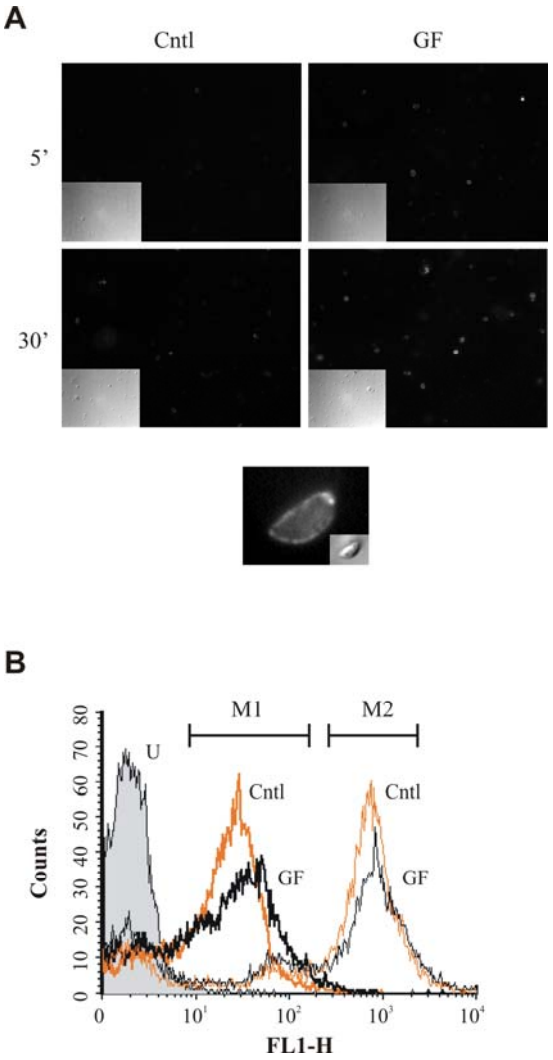

Figure 3: GF120918 treatment increases MIC2 secretion. A. Isolated parasites were treated with 10 µM GF120918 (GF) or solvent (cntl) for 5 or 30 min, fixed and stained with anti-MIC2 antibody without cell permeabilization. Central panel, magnification of *T. gondii* treated with GF120918 for 30 min showing MIC2 surface staining. Insets, differential interference contrast images. B. Isolated parasites treated with 10 µM GF120918 (GF) or solvent (cntl) for 30 min were stained with anti-MIC2 antibody without (thick lines) or with (thin lines) cell permeabilization and quantified by flow cytometry. Overlay histogram showing cells treated with solvent (cntl, yellow lines) or GF120918 (GF, black lines). U, unstained cells.

motility [24]. To analyse whether GF120918 affected microneme secretion, we examined the discharge of the microneme protein MIC2, which is secreted on the parasite surface and then shed after proteolytic processing [25]. Parasites treated for 5 and 30 min with GF120918 showed a time dependent increase in MIC2 surface staining compared with control cells (Fig. 3A). Population-wide quantification by flow cytometry revealed that MIC2 surface staining in non-permeabilized cells increased following GF120918 treatment in ~25% of the cells (Fig. 3B, thick lines). The staining was not due to cell permeabilization induced by inhibitor treatment, as detergent-permeabilized cells showed a much stronger signal (Fig. 3B, thin lines). In addition, analysis of permeabilized cells revealed that in control samples 64.44% of the total cell number (n=10'000) showed high MIC2 signal, while GF120918 treatment decreased this number to 48.47%, suggesting a loss of cell associated MIC2 following secretion. Collectively, these data indicate that GF120918 treatment induced microneme secretion without increasing the permeability of parasite plasma membrane.

GF120918 treatment induces parasite egress.
As we observed that GF120918 treatment of extracellular *T. gondii* enhanced parasite motility, we reasoned that if GF120918 could activate motility also in intracellular parasites, it would promote active egress of *T. gondii* from the host cells, a process which depends on parasite motility and is triggered by changes in the host cells ionic environment [26]. When infected cultures were treated for 4 h with GF120918, a two fold increase in parasite egress was observed compared with untreated cells (Fig. 4A, w/o CaI).
Contrary to the natural egress which occurs at the end of the parasite lytic cycle and does not require parasite motility [27], the motility-

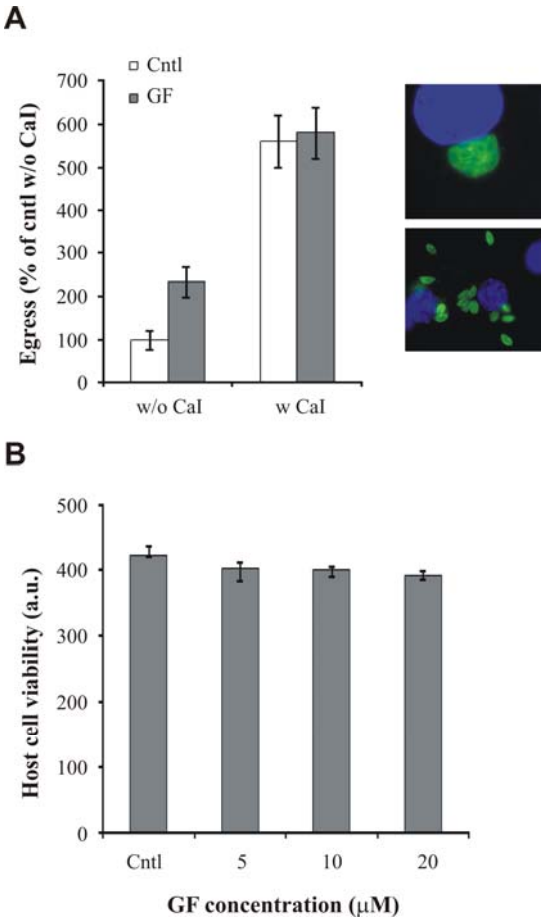

Figure 4: GF120918 treatment increases *T. gondii* egress. A. *T. gondii* was allowed to replicate in P-gp DKO host cells for 30 h, treated with 10 μM GF120918 (GF) or solvent (cntl) for 4 h and egress quantified after parasite immunolabeling. For Ca^{2+} ionophore (CaI)-induced egress, infected monolayers were treated with GF120918 as before and additionally incubated with 1 μM A23187 for 10 min. Data are average of egressed parasites per field ± SE (n=20) expressed as percentage of cntl without CaI. Right panels, examples of intravacuolar and egressed parasites. B. Metabolic activity of P-gp DKO host cells treated for 24 h with solvent (cntl) or GF120918 (GF) at the indicated concentrations was assessed by measuring AlamarBlue reduction (Biosource). Results are average ± SE (n = 6).

dependent active egress is thought to be employed by the parasite as an escape mechanism from a dying host cell [28]. To determine whether the GF120918-mediated egress was caused by host cell lethality, we analyzed the viability of host cells treated with the inhibitor. Incubation with GF120918 for 24 h did not reduce host cell viability, indicating that the increased egress induced by GF120918 was not a response to inhibitor-mediated host cell toxicity (Fig. 4B).

Next we analyzed the effect of GF120918 during experimental induction of active egress. As with microneme secretion, active egress can also be induced by adding the Ca^{2+} ionophore A23187 [29], which raises intracellular calcium levels and activates parasite motility (rev. in [30]). When parasite egress was induced with A23187 incubation, a similar increase in egress was observed in presence or absence of GF120918, indicating that GF120918 treatment was not able to further increase egress when used in combination with the Ca^{2+} ionophore (Fig. 4A, w CaI).

Intracellular localization of T. gondii P-gp. We showed that treatment of *T. gondii* with the P-gp inhibitor GF120918 strongly correlated with alterations in Ca^{2+}-dependent processes; thus, it is possible that P-gp plays a role in Ca^{2+} regulation in this parasite. To investigate this hypothesis, we analyzed whether P-gp localized in parasite organelles involved in Ca^{2+} homeostasis. For this aim we used the P-gp-specific monoclonal antibody C219, which recognizes a conserved epitope also present in the *T. gondii* orthologue (Fig. S1B). Western blot analysis confirmed that the antibody reacts with a parasite protein corresponding to the predicted mass of P-gp (Fig. S1A). Immunoelectron microscopy of infected cells showed a distinct staining concentrated in conspicuous membrane bound electron-lucent vesicles of 100-400 nm

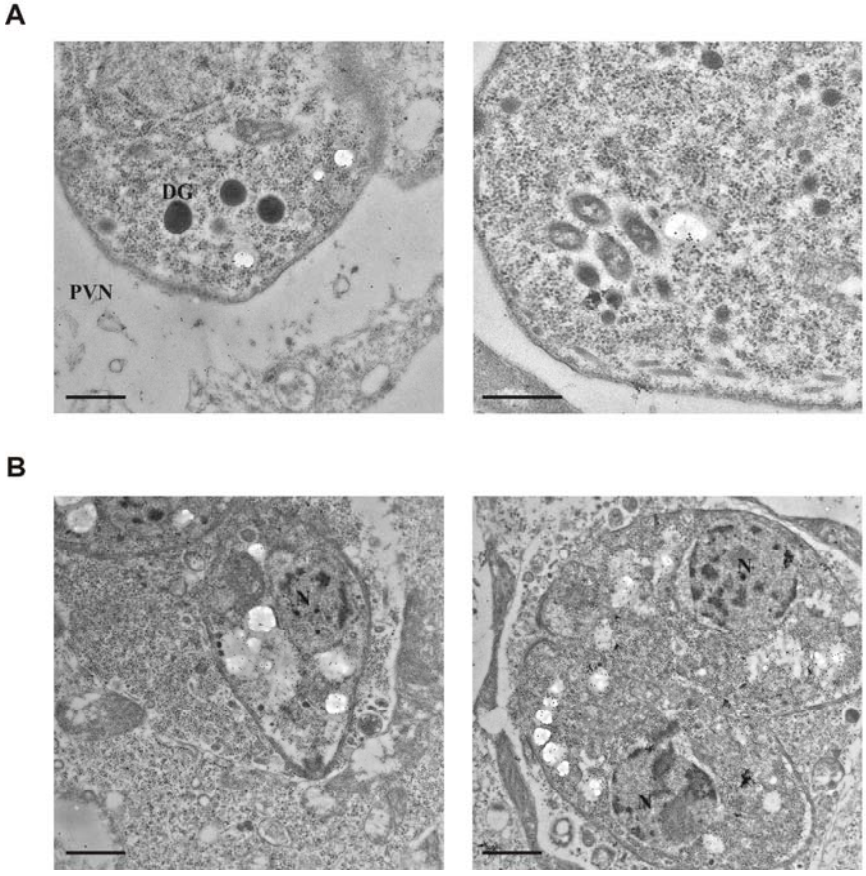

Figure 5: Ultrastructural localization of *T. gondii* P-gp. A. *T. gondii* was allowed to replicate in P-gp DKO host cells for 24 h and immunoelectron microscopy performed with anti-Pgp antibody C219. PVN, parasitophorous network. DG, dense granules. N, nucleus. Scale bars, 0.5 μm. B. Co-localization of C219 (15 nm gold, arrows) and anti-VP1 (5 nm gold, arrowheads). Scale bars, 0.5 μm. C. Examples of P-gp localization in damaged parasite vacuoles. Scale bars, 1 μm.

diameter, which morphologically resembled acidocalcisomes, the largest intracellular store of Ca^{2+} in the parasite [31] (Fig. 5A). Co-immunostaining with antibodies against the acidocalcisome marker VP1 [32] revealed that both proteins are indeed present in morphologically similar structures (Fig. 5B).

In addition, P-gp labeling was found in the tubulovesicular network within the parasite vacuole. The plasma membrane of theparasite was less intensely labeled with this antibody, and no staining of other vesicular structures, such as rhoptries and dense granules was observed. Strikingly, P-gp staining drastically increased in the rare vacuoles which contained dying parasites, characterized by high intracellular vacuolization, plasma membrane rupture and release of cytosolic content in the parasite vacuolar space (Fig. 5C).

Next, we investigated the localization of P-gp by immunofluorescence analysis. As the monoclonal antibody C219 is suitable for this technique only in case of P-gp overexpression, we engineered a P-gp minigene composed of three sequences of the parasite protein showing low degree of similarity with the mammalian P-gp (Fig S1B), and which encompassed the peptide sequence used in a previous study to raise anti-*T. gondii* P-gp antibodies [9]. Similar to the C219 antibody, the immune serum against P-gp minigene reacted with a band of mass expected for P-gp (Fig. S1A). As previously reported [9], lower molecular weight bands were also detected; it is currently not known if they constitute protein degradation or processing products. Immunofluorescence analysis of *T. gondii* infected cells using the

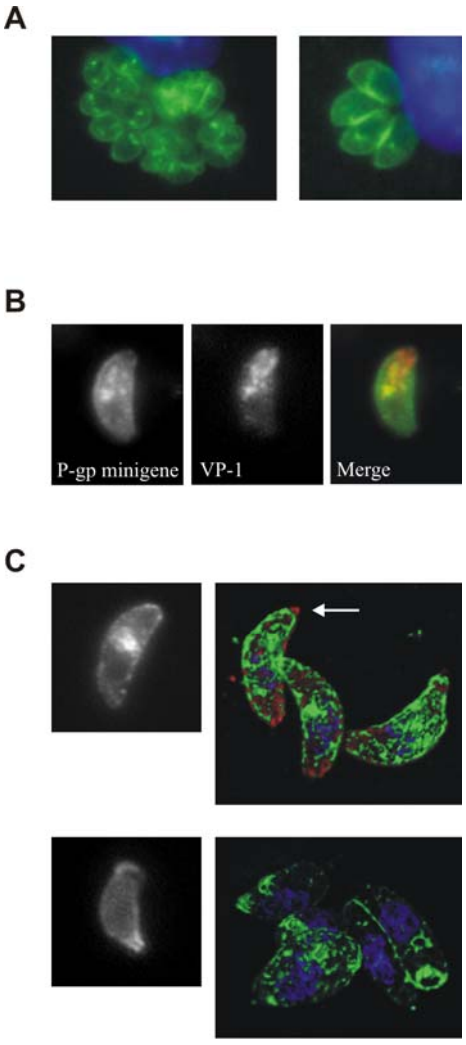

Figure 6: Intracellular localization of *T. gondii* P-gp. A. Fluorescence microscopy of intracellular *T. gondii* at 24 h post infection using anti-P-gp minigene antibody. Nuclear DNA was stained with DAPI. B. Dual staining of isolated *T.gondii* using anti-P-gp minigene (green) and anti-VP1 (red) antibodies, showing partial co-localization of the two proteins. C. Fluorescence (left panels) and confocal (right panels) microscopy showing differential P-gp distribution in extracellular parasites stained with anti-P-gp minigene antibody (green). The arrow indicates the absence of P-gp staining in the conoid area labeled with anti- *T. gondii* antibody (red). Nuclear DNA was stained with DAPI (blue).

P-gp minigene antibody showed a strong labeling of distinct intracellular structures distributed throughout the cell and, less intensely, of plasma membrane (Fig. 6A). Similar to the observations with electron microscopy, these intracellular structures partially co-localized with VP1, strongly suggesting that P-gp is indeed localized in acidocalcisomes (Fig. 6B).

Interestingly, when extracellular *T. gondii* were probed with the P-gp minigene antibody, a subgroup of parasites showed P-gp labeling exclusively on the plasma membrane and labeling of the internal structures was no longer evident. In addition, the staining concentrated at the apical end of the parasite and formed a collar around the conoid, which in turn remained unlabeled (Fig. 6C). These results suggest that P-gp transiently re-localized in extracellular parasites.

GF120918 treatment inhibits T. gondii replication and lipid synthesis. To determine whether GF120918 treatment affected parasite replication, P-gp DKO host cells were infected with *T. gondii* and subsequently treated with different concentrations of the inhibitor. Analysis of parasite burden 48 h post infection revealed a marked dose-dependent inhibition of parasite replication (Fig. 7A). Immunofluorescence analysis did not show any cells positive for the bradyzoite-specific antigen BAG1 (data not shown), indicating that GF120918 treatment reduced parasite replication without triggering parasite stage conversion to the quiescent bradyzoite form. Treatment with verapamil, an earlier generation P-gp inhibitor reported to be less potent than GF120918 [33], was less effective in blocking parasite replication. However, longer incubation times with verapamil strongly inhibited *T. gondii* replication as well (Fig. 7B), without affecting host cell viability (data not shown). In addition, GF120918-mediated inhibition of parasite replication was not reversed following removal of the

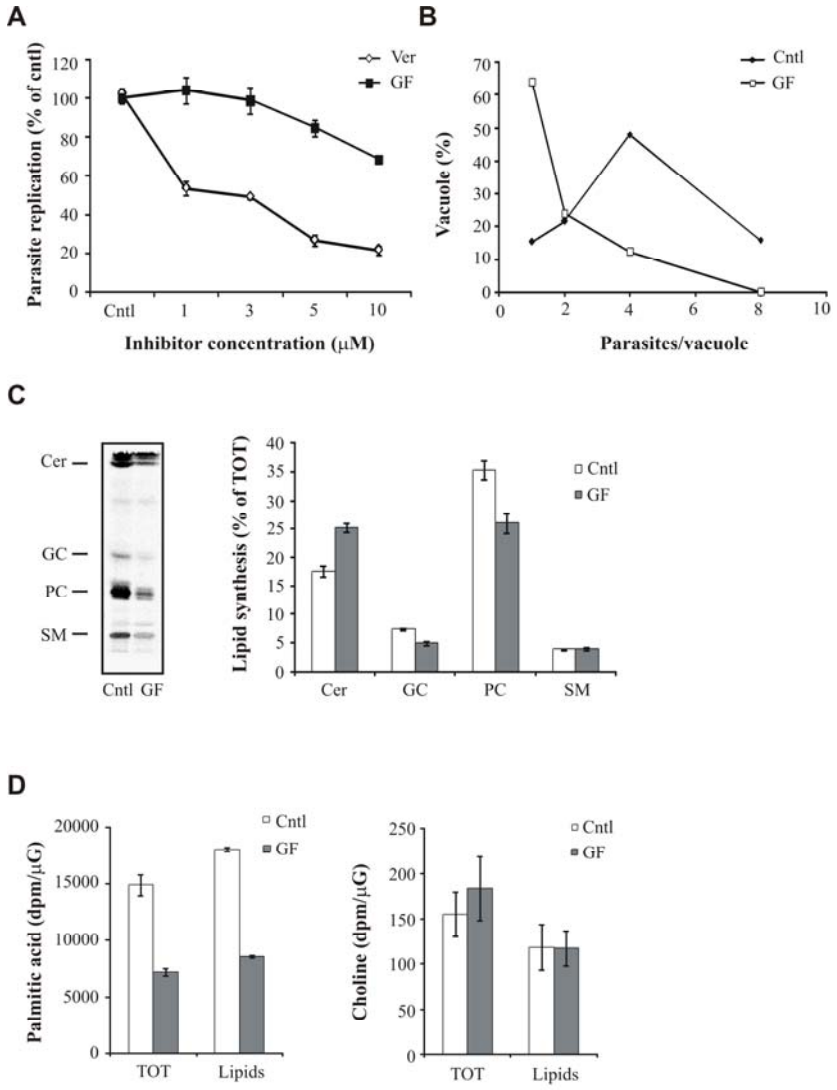

Figure 7: GF120918 treatment inhibits parasite replication and lipid synthesis. A. *T. gondii* were allowed to infect P-gp DKO host cells and subsequently treated with the indicated concentrations of GF120918 (GF) and verapamil (Ver). Parasite burden was quantified 48 h post infection by a colorimetric assay measuring the amount of parasite-expressed β-galactosidase. Results are expressed as percentage of parasite number in control untreated cells ± SE (n=5). B. Time course of parasite replication inhibition by verapamil. *T. gondii* infected host cells were treated with the indicated concentrations of verapamil or solvent (cntl). Parasite burden was quantified at the indicated times post infection as described above. Results are expressed as percentage of parasite number in control untreated cells ± SE (n=3). C. *T. gondii* were treated with 10 μM GF120918 (GF) or solvent (cntl) for 4 h, washed and incubated with P-gp DKO host cells for 24 h in absence of the drug. Intracellular parasites were quantified by direct counting after immunostaining. The distribution of the parasite number in single vacuoles is expressed as percentage of total vacuoles examined (n>100). D. Isolated parasites were labeled with 0.5 μCi/mL of [^{3}H]palmitic acid for 3 h in presence of 10 μM GF120918 (GF) or solvent (cntl) and lipid were extracted. Left panel, TLC separation of de novo synthesized lipids. Lipid standard used: ceramide (Cer), glucosylceramide (GC), phosphatidylcholine (PC), sphingomyelin (SM). Right panel, quantification of the relative amount of newly synthesized lipid species expressed as percentage of total lipids. Data are average ± SE (n=3). E. Isolated parasites were labeled with 0.5 μCi/mL of [^{3}H]palmitic acid or 4 μCi/mL [^{3}H]choline for 3 h in presence of 10 μM GF120918 (GF) or solvent (cntl). [^{3}H] incorporation was measured in both whole cell (TOT) and lipid extracts by liquid scintillation and normalized by protein content. Data are average ± SE (n=6).

drug: parasites treated with the inhibitor prior to contact with host cells not only showed defective invasion (Fig. 1B), but also formed smaller vacuoles containing fewer parasites than control cells after 24 h incubation in the absence of the drug (Fig. 7C).

As we previously showed that host P-gp is involved in cholesterol transport from the host cell to the parasite vacuoles, a critical process for proper parasite replication [11], we hypothesized that the defective parasite replication observed during *T. gondii* treatment with the P-gp inhibitor GF120918 may derive from impaired lipid transport and/or synthesis. To test this, we treated isolated parasites with the inhibitor and monitored lipid synthesis after metabolic labeling. The fatty acid precursor [^{3}H]palmitic acid was readily incorporated in phospho- and sphingolipid species of control parasites (Fig. 7D). However, incubation with GF120918 induced a general decrease in parasite lipid synthesis. Interestingly, the inhibitor did not reduce the synthesis of all labeled lipids in a similar manner, but differently affected the relative amount of the lipid species, with PC synthesis being the most down-regulated while ceramide synthesis was increased compared with control cells. Next, we determined whether GF120918 affected not only lipid synthesis but also lipid precursor uptake. Liquid scintillation analysis revealed that inhibitor treatment strongly inhibited the incorporation of [^{3}H]palmitic acid in both total cell extracts and lipid fraction (Fig. 7E). This reduced incorporation was specific for [^{3}H]palmitic acid as incorporation of [^{3}H]choline was not affected by GF120918 treatment. Collectively, these data show that GF120918-induced inhibition of *T. gondii* replication was likely mediated by a reduction in parasite lipid uptake and synthesis.

Down-regulation of T. gondii P-gp correlates with reduced parasite replication and lipid synthesis. While *T. gondii* is able to grow in P-gp DKO host cells, its replication rate is reduced due to defective cholesterol trafficking to the parasite vacuole [11]. When we analyzed *T. gondii* maintained for more than 4 lysis cycles in P-gp DKO host cells, we found that the sub-optimal growth conditions did not trigger parasite stage conversion to the quiescent bradyzoite form (Fig. 8A). In addition, parasites isolated from P-gp DKO host cells after more than 4 passages were able to infect (Fig. 8B) and to egress from (Fig. 8C) new host cells as efficiently as parasites maintained in WT host cells. These finding suggest that the lower parasite burden observed was not caused by compromised infection or exit from host cells, but by a specific defect in replication, consistent with the limited access to host cholesterol demonstrated previously [11]. However, when parasites isolated from P-gp DKO host cells were allowed to infect WT host cells with a normal cholesterol trafficking, their replication rate remained slower compared with parasites isolated from WT host cells, as monitored up to 72 h post infection (Fig. 8D and not shown). While it is conceivable that cholesterol storage still depleted in the parasite after prolonged growth in P-gp DKO host cells affected *T. gondii* replication, it is also possible that lipid transport and/or synthesis are altered in these parasites. To test this hypothesis, we monitored the lipid synthesis in *T. gondii* isolated from P-gp DKO host cells after more than 4 lysis cycles. Surprisingly, [^{3}H]palmitic acid labeled cells showed an overall decrease in lipid synthesis with a profile similar to what was observed during P-gp inhibition with GF120918 (Fig. 8E). To investigate whether the inhibition of lipid synthesis correlated with inhibition of *T. gondii* P-gp, we performed real-time PCR (Fig. 8F) and P-gp functionality assay (Fig. 8G) on parasites isolated from WT or P-gp

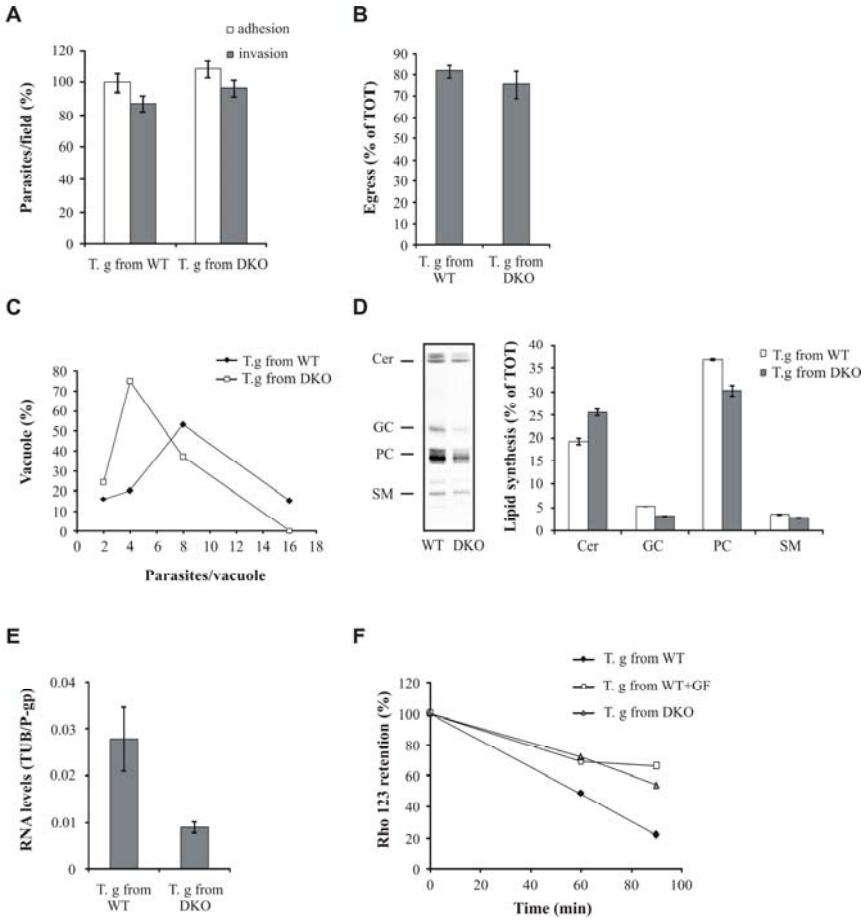

Figure 8: Down-regulation of *T. gondii* P-gp correlates with decreased lipid synthesis. A. Immunoflorescence analysis using antibodies against the bradyzoite-specific antigen BAG1 showing the absence of parasite stage conversion into bradyzoites after more than 4 lysis cycles in P-gp DKO host cells (upper panels). Lower panels, positive control of parasites induced to differentiate by alkaline treatment as described in the Materials and Methods section. Arrows, parasite vacuoles. DIC, differential interference contrast images. B. Adhesion/invasion assay in WT host cells of *T. gondii* isolated from P-gp WT or DKO host cells after more than 4 lysis cycles. Adherent and invaded parasites were counted after dual color immunostaining. Data are average of parasites per field ± SE (n=10) and expressed as percentage of cntl adhesion of *T. gondii* maintained in WT host cells. C. The same isolated parasites were allowed to replicate in WT host cells for 30 h, following induction of egress with 1 µM A23187 for 10 min. Data are average of egressed parasites per field ± SE (n=15) expressed as percentage of the total (egressed + intravacuolar) parasites. D. Parasites isolated from P-gp WT or DKO host cells after more than 4 lysis cycles were incubated with WT host cells for 24 h. Intracellular parasites were quantified by direct counting after immunostaining. The distribution of the parasite number in single vacuoles is expressed as percentage of total vacuoles examined (n>100). E. Parasites isolated from P-gp WT or DKO host cells after more than 4 lysis cycles were labeled with 0.5 µCi/mL of [^{3}H]palmitic acid for 3 h and lipid were extracted. Left panel, TLC separation of de novo synthesized lipids. Lipid standard used: ceramide (Cer), glucosylceramide (GC), phosphatidylcholine (PC), sphingomyelin (SM). Right panel, quantification of the relative amount of newly synthesized lipid species expressed as percentage of total lipids. Data are average ± SE (n=3). F. Semi-quantitative real time PCR of P-gp expression levels in parasites isolated from P-gp WT or DKO host cells after more than 4 lysis cycles. Gene expression levels were given as values in arbitrary units relative to the amount of the constitutively expressed house-keeping gene tubulin. Data are average ± SE (n =5). G. Functionality assay of P-gp in *T. gondii* isolated from P-gp WT or DKO host cells after more than 4 lysis cycles. Parasites from WT host cells were treated with 5 µM GF120918 (GF) as positive control for inhibition of P-gp functionality. Intracellular rhodamine 123 (Rho 123) retention is expressed as percentage of mean fluorescence of intracellular Rho 123 at time 0.

DKO host cells. Both approaches indicated that P-gp expression and activity were reduced in parasites grown in P-gp DKO host cells, supporting the correlation between lipid synthesis and P-gp activity revealed by pharmacological P-gp inhibition.

Discussion

P-gp has been shown to be a major mechanism of multidrug resistance in pathogenic organisms, including protozoan parasites (rev. in [34]). However, the physiological roles of P-gp in the absence of drug pressure remain poorly understood. In the present study we investigated the effects of the potent, third generation P-gp inhibitor GF120918 in the pathogenic parasite *T. gondii*. We found a dual role of GF120918 in the parasite physiology, namely in Ca^{2+}-dependent processes and lipid synthesis.

GF120918 treatment and Ca^{2+}-regulated processes. Ca^{2+} fluxes have been shown to play a key role in *T. gondii* invasion by regulating the secretion of microneme proteins, which serve as a bridge between the internal actin-myosin motor system and external substrates, and thus mediate both *T. gondii* adhesion and movement [35]. However, the molecular mechanisms regulating Ca^{2+} homeostasis in the parasite are not completely elucidated [36]. Here we showed that GF120918 treatment induced the secretion of the microneme protein MIC2 in absence of contact with host cells. In addition, increased MIC2 secretion correlated with increased parasite motility, in terms of number and length of trails left by the parasite while gliding on a substrate. Increased motility was not reported in a previous study using an early generation P-gp inhibitor [6]. While the different methods used by the authors to quantify parasite movement could account for this discrepancy, another explanation derives from different potency and binding capacity of the inhibitors to P-gp, which is also suggested by the different reversibility of the compounds observed in replication and invasion assays. Consistent with a role in promoting Ca^{2+}-mediated motility, GF120918 treatment induced *T. gondii* egress from infected host cells, a process known to depend on parasite motility and Ca^{2+} fluxes [26].

Increased *T. gondii* motility has been reported only rarely, and is generally characterized by fast and unregulated movement not resulting in productive locomotion. Examples are treatments with jasplakinolide, an actin filament stabilizer [37], or selected small molecules identified in a screen for parasite invasion inhibitors [38]. However treatment with calmidazolium, which increased intracellular Ca^{2+} levels in the parasite, induced both microneme secretion and productive motility [39]. The mechanism of calmidazolium-mediated increase of Ca^{2+} levels has not been identified in the parasite as yet; however the fact that chelation of extracellular Ca^{2+} decreased the calmidazolium-induced parasite motility led to the hypothesis that the compound may promote the influx of extracellular Ca^{2+} by modulating a Ca^{2+} transporter localized on the parasite plasma membrane [39]. Importantly, in our experimental conditions, extracellular Ca^{2+}chelation decreased the GF120918-induced parasite motility as well. The striking similarity of the calmidazolium and GF120918 effect on parasite motility strongly suggests that the two compounds operate on a similar molecular mechanism and reveal a possible involvement of P-gp in Ca^{2+} signaling in the parasite. In addition, it is possible that calmidazolium, which is marketed as a calmodulin inhibitor, induced the *T. gondii* phenotype by interfering with P-gp function, as Pgp is inactivated by calmodulin antagonists [40]. Conversely, GF120918 has not been reported thus far to interfere with Ca^{2+} transport or Ca^{2+}-

dependent processes. Analysis of P-gp-dependent Ca^{2+} fluxes is limited by the fact that commonly used Ca^{2+} indicators are known P-gp substrates and are actively exported from the cell interior [41]. However studies performed with radiolabeled Ca^{2+} in mammalian cells indicated that this ion accumulated more in P-gp over-expressing than in control cells [42-44]. Two P-type Ca^{2+} transporters, the plasma membrane Ca^{2+}-ATPase (PMCA) and the sarcoplasmic reticulum Ca^{2+}-ATPase (SERCA), play a crucial role in maintaining Ca^{2+} homeostasis. Both proteins counter-transport protons and alteration of intracellular pH has been shown to produce changes in Ca^{2+} levels (Rev. in [45]). Interestingly, P-gp expression has been associated with outward proton movement and intracellular alkalinization as a consequence of increased Cl^-/H^+ antiport [46]; similar data were also obtained in the analysis of human P-gp over-expression in yeast cells [47] and in the characterization of a bacterial P-gp homologue [48]. While the direct mechanism regulating the P-gp-mediated ion transport is not known, it is conceivable that P-gp may play a role in Ca^{2+} homeostasis by regulating cellular concentration of protons and pH-dependent Ca^{2+} transporters. Ca^{2+} regulation via PMCA and SERCA homologues is operational in *T. gondii* (rev. in [36,49]). Importantly, a PMCA-type Ca^{2+}-ATPase (TgA1) involved in Ca^{2+} influx, is localized to acidocalcisomes, the largest Ca^{2+} storage in *T. gondii* (rev. in [31]). TgA1 deficiency reduced *T. gondii* invasion and decreased parasite virulence [32], confirming that these organelles play an essential role in Ca^{2+} homeostasis and cellular processes in the parasite. Surprisingly, our localization data revealed that P-gp was found not only on the plasma membrane of the parasite, but also in acidocalcisomes, further supporting a P-gp involvement in Ca^{2+} regulation. Similarly to the observations with the acidocalcisome marker type I vacuolar-type H^+-pyrophosphatase [50], P-gp transiently re-localized in a collar-like structure at the apical end of extracellular parasites. Thus, we can propose a model where P-gp may participate in the Ca^{2+} homeostasis via facilitating Ca^{2+} uptake in acidocalcisomes by contributing to the establishment of the proton gradient in the organelles and, in addition, via promoting the function of TgA1. In addition, P-gp may also facilitate the activity of PMCA and its inhibition would promote the entry of extracellular Ca^{2+} and increase parasite motility. In support of this hypothesis, chelation of extracellular Ca^{2+} reduced GF120918-stimulated parasite motility.

P-gp has also been proposed as a regulator for Cl^- selective channels with a role in cell volume regulation [51]. As acidocalcisomes have been implicated in maintaining ionic homeostasis and regulating cell volume in Leishmania parasites [52], it is tempting to speculate that *T. gondii* P-gp present in these organelles may contribute to this regulatory function as well.

One intriguing finding of *T. gondii* treatment with GF120918 was the inhibition of host cell invasion despite increased microneme secretion. Microneme secretion is necessary for a successful host cell invasion; however several results suggest that it is not sufficient to promote this process. Strong stimulation of micronemes via prolonged Ca^{2+} increase inhibits parasite invasion ([24,53] and our study), presumably due to the exhaustion of required invasion factors. The increased inhibition of *T. gondii* invasion we observed following prolongation of the GF120918 incubation time suggested that a similar mechanism is responsible for the observed time dependent inhibition. In addition, *T. gondii* deficient for the acidocalcisome Ca^{2+} transporter AP1 also showed increased and

disregulated microneme secretion and invasion inhibition [32]. Interestingly, no invasion defect was observed in *T. gondii* with down-regulated P-gp expression, suggesting either that the reduced P-gp activity may still be sufficient to guarantee a normal infection rate, or that compensatory mechanisms are in place to maintain proper Ca^{2+} regulation.

GF120918 treatment and parasite replication. Our previous work demonstrated that functional host cell P-gp is required for normal parasite replication [11]. In contrast with mammalian cells where P-gp inhibition or absence does not affect cell replication, in this study we showed that GF120918 treatment inhibits parasite replication. Our analyses also indicated that the replication inhibition was likely caused by defective lipid synthesis, as GF120918 treatment selectively reduced palmitic acid incorporation in both total cell and lipid extracts. Conversely the normal choline incorporation in presence of GF120918 treatment suggested that the observed defect in palmitic acid incorporation is likely to occur also at the level of fatty acid uptake. The role of P-gp as a lipid transporter/flippase has been confirmed using labeled short chain lipid analogues [5]. In addition, the recently resolved X-ray structure of P-gp revealed the presence of portals open to both the cytoplasm and the inner leaflet of the plasma membrane, consistent with a function as a lipid flippase [54]. However, experiments with naturally occurring lipids are scarce and the physiological role of P-gp in endogenous lipid transport is still uncharacterized, with the only exception of platelet-activating factor (PAF) [55]. *T. gondii* has been shown to scavenge not only cholesterol [56], but also a variety of lipids from the host cells [57]. While the mechanisms by which host–derived lipids reach the parasite are not completely elucidated, the formation of H.O.S.T., a unique system of tubular structures, has been proposed to be a key event to sequester endo-lysosomes from the host cytoplasm into the parasite vacuole, thus providing *T. gondii* with cholesterol and possibly other lipids [58]. As our analyses showed that P-gp localized in the tubular structures forming the intravacuolar network, it is tempting to speculate that parasite P-gp is involved in the uptake of host–derived lipids, either directly or via modulation of other transporters. A broad analysis of lipid transport by *T. gondii* P-gp and related transporters will be an important area for future investigation.

Quite surprisingly, our localization studies also revealed an increased P-gp labeling in damaged parasite vacuoles, thus raising the question of a possible role of P-gp during cellular stress in the parasite. In support of this hypothesis, increased P-gp expression was observed in mammalian cells after radiation exposure and was associated with resistance to apoptotic signals and radioprotection [59], indicating that P-gp plays a role not only in cell protection during xenobiotic exposure, but also in cell survival during cell damage.

Finally, we found unexpectedly that parasites grown in P-gp deficient host cells had reduced P-gp expression. The molecular mechanisms leading to P-gp down-regulation remain to be determined. One possibility is that the reduced cholesterol content found in these parasites [11] affected P-gp expression, as cholesterol depletion has been shown to down-regulate P-gp expression [60]. Alternatively, the slower *T. gondii* replication rate observed during infection of P-gp deficient host cells may result in reduced P-gp expression. Consistent with this hypothesis, less virulent *T. gondii* strains which are characterized by a slower replication rate showed a reduced P-gp expression compared

with the virulent and fast replicating RH strain [9].

In summary, this study demonstrated that GF120918 treatment potently inhibits parasite invasion and replication, thus validating the potential of P-gp inhibitors as a therapeutic strategy against *T. gondii*. In addition, we also showed that GF120918 affected Ca^{2+}-dependent processes and lipid metabolism in the parasite. Finally, our results indicated that GF120918 can be used to specifically uncouple parasite motility and host cell invasion, thus providing a useful tool to study these processes. While our data on P-gp localization and expression are in support for a direct involvement of P-gp in these events, additional investigations using genetic approaches will be required to further our understanding of the function of P-gp and possibly other ABC transporters in the biology of *T. gondii*.

Materials and Methods

Biochemical reagents. Unless otherwise stated, all chemicals were purchased from Sigma and cell culture reagents from Gibco-BRL. GF120918 was a kind gift of GlaxoSmithKline. Reagents stock solutions were prepared at the following concentrations: 2 mM GF120918 in DMSO, 10 mM BAPTA (1,2-bis (2-aminophenoxy) ethane-N, N, N', N' tetracetic acid) in 0.3 M $NaHCO_3$, 1 mM A23187 in DMSO, 1 mg/mL rhodamine 123 in EtOH, 4.1 mM verapamil in PBS. Reagents were freshly diluted to the concentrations required for the individual experiment. Radiolabeled palmitic acid and choline were purchased from Amersham Pharmacia Biotech. Anti-P-gp monoclonal antibody C219 was purchased from Alexis Biochemicals; anti-*T. gondii* MIC2 and VP1 were a kind gift from J.F. Dubremetz (Université de Montpellier 2, Montpellier, France) and S. Moreno (University of Georgia, Athens, GA), respectively. Conjugated secondary antibodies were from Invitrogen. Lipid standards were from Avanti Polar Lipids, Alabaster, Alabama.

Mammalian cell and parasite culture. Mouse embryonic fibroblasts (MEF) double knocked out (DKO) for P-gp, (77.1 , $Mdr1a^{-/-}/Mdr1b^{-/-}$) [3] and parental cells were kindly provided by A. Schinkel (The Netherlands Cancer Institute, Amsterdam, The Nederlands). Cells were routinely cultured in Dulbecco's modified Eagle medium (DMEM) supplemented with 10% fetal calf serum (FCS), 2 mM glutamine, 50 U of penicillin/mL, and 50 µg of streptomycin/mL at 37°C with 5% CO_2. β-galactosidase expressing *T. gondii* were a kind gift from J. Boothroyd (Stanford University School of Medicine, Stanford, CA). *T. gondii* tachyzoites of the RH strain expressing *Escherichia coli* β-galactosidase [61] were used in this study. Parasites were maintained by serial passages in MEF, harvested from infected host cells by passage through a 26-gauge needle and purified by separation on Sephadex-G25 columns (Amersham) as described [62]. Purified parasites were counted in a hemocytometer chamber and used for a new cycle of host cell invasion.

For determination of parasite invasion, parasite were pre-treated with 10 µM GF120918 for 30 min at 37°C and allowed to infect for 4 h host cell monolayers at a multiplicity of infection (MOI) of 3 in presence of the drug. Alternatively, parasites were pre-treated with 10 µM GF120918 for 4 h, washed, and allowed to infect host cell monolayers in absence of the drug. After removal of residual extracellular parasites, infected cells were incubated for 20 h in absence of the drug and invasion was quantified by enumerating the parasite vacuoles per field.

For adhesion/invasion assay, parasites were pre-treated with 10 µM GF120918 for 30 min

at 37°C and allowed to infect host cell monolayers at MOI 3 for 2 h in presence of the drug. Alternatively, drug pre-treatment was omitted and 10 μM GF120918 added at the time of invasion. Parasites were analyzed by dual color immunostaining with anti-*T. gondii* antiserum to differentiate adherent (extracellular + intracellular) and invaded (intracellular) parasites, as described [63].

For determination of parasite replication, host cell monolyers were infected at a MOI of 3; and parasite burden was quantified after 24 hrs by direct parasite counting or after 48 or 72 hrs by colorimetric detection of parasite β-galactosidase using chlorophenol red-β-D galactopyranoside as substrate, as described [64]. During inhibitor analyses, GF120918 was added 2 h after infection at the concentration indicated in the figure legends.

Bradyzoite differentiation was induced in vitro by alkaline treatment as described [65]. Briefly, *T. gondii* tachyzoites were allowed to infect a host cell monolayer for 2 h and then the medium was replaced with RPMI-1640 containing 1g/L $NaHCO_3$ and 50mM tricine that had been adjusted to pH 8.1 with NaOH. Cultures were incubated at 37°C and ambient CO_2 for 4 days.

Cell viability of parasites was tested by trypan blue exclusion; metabolic activity of host cells was tested by using the AlamarBlue™ assay (BioSource, Camarillo, CA), according to the manufacturer instructions.

P-glycoprotein functional assay. P-gp activity was assessed by cellular retention of the P-gp substrate rhodamine 123 (Rho). Briefly, cells were incubated with 0.5 mg/mL Rho in PBS for 30 min at 37˚C in presence or absence of GF120918, at the concentrations indicated in the figure legends. After washing in PBS, cells were incubated in medium at 37˚C in absence or presence of the inhibitor for the time points indicated in the figure legend. The kinetic of rhodamine retention was quantified using a FACSCalibur flow cytometer (Becton & Dickinson, Basel, Switzerland).

Motility assay. Motility was assayed by trail deposition visualization, as described [38] with the following modifications. Freshly harvested parasites were resuspended in HBSS containing 1% FCS and 10 mM Hepes, pre-treated with 10 μM GF120918 or DMSO for 15 min at 4°C, then added to poly-lysine coated slides (Thermo Fisher, Portsmouth, NH) for 15 min at room temperature and allowed to glide for 30 min at 37°C. After buffer removal, parasite trails were fixed in PBS containing 3.6% formaldehyde, blocked and stained with anti-*T. gondii* antiserum, 1: 400 dilution, followed by Alexa 488-conjugated goat anti-rabbit IgG, 1:200 dilution.

Egress. Egress was assayed as described [66], with the following modifications. P-gp DKO MEF monolayers were grown on 10-well glass slides (Thermo Fisher, Portsmouth, NH), infected with *T. gondii* at an MOI of 3 and parasites were allowed to replicate for 30 h at 37°C. 10 μM GF120918 was added in the last 4 h of replication, then cells were fixed with 3.6% formaldehyde, blocked and stained with anti-*T. gondii* antiserum, 1: 2000 dilution, followed by Alexa 488-conjugated goat anti-rabbit IgG,1:200 dilution. For induced egress, infected monolayers were treated with 10 μM GF120918 as before, washed, incubated with 1 μM A23187 in warm HBSS buffer for 10 min at 37°C and stained as described before. Lysed and intact vacuoles were quantified and egress was expressed as percentage of lysed vacuoles out of the total vacuoles present in a given field.

Antibody production. *T. gondii* P-gp minigene was obtained by fusing three sequences of the parasite protein (aa 1-52, 295-331, 625-755) showing low degree of similarity with the mammalian P-gp. Oligonucleotides (5'-3' orientation) used in this study were:

s1 BamHI CGGGATCCATGGCCACCTCAGACGACT CATC, as1 XbaI GCTCTAGA TTCT GTTCCAGAGACGAAGTGGAAC, s2 XbaI GCTCTAGAGGACAAGTGATCTCCGAC GGA
TTG, as2 EcoRI CGGAATTC AGCGTCGCCACCCTGAAACTCCAG, s3 EcoRI
CGGAATTCATGAAAGACGAGAGCGGT CTG, as3 HindIII CCCAAGCTTAGGCCAGTAG CGGAGAGCGAG.

The P-gp minigene was inserted downstream of the maltose binding protein (MBP) in the plasmid vector pMal-2Cx (New England Biolabs, MA). The fusion protein was produced in transgenic *Escherichia coli* by induction with 0.3 mM IPTG (isopropyl-β-D-thiogalactopyranoside) for 2 h at 37°C. Following protein isolation by affinity purification on amylose resin according to the manufacturers protocol (New England Biolabs, MA), P-gp minigene was dialyzed, lyophilized and 150 µg used to immunize intraperitoneally with RIBI adjuvant (Corixa, Hamilton MT, USA) NMRI mice on days 0, 15, and 30 and 50.

Immunofluorescence analysis. Host cells infected with *T. gondii* or extracellular parasites were fixed in 3.6 % formaldehyde, permeabilized with 0.2% Triton X-100 in PBS for 20 min, when indicated in the figure legends, blocked and incubated with primary antibodies for 1 h. The primary antibodies used in this study were: anti-*T. gondii* tachyzoite rabbit antiserum [67], 1:2000 dilution, anti-*T. gondii* MIC2 monoclonal antiserum, 1:1000 dilution; anti-*T. gondii* VP1 rabbit antiserum, 1:2000 dilution; anti-*T. gondii* BAG1 rabbit antiserum [68], 1: 250 dilution; anti-*T. gondii* P-gp minigene mouse antiserum, 1:250 dilution. Fluorophore-conjugated secondary antibodies were used at 1: 200 dilution. Nuclei were visualized with 4', 6-diamidino-2-phenylindole (DAPI).

Microscopy analyses were performed on a Leica DM IRBE fluorescence microscope or on a Leica SP2 AOBS confocal laser-scanning microscope (Leica Microsystems, Wetzlar, Germany), using the appropriate settings. Image stacks of optical sections were further processed using the Huygens deconvolution software package version 2.7 (Scientific Volume Imaging, Hilversum, NL).

Transmission electron microscopy analysis. P-gp DKO host cells were grown in 75 cm^2 flasks, infected with *T. gondii* tachyzoites at MOI 1 and incubated at 37°C for 24 h prior to fixation with 3% paraformaldehyde and 0.5% glutaraldehyde. Ultrathin sections were stained with anti-P-gp C219, 1:2 dilution, followed by 10 nm gold conjugated anti-mouse antibodies, or double labeled with anti-P-gp C219, followed by 15 nm gold conjugated anti-mouse antibodies, and anti-VP1, 1:250 dilution, followed by 5 nm gold conjugated anti-rabbit antibodies. Sections were counterstained with uranyl acetate and lead citrate and analyzed in a transmission electron microscope (CM12, Philips, Eindhoven, The Netherlands) equipped with a CCD camera (Ultrascan 1000; Gatan, Pleasanton, CA) at an acceleration voltage of 100 kV.

Lipid analyses. For analysis of *T. gondii* lipid synthesis, purified parasites were labeled with 0.5 µCi/mL [^{3}H]palmitic acid or 4 µCi/mL [^{3}H]choline for 3 h in DMEM supplemented with 10% FCS. After extensive washing with PBS and 0.05% fat free BSA in PBS, lipids were extracted according to [69] and aliquots corresponding to equal protein content were separated by high performance thin layer chromatography (HPTLC) on Silica Gel 60 plates using chloroform/methanol/25% NH_4OH (65:25:4.5). Radiolabeled bands were visualized by use of a tritium-sensitive screen (Perkin-Elmer, Boston, MA) in a Personal

Molecular PhosphoImager FX (Biorad), identified according to co-migrating standards (Avanti Polar Lipids, Alabaster, Alabama) visualized by iodine vapors and quantified using ImageQuant software (Amersham, Otelfingen, Switzerland). For determination of radioactivity associated with total cell extract or lipid fraction, labeled cells aliquots were solubilized in 0.1N NaOH or lipid extracted as described above and radioactivity measured by liquid scintillation.

Semi-quantitative real time-PCR (RT-PCR). RNA was isolated from 10^7 parasites isolated from WT or P-gp DKO host cells after five lysis cycles using an RNAeasy kit (Qiagen, Stanford, CA) following the "Animal Cells Spin" protocol. Residual genomic DNA was removed with DNase I digestion according to the manufacturer's protocol. First strand cDNA synthesis was performed using ~250 ng RNA and Omniscript reverse transcriptase (Qiagen), according to manufacturer's protocol. Amplification was performed in an iCycler iQ (Biorad, Hercules, CA) Primer pairs (5'-3' orientation) used for amplification of parasite tubulin (TUB), and P-gp were: T.gTUB s CCAGGAGATGTTCAAG, T.gTUB as ACTCGGACACCAGGTCGTTC, T.gPgp s AAGGACAGCCGAAGGAAGAC, T.gPgp as GATGATGTCCGTCTGTGAC. Control PCR showed absence of contamination from host cell RNA or parasite genomic DNA. To assess the efficiency of the amplification reactions, standard curves for every primer pair and cDNA were generated from six-fold serial dilutions in duplicate, using the iQ5 software. Expression levels of the genes were given as values in arbitrary units relative to the amount of the constitutively expressed house-keeping gene tubulin.

Western blot analysis. Cell lysates for immunoblots were prepared by sonicating cells at 10^7/ml in 50 mM Tris-HCl (pH 6.8), 10% glycerol, 2% SDS, 5 mM DTT, 0.5 mM phenylmethylsulfonylfluoride and complete protease inhibitor mixture (Calbiochem). Samples corresponding to 40 μg proteins were mixed with SDS-PAGE loading buffer and incubated 10 min at room temperature to prevent P-gp aggregation. Samples were separated on 7.5% SDS-PAGE gels, transferred to nitrocellulose membranes, and probed using anti-P-gp C219 (1: 50), anti-*T. gondii* P-gp minigene (1:1000) and anti-tubulin (1:2000) antibodies. Immunoreactive bands were visualized with horseradish peroxidase-conjugated secondary antibodies and enhanced chemiluminescence (ECL).

Determination of protein concentration. Protein content was determined using the Bio-Rad Protein Assay according to the instructions provided by the manufacturer. Bovine serum albumin was used for the standard curve.

Acknowledgments

We thank GlaxoSmithKline AG for their kind gift of GF120918 compound, Jean-François Dubremetz and Silvia Moreno for kindly providing the anti-MIC2 and anti-VP1 antibodies and Mihaela Zavolan for bioinformatic analysis of *T. gondii* P-gp. We are grateful to John Boothroyd for the β-galactosidase-expressing *T. gondii*, Alfred Schinkel for kindly providing the P-gp deficient murine embryonic fibroblasts and Therese Michel for technical assistance.

References

1. Allikmets R, Gerrard B, Hutchinson A, Dean M (1996) Characterization of the human ABC superfamily: isolation and mapping of 21 new genes using the expressed sequence tags database. Hum Mol Genet 5: 1649-1655.
2. Higgins CF (1992) ABC transporters: from microorganisms to man. Annu Rev Cell Biol 8: 67-113.
3. Schinkel AH, Mayer U, Wagenaar E, Mol CA, van Deemter L, et al. (1997) Normal viability and altered pharmacokinetics in mice lacking mdr1-type (drug-transporting) P-glycoproteins. Proc Natl Acad Sci U S A 94: 4028-4033.
4. Ueda K, Okamura N, Hirai M, Tanigawara Y, Saeki T, et al. (1992) Human P-glycoprotein transports cortisol, aldosterone, and dexamethasone, but not progesterone. J Biol Chem 267: 24248-24252.
5. Orlowski S, Martin S, Escargueil A (2006) P-glycoprotein and 'lipid rafts': some ambiguous mutual relationships (floating on them, building them or meeting them by chance?). Cell Mol Life Sci 63: 1038-1059.
6. Silverman JA, Hayes ML, Luft BJ, Joiner KA (1997) Characterization of anti-Toxoplasma activity of SDZ 215-918, a cyclosporin derivative lacking immunosuppressive and peptidyl-prolyl-isomerase-inhibiting activity: possible role of a P glycoprotein in Toxoplasma physiology. Antimicrob Agents Chemother 41: 1859-1866.
7. Sauvage V, Aubert D, Bonhomme A, Pinon JM, Millot JM (2004) P-glycoprotein inhibitors modulate accumulation and efflux of xenobiotics in extra and intracellular Toxoplasma gondii. Mol Biochem Parasitol 134: 89-95.
8. Sauvage V, Millot JM, Aubert D, Visneux V, Marle-Plistat M, et al. (2006) Identification and expression analysis of ABC protein-encoding genes in Toxoplasma gondii. Toxoplasma gondii ATP-binding cassette superfamily. Mol Biochem Parasitol 147: 177-192.
9. Schmid A, Sauvage V, Escotte-Binet S, Aubert D, Terryn C, et al. (2009) Molecular characterization and expression analysis of a P-glycoprotein homologue in Toxoplasma gondii. Mol Biochem Parasitol 163: 54-60.
10. High KP (1994) The antimicrobial activities of cyclosporine, FK506, and rapamycin. Transplantation 57: 1689-1700.
11. Bottova I, Hehl AB, Stefanic S, Fabrias G, Casas J, et al. (2009) Host cell P-glycoprotein is essential for cholesterol uptake and replication of Toxoplasma gondii. J Biol Chem 284: 17438-17448.
12. Wallstab A, Koester M, Bohme M, Keppler D (1999) Selective inhibition of MDR1 P-glycoprotein-mediated transport by the acridone carboxamide derivative GG918. Br J Cancer 79: 1053-1060.
13. Hyafil F, Vergely C, Du Vignaud P, Grand-Perret T (1993) In vitro and in vivo reversal of multidrug resistance by GF120918, an acridonecarboxamide derivative. Cancer Res 53: 4595-4602.
14. Tamai I, Tsuji A (2000) Transporter-mediated permeation of drugs across the blood-brain barrier. J Pharm Sci 89: 1371-1388.
15. Zhang Y, Bachmeier C, Miller DW (2003) In vitro and in vivo models for

assessing drug efflux transporter activity. Adv Drug Deliv Rev 55: 31-51.
16. Bardelmeijer HA, Ouwehand M, Beijnen JH, Schellens JH, van Tellingen O (2004) Efficacy of novel P-glycoprotein inhibitors to increase the oral uptake of paclitaxel in mice. Invest New Drugs 22: 219-229.
17. Evers R, Kool M, Smith AJ, van Deemter L, de Haas M, et al. (2000) Inhibitory effect of the reversal agents V-104, GF120918 and Pluronic L61 on MDR1 Pgp-, MRP1- and MRP2-mediated transport. Br J Cancer 83: 366-374.
18. Ward KW, Azzarano LM (2004) Preclinical pharmacokinetic properties of the P-glycoprotein inhibitor GF120918A (HCl salt of GF120918, 9,10-dihydro-5-methoxy-9-oxo-N-[4-[2-(1,2,3,4-tetrahydro-6,7-dimethoxy-2-i soquinolinyl)ethyl]phenyl]-4-acridine-carboxamide) in the mouse, rat, dog, and monkey. J Pharmacol Exp Ther 310: 703-709.
19. Witherspoon SM, Emerson DL, Kerr BM, Lloyd TL, Dalton WS, et al. (1996) Flow cytometric assay of modulation of P-glycoprotein function in whole blood by the multidrug resistance inhibitor GG918. Clin Cancer Res 2: 7-12.
20. Huynh MH, Rabenau KE, Harper JM, Beatty WL, Sibley LD, et al. (2003) Rapid invasion of host cells by Toxoplasma requires secretion of the MIC2-M2AP adhesive protein complex. Embo J 22: 2082-2090.
21. Soldati D, Meissner M (2004) Toxoplasma as a novel system for motility. Curr Opin Cell Biol 16: 32-40.
22. Hakansson S, Morisaki H, Heuser J, Sibley LD (1999) Time-lapse video microscopy of gliding motility in Toxoplasma gondii reveals a novel, biphasic mechanism of cell locomotion. Mol Biol Cell 10: 3539-3547.
23. Lovett JL, Sibley LD (2003) Intracellular calcium stores in Toxoplasma gondii govern invasion of host cells. J Cell Sci 116: 3009-3016.
24. Carruthers VB, Giddings OK, Sibley LD (1999) Secretion of micronemal proteins is associated with toxoplasma invasion of host cells. Cell Microbiol 1: 225-235.
25. Carruthers VB, Sherman GD, Sibley LD (2000) The Toxoplasma adhesive protein MIC2 is proteolytically processed at multiple sites by two parasite-derived proteases. J Biol Chem 275: 14346-14353.
26. Moudy R, Manning TJ, Beckers CJ (2001) The loss of cytoplasmic potassium upon host cell breakdown triggers egress of Toxoplasma gondii. J Biol Chem 276: 41492-41501.
27. Lavine MD, Arrizabalaga G (2008) Exit from host cells by the pathogenic parasite Toxoplasma gondii does not require motility. Eukaryot Cell 7: 131-140.
28. Persson EK, Agnarson AM, Lambert H, Hitziger N, Yagita H, et al. (2007) Death receptor ligation or exposure to perforin trigger rapid egress of the intracellular parasite Toxoplasma gondii. J Immunol 179: 8357-8365.
29. Endo T, Sethi KK, Piekarski G (1982) Toxoplasma gondii: calcium ionophore A23187-mediated exit of trophozoites from infected murine macrophages. Exp Parasitol 53: 179-188.
30. Hoff EF, Carruthers VB (2002) Is Toxoplasma egress the first step in

invasion? Trends Parasitol 18: 251-255.
31. Miranda K, de Souza W, Plattner H, Hentschel J, Kawazoe U, et al. (2008) Acidocalcisomes in Apicomplexan parasites. Exp Parasitol 118: 2-9.
32. Luo S, Ruiz FA, Moreno SN (2005) The acidocalcisome Ca2+-ATPase (TgA1) of Toxoplasma gondii is required for polyphosphate storage, intracellular calcium homeostasis and virulence. Mol Microbiol 55: 1034-1045.
33. Robert J (1998) Approaches to multidrug resistance reversal. Expert Opin Investig Drugs 7: 929-939.
34. Sauvage V, Aubert D, Escotte-Binet S, Villena I (2009) The role of ATP-binding cassette (ABC) proteins in protozoan parasites. Mol Biochem Parasitol 167: 81-94.
35. Jewett TJ, Sibley LD (2003) Aldolase forms a bridge between cell surface adhesins and the actin cytoskeleton in apicomplexan parasites. Mol Cell 11: 885-894.
36. Moreno SN, Docampo R (2003) Calcium regulation in protozoan parasites. Curr Opin Microbiol 6: 359-364.
37. Wetzel DM, Hakansson S, Hu K, Roos D, Sibley LD (2003) Actin filament polymerization regulates gliding motility by apicomplexan parasites. Mol Biol Cell 14: 396-406.
38. Carey KL, Westwood NJ, Mitchison TJ, Ward GE (2004) A small-molecule approach to studying invasive mechanisms of Toxoplasma gondii. Proc Natl Acad Sci U S A 101: 7433-7438.
39. Wetzel DM, Chen LA, Ruiz FA, Moreno SN, Sibley LD (2004) Calcium-mediated protein secretion potentiates motility in Toxoplasma gondii. J Cell Sci 117: 5739-5748.
40. Ford JM (1996) Experimental reversal of P-glycoprotein-mediated multidrug resistance by pharmacological chemosensitisers. Eur J Cancer 32A: 991-1001.
41. Homolya L, Hollo Z, Germann UA, Pastan I, Gottesman MM, et al. (1993) Fluorescent cellular indicators are extruded by the multidrug resistance protein. J Biol Chem 268: 21493-21496.
42. Tsuruo T, Iida H, Kawabata H, Tsukagoshi S, Sakurai Y (1984) High calcium content of pleiotropic drug-resistant P388 and K562 leukemia and Chinese hamster ovary cells. Cancer Res 44: 5095-5099.
43. Sulova Z, Orlicky J, Fiala R, Dovinova I, Uhrik B, et al. (2005) Expression of P-glycoprotein in L1210 cells is linked with rise in sensitivity to Ca2+. Biochem Biophys Res Commun 335: 777-784.
44. Mestdagh N, Vandewalle B, Hornez L, Henichart JP (1994) Comparative study of intracellular calcium and adenosine 3',5'-cyclic monophosphate levels in human breast carcinoma cells sensitive or resistant to Adriamycin: contribution to reversion of chemoresistance. Biochem Pharmacol 48: 709-716.
45. Austin C, Wray S (2000) Interactions between Ca(2+) and H(+) and functional consequences in vascular smooth muscle. Circ Res 86: 355-363.
46. Hoffman MM, Roepe PD (1997) Analysis of ion transport perturbations caused by hu MDR 1 protein overexpression. Biochemistry 36: 11153-11168.
47. Fritz F, Howard EM, Hoffman MM, Roepe PD (1999) Evidence for altered ion transport in Saccharomyces cerevisiae overexpressing human

MDR 1 protein. Biochemistry 38: 4214-4226.
48. Velamakanni S, Lau CH, Gutmann DA, Venter H, Barrera NP, et al. (2009) A multidrug ABC transporter with a taste for salt. PLoS One 4: e6137.
49. Nagamune K, Moreno SN, Chini EN, Sibley LD (2008) Calcium regulation and signaling in apicomplexan parasites. Subcell Biochem 47: 70-81.
50. Drozdowicz YM, Shaw M, Nishi M, Striepen B, Liwinski HA, et al. (2003) Isolation and characterization of TgVP1, a type I vacuolar H+-translocating pyrophosphatase from Toxoplasma gondii. The dynamics of its subcellular localization and the cellular effects of a diphosphonate inhibitor. J Biol Chem 278: 1075-1085.
51. Valverde MA, Bond TD, Hardy SP, Taylor JC, Higgins CF, et al. (1996) The multidrug resistance P-glycoprotein modulates cell regulatory volume decrease. Embo J 15: 4460-4468.
52. Lefurgey A, Gannon M, Blum J, Ingram P (2005) Leishmania donovani amastigotes mobilize organic and inorganic osmolytes during regulatory volume decrease. J Eukaryot Microbiol 52: 277-289.
53. Mondragon R, Frixione E (1996) Ca(2+)-dependence of conoid extrusion in Toxoplasma gondii tachyzoites. J Eukaryot Microbiol 43: 120-127.
54. Aller SG, Yu J, Ward A, Weng Y, Chittaboina S, et al. (2009) Structure of P-glycoprotein reveals a molecular basis for poly-specific drug binding. Science 323: 1718-1722.
55. Ernest S, Bello-Reuss E (1999) Secretion of platelet-activating factor is mediated by MDR1 P-glycoprotein in cultured human mesangial cells. J Am Soc Nephrol 10: 2306-2313.
56. Coppens I, Sinai AP, Joiner KA (2000) Toxoplasma gondii exploits host low-density lipoprotein receptor-mediated endocytosis for cholesterol acquisition. J Cell Biol 149: 167-180.
57. Charron AJ, Sibley LD (2002) Host cells: mobilizable lipid resources for the intracellular parasite Toxoplasma gondii. J Cell Sci 115: 3049-3059.
58. Coppens I, Dunn JD, Romano JD, Pypaert M, Zhang H, et al. (2006) Toxoplasma gondii sequesters lysosomes from mammalian hosts in the vacuolar space. Cell 125: 261-274.
59. Maier P, Fleckenstein K, Li L, Laufs S, Zeller WJ, et al. (2006) Overexpression of MDR1 using a retroviral vector differentially regulates genes involved in detoxification and apoptosis and confers radioprotection. Radiat Res 166: 463-473.
60. Rodrigues AC, Curi R, Hirata MH, Hirata RD (2009) Decreased ABCB1 mRNA expression induced by atorvastatin results from enhanced mRNA degradation in HepG2 cells. Eur J Pharm Sci 37: 486-491.
61. Seeber F, Boothroyd JC (1996) Escherichia coli beta-galactosidase as an in vitro and in vivo reporter enzyme and stable transfection marker in the intracellular protozoan parasite Toxoplasma gondii. Gene 169: 39-45.
62. Hemphill A, Gottstein B, Kaufmann H (1996) Adhesion and invasion of bovine endothelial cells by Neospora caninum. Parasitology 112 (Pt 2): 183-197.
63. Hemphill A (1996) Subcellular localization and functional characterization of Nc-p43, a major

Neospora caninum tachyzoite surface protein. Infect Immun 64: 4279-4287.
64. Sonda S, Ting LM, Novak S, Kim K, Maher JJ, et al. (2001) Cholesterol esterification by host and parasite is essential for optimal proliferation of Toxoplasma gondii. J Biol Chem 276: 34434-34440.
65. Soete M, Camus D, Dubremetz JF (1994) Experimental induction of bradyzoite-specific antigen expression and cyst formation by the RH strain of Toxoplasma gondii in vitro. Exp Parasitol 78: 361-370.
66. Black MW, Arrizabalaga G, Boothroyd JC (2000) Ionophore-resistant mutants of Toxoplasma gondii reveal host cell permeabilization as an early event in egress. Mol Cell Biol 20: 9399-9408.
67. Fuchs N, Sonda S, Gottstein B, Hemphill A (1998) Differential expression of cell surface- and dense granule-associated Neospora caninum proteins in tachyzoites and bradyzoites. J Parasitol 84: 753-758.
68. McAllister MM, Parmley SF, Weiss LM, Welch VJ, McGuire AM (1996) An immunohistochemical method for detecting bradyzoite antigen (BAG5) in Toxoplasma gondii-infected tissues cross-reacts with a Neospora caninum bradyzoite antigen. J Parasitol 82: 354-355.
69. Bligh EG, Dyer WJ (1959) A rapid method of total lipid extraction and purification. Can J Med Sci 37: 911-917.

Supporting online material

A

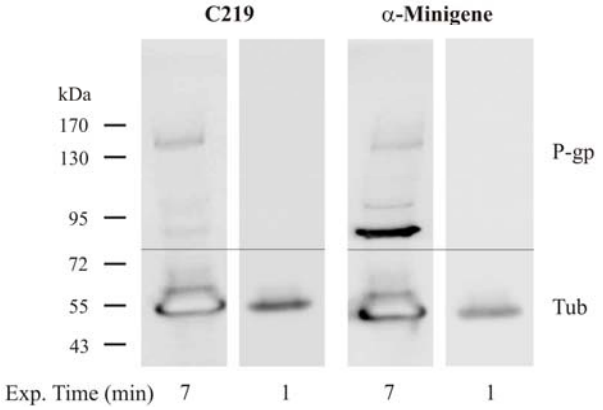

B

Figure S1: Detection of P-gp in *T. gondii*. A. Immunoblot analysis of *T. gondii* extracts probed with the P-gp specific monoclonal antibody C219 or with the anti-*T. gondii* P-gp minigene antibody. Tubulin staining was used as a loading control. Due to the low levels of P-gp expression compared with tubulin, probed membranes were exposed for different times to record unsaturated signal for both proteins. B. Protein sequence alignment of *T. gondii* P-gp (Tgmdr1) with the two mouse homologues. Highlighted in yellow are the sequences used to create the P-gp minigene fusion protein. Red box, sequence used in a previous study [1] to raise antibodies specific for *T. gondii* P-gp. Green box, epitope recognized by the P-gp specific monoclonal antibody C219. Gene bank accession numbers: T.g mdr1, DQ094188; Mmdr1a, NP_035206; Mmdr1b, NP_035205.

1. Schmid A, Sauvage V, Escotte-Binet S, Aubert D, Terryn C, et al. (2009) Molecular characterization and expression analysis of a P-glycoprotein homologue in Toxoplasma gondii. Mol Biochem Parasitol 163: 54-60.

Manuscript 3

Epigenetic mechanisms regulate stage differentiation in the minimized protozoan *Giardia lamblia*

Epigenetic mechanisms regulate stage differentiation in the minimized protozoan *Giardia lamblia*.

Sabrina Sonda[1§]*, Laura Morf[1§], Iveta Bottova[1], Hansruedi Baetschmann[2], Hubert Rehrauer[2], Amedeo Caflisch[3], Mohamed-Ali Hakimi[4] and Adrian B. Hehl[1]*

[1]Institute of Parasitology and [3]Department of Biochemistry, University of Zurich, 8057 Zurich, Switzerland; [2] Functional Genomics Center Zurich, 8057 Zurich, Switzerland, [4]UMR5163, Laboratoire Adaptation et Pathogénie des Micro-organismes, Centre National de la Recherche Scientifique (CNRS), Université Joseph Fourier Grenoble 1, BP 170, 38042 Grenoble, Cedex 09, France

[§]These authors contributed equally to this work

Address correspondence to:
Sabrina Sonda, E-mail: sabrina.sonda@vetparas.uzh.ch
Adrian B. Hehl, E-mail: adrian.hehl@access.uzh.ch *Address correspondence to:

SUMMARY

Histone modification is an important mechanism regulating both gene expression and the establishment and maintenance of cellular phenotypes during development. Regulation of histone acetylation via histone acetylases (HAT) and deacetylases (HDAC) appears to be particularly crucial in determining gene expression patterns. In this study we explored the effect of HDAC inhibition on the life cycle of the human pathogen *Giardia lamblia*, a highly reduced parasitic protozoan characterized by minimized cellular processes. We found that the HDAC inhibitor FR235222 increased the level of histone acetylation and induced transcriptional regulation of ~2% of genes in proliferating and encysting parasites. In addition, our analyses showed that the levels of histone acetylation decreased during differentiation into cysts, the infective stage of the parasite. Importantly, FR235222 treatment during encystation reversed this histone hypo-acetylation and potently blocked the formation of cysts. These results provide the first direct evidence for epigenetic regulation of gene expression in this simple eukaryote. This suggests that regulation of histone acetylation is involved in the control of *Giardia* stage differentiation, and identifies epigenetic mechanisms as a promising target to prevent *Giardia* transmission.

INTRODUCTION

Regulation of gene expression is a complex process controlled by several molecular mechanisms including modification of chromatin structure, activity of sequence-specific DNA binding proteins, and post-transcriptional modulation of mRNA levels. Epigenetic histone modifications result in alteration of chromatin structure, which in turn induces changes in gene expression (reviewed in (Jenuwein and Allis, 2001; Kouzarides, 2007)). In general terms, the process of covalent histone acetylation regulates gene expression by modifying DNA packaging, with histone hyperacetylation leading to chromatin decondensation and activation of transcription. Conversely, histone hypoacetylation leads to a tighter DNA-histone binding, with consequent chromatin condensation and gene silencing. The level of histone acetylation is strictly controlled by the concerted activity of histone acetylases (HAT) and deacetylases (HDACs), which act as central organizers of chromatin remodeling and gene transcription. The correct regulation of HDACs is critical for cellular homeostasis. The importance of a tight control of HDAC activity is exemplified by its up-regulation associated with uncontrolled cell growth at the onset of cancer (Glozak and Seto, 2007). In this context, considerable efforts have been invested to develop inhibitors of HDAC activity (HDACi) as anti-cancer drugs, as HDACi were shown to counteract aberrant cell cycle

regulation in cancer cells both *in vitro* and *in vivo* (Bolden et al., 2006). In addition, recent studies revealed that the activity of HDACs is crucial not only for cell cycle regulation but also for the orchestration of development and cell differentiation in different mammalian organs (Haumaitre et al., 2009; Margueron et al., 2005). Despite these recent advances, our understanding of the roles HDACs play remains limited.

In this study we investigated whether HDAC activity also plays a role in the differentiation process of the intestinal pathogenic parasite *Giardia lamblia*, a protozoan characterized by a highly reduced genome and significant minimization of most cellular systems due to secondary reduction (Morrison et al., 2007). In this respect, the parasite is a useful model organism to study basic biological processes of other higher eukaryotes. The *G. lamblia* life cycle is comprised of highly motile flagellated trophozoites and quiescent cyst surrounded by a protective cyst wall (Gerwig et al., 2002). Differentiation from the trophozoite to the cyst stage is critical for the parasite survival in the environment and disease transmission.

G. lamblia encystation is a complex process that involves both expression of specific proteins and also changes in the parasite's metabolism (Adam, 2001). The encystation process begins with an early phase where cyst wall components, including CWPs1-3, are synthesized and accumulated in encystation-specific secretory vesicles (ESVs). ESVs are formed transiently only during the time of encystation and display Golgi-like characteristics (Hehl and Marti, 2004; Lujan *et al.*, 1998; Marti and Hehl, 2003; Stefanic *et al.*, 2009), allowing both maturation and export of the CWPs to the cell exterior to form the cyst wall. This late phase is completed with the sequential secretion of two layers of cyst wall material to the parasite surface 20-24 h after induction of encystation, where it polymerizes to a rigid extracellular matrix, the cyst wall.

Despite recent discoveries in the field of *G. lamblia* encystation, our understanding of the molecular mechanisms initiating and regulating gene expression during this critical process remains incomplete. Several factors have been found to be implicated, including kinase and phosphatase-mediated signal transduction (Bazan-Tejeda *et al.*, 2007; Ellis *et al.*, 2003; Lauwaet *et al.*, 2007; Pan *et al.*, 2009), arginine deiminase activity (Touz et al., 2008), proteinases (Touz et al., 2002a) and dipeptidyl peptidase IV (Touz et al., 2002b). In addition, we recently showed that the synthesis of the sphingolipid glucosylceramide is also essential for complete cyst formation in *G. lamblia* (Štefanić et al., submitted). However, much less is known about transcriptional regulation of encystation-specific genes. To date only a few putative encystation-related transcription factors have been identified and partially characterized in *G. lamblia*: a Myb2 homolog (Huang et al., 2008; Sun et al., 2002), two members of the GARP family (Sun et al., 2006), one ARID family member (Wang et al., 2007) and a recently described WRKY protein (Pan et al., 2009). All these transcription factors, whose expression increases during encystation, bind to the short promoter of encystation-induced genes and act as *trans*-activators of transcription. In addition to trans-activating factors, mechanisms for negative regulation have also been suggested to control CWP expression in vegetative trophozoites, including regulation of mRNA stability via the 3' untranslated region (UTR) (Hehl et al., 2000), the nonsense-mediated mRNA decay (NMD) factor UPF1 (Chen et al., 2008), and presence of negative *cis*-acting elements in the CWP promoters (Davis-Hayman et al., 2003).

Because *G. lamblia* encystation is associated with clearly detectable changes in mRNA levels and the degree of histone acetylation is critical for transcriptional control, we hypothesized that epigenetic chromatin modifications via histone acetylation may participate in the modulation of stage differentiation in this parasite. To test this, we analyzed whether modifying histone acetylation levels by inhibiting giardial HDAC affected parasite encystation.

RESULTS

Histone acetylation decreases during *G. lamblia* stage conversion. *G. lamblia* encystation is regulated at the transcriptional level and results in high levels of transcription of encystation-specific genes during the first 7-9 h post induction. To investigate whether epigenetic mechanisms dependent on histone

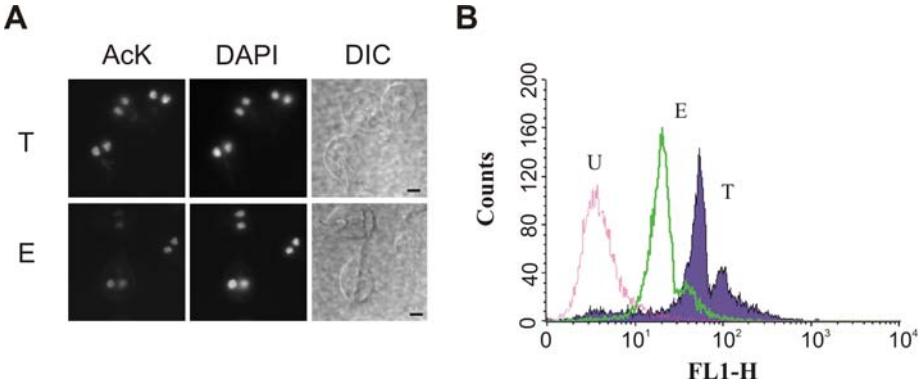

Figure 1: Acetylation levels decrease in *G. lamblia* upon induction of encystation. Trophozoites (T) and parasites induced to encyst for 16 h (E) were probed for acetylated lysine (AcK). A. Immunofluorescence analysis showing the staining restricted to the nuclei in both stages of the parasite. DAPI, nuclear staining; DIC, differential interference contrast. Scale bar: 3 μm. B. Overlay histogram of the FACS analysis showing trophozoites (T) and encysting cells (E) stained for AcK. U, unstained cells. Note the decreased intensity of AcK staining in encysting cells compared with trophozoites (logarithmic scale on x-axis).

acetylation are involved in the stage conversion of *G. lamblia*, we compared the histone acetylation levels in trophozoites and encysting cells. To test this, we incubated isolated parasites with an anti-acetyl lysine antibody after chemical fixation and detergent permeabilization. Immunofluorescence analysis revealed that the labeling was restricted to the nuclei and that it overlapped with DAPI-stained DNA, as expected for labeled histones (Fig. 1A). As previously shown for the labeling of methyl-modified histones (Dawson et al., 2007), the two giardial nuclei were similarly stained, indicating that the chromatin of both nuclei can be modified by the acetylation mark. Importantly, no cross-reaction was observed with cytosolic acetylated proteins, including tubulin (Fig. 4B), indicating that the antibody exclusively recognizes acetylated proteins restricted to the nucleus.
Next we quantified the degree of histone acetylation in trophozoites and encysting cells by flow cytometry. Our analysis showed that the staining intensity decreased in differentiating trophozoites (Fig. 1B), suggesting that the levels of histone acetylation are regulated in the parasite in a stage-specific manner.

Characterization of *G. lamblia* HDAC. As the cellular levels of histone acetylation are maintained by the concerted activity of HAT and HDAC enzymes, we investigated whether these enzymes are present in the parasite.
Analysis of the Giardia Genome Database (www.giardiadb.org) revealed the presence of putative enzymes responsible for histone modification, including HDACs (Table 1). In mammalian cells, the classical HDAC family consists of the ubiquitously expressed class I (HDAC1-3, 8) and the tissue-specific classes II (HDAC4-7, 9, 10) and IV (HDAC11), while the structurally unrelated class III is composed of sirtuin proteins 1-7. Interestingly, the *G. lamblia* genome codes for only one predicted homologue of the classical HDAC family, and four additional predicted sirtuin type 2 family homologues. Multiple sequence alignments showed a high level of similarity between the single giardial HDAC and orthologues of protozoan and metazoan species (Fig. 2 and Table 2), indicating that the protein is highly conserved in this parasite. Importantly the amino acids thought to be critical for human HDAC1 activity, including the residues in the catalytic pocket that co-ordinate binding to the co-factor Zn^{2+}, and that are in contact with the HDAC inhibitor Trichostatin A (Finnin et al., 1999; Vannini et al., 2004) are also present

Table 1. Putative histone modifying enzymes in *G. lamblia*	
Histone acetylases	
GL50803_10666	Histone acetyltransferase GCN5
GL50803_2851	Histone acetyltransferase MYST2
GL50803_16639	Histone acetyltransferase Elp3
GL50803_14753	Histone acetyltransferase type B subunit 2
GL50803_17263	Histone acetyltransferase MYST1
Histone deacetylases	
GL50803_3281	Histone deacetylase I
GL50803_10707	NAD-dependent histone deacetylase Sir2
GL50803_10708	Hypothetical protein, Sir2 domain
GL50803_16569	Transcriptional regulator, Sir2 family
GL50803_6942	Sir2 family protein
GL50803_11676	Sirtuin type 2
Histone methylases	
GL50803_8921	Set-2, putative
GL50803_13838	Hypothetical protein
GL50803_13790	Hypothetical protein
GL50803_9130	Histone methyltransferase HMT1
GL50803_17036	Hypothetical protein
GL50803_221691	Histone methyltransferase HMT2

Table 2. Sequence comparison of Gl HDAC with selected orthologues

Name	Identity (%)	Similarity (%)	AA overlap
Tg_ HDAC3	48	68	376
Eh_ HDAC	46	64	377
Mm_ HDAC1	50	72	368
Hs_ HDAC1	50	72	368
Sc_ RPD3	51	69	372
Hs _HDAC3	45	66	432
Hs _HDAC8	41	62	368

in the giardial HDAC. Interestingly, the predicted giardial HDAC does not possess an AT insertion which is typical of Apicomplexa (Bougdour et al., 2009), but contains a unique four-residue insertion in position 283-286, which is not found in other species.

To analyze the localization of giardial HDAC, a recombinant variant fused to a C-terminal HA tag was expressed in the parasites. Immunofluorescence analysis of transgenic cells revealed that the protein localizes to the parasite nuclei, suggesting that the giardial HDAC is likely to function in this subcellular location (Fig. 3A).

To gain further insights into the structure-function basis of giardial HDAC, a homology model was generated using the recently resolved structure of human HDAC8 as a template (Fig. 3B) (Vannini *et al.*, 2007). The predicted 3-D structure revealed a striking similarity with the human homologue. In addition, position and orientation of the active site residues are essentially identical in the giardial and human structures, further supporting the predicted catalytic activity of *G. lamblia* HDAC.

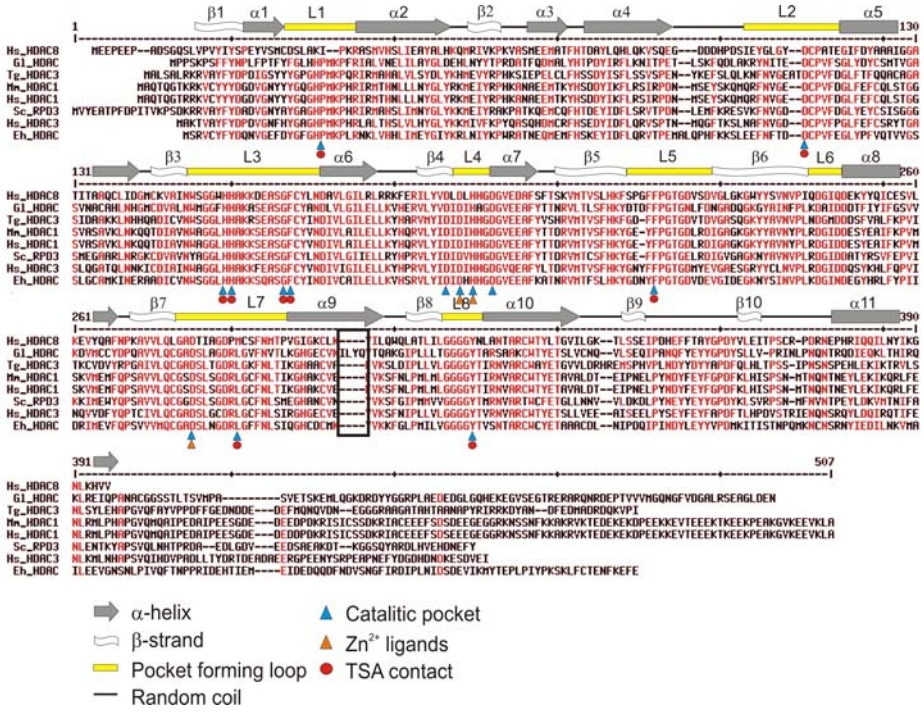

Figure 2: Multiple sequence alignment of selected deacetylases. Protein sequence alignment of giardial HDAC with selected orthologues. Indicated are the residues important for catalytic activity and involved in zinc and TSA binding, based on crystal structure of related HDAC (Finnin et al., 1999; Vannini et al., 2004). The four residues of the *G. lamblia*-specific insertion are boxed. Alignments were performed with Multalin (http://bioinfo.genopole-toulouse.prd.fr/multalin/). Gene bank accession numbers: GlHDAC (AAU89077), TgHDAC3 (AAY53803; ToxoDB accession no. 42.m00014), EhHDAC (AAV33348), HsHDAC1 (CAG46518), HsHDAC3 (NP_003874.2), HsHDAC8 (AF245664), MsHDAC1 (AAI08372), ScRPD3 (AAB20328).

To investigate whether the catalytic pocket of giardial HDAC could accommodate HDAC inhibitors, we modeled the structure of the protein in complex with the cyclic tetrapeptide FR235222 (Mori et al., 2003), a potent inhibitory that was recently shown to specifically target HDAC3 in the Apicomplexan parasite *Toxoplasma gondii* (Bougdour et al., 2009) (Fig. 3C). The 3-D structure of FR235222 was built using the values of the backbone dihedral angles as they are in the NMR solution conformation (Rodriquez *et al.*, 2006). Three binding modes of FR235222 in the homology model of *G. lamblia* HDAC were generated by manual docking using the program WITNOTP (Armin Widmer, Novartis Pharma, Basel, Switzerland). In all binding modes, the long side chain of FR235222 was positioned in the deep pocket of HDAC with the ketone moiety at the tip of the side chain chelating the zinc. The three binding modes differ from each other in the orientations of the phenylalanine, isovaline, and 4-methyl-proline side chains on the rim of the deep pocket. Each binding mode was energy minimized with rigid protein and zinc atom using the TAFF force field (Clark *et al.*, 1989). Upon energy minimization there is good surface complementarity in all of the three binding modes. Furthermore, the binding energy is similar in the three minimized structures, which is consistent with the heterogeneity of orientations observed for a set of inhibitors of human HDAC 8 (Dowling *et al.*, 2008).

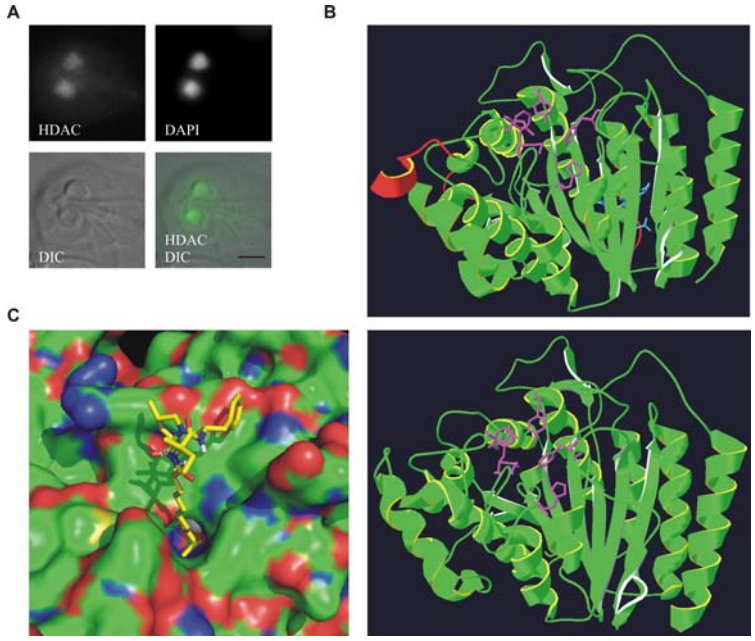

Figure 3: Characterization of *G. lamblia* HDAC. A. Fluorescence analysis of parasites expressing recombinant giardial HDAC fused to a C-terminal HA tag and encysted for 16 h. Cells were co-stained for nuclei (DAPI). DIC: differential interference contrast image. Scale bars: 3 µm. B. 3-D homology model of GlHDAC (upper panel) built with the SWISS-MODEL program and X-ray structure of HsHDAC8 (lower panel) used as a template. Key residues of the active-site are violet (Asp 101, His 142, Phe 152, Phe 208, Tyr 306 in HsHDAC8; Asp 94, His 135, Phe 145, Phe 201, Tyr 303 in GlHDAC). The four amino acids of GlHDAC insertion are blue. The GlHDAC region not covered by the HsHDAC8 template is red. C. Predicted binding mode of FR235222 (sticks) in the homology model of GlHDAC (surface rendering). The energy minimization was performed with rigid protein. The atoms of FR235222 are colored according to atomic element with carbon in yellow, nitrogen in blue, oxygen in red, and hydrogen in gray. Hydrogen atoms on the side chains are not shown to avoid overcrowding. The polar surface of HDAC is colored according to atomic element (nitrogen in blue and oxygen in red) while the nonpolar surface is green. The zinc atom is the white sphere that is visible only partially at the bottom of the deep pocket close to the center of the image. The long side chain of FR235222 fits nicely in the cavity, and the two oxygen atoms at its tip chelate the zinc atom. Figure prepared with the program PyMOL (DeLano Scientific, USA).

Inhibition of HDAC increases histone acetylation levels in *G. lamblia*. Because the stage conversion of *G. lamblia* correlated with decreased levels of histone acetylation, we investigated whether reversing the decrease in acetylation by inhibiting HDAC could prevent parasite encystation. To this aim, we tested in the parasite the inhibitory activity of FR235222, the potent HDAC inhibitor which was predicted to fit in the active site of *G. lamblia* HDAC in our 3-D model. Immunofluorescence and quantitative analysis by flow cytometry revealed that treatment with FR235222 increased acetylation levels in encysting parasites (Fig. 4A). Selected subtypes of HDACs have been shown to target cytosolic non-histone proteins, including tubulin (Schemies et al., 2009). In our experiments, FR235222 treatment did not increase the acetylation levels of tubulin (Fig. 4B), implying not only that the inhibitor is not affecting the activity of other cellular deacetylases in a non-specific manner, but also that the single giardial HDAC is likely not able to accept tubulin as a substrate. In addition, nuclear basic proteins were isolated by acid extraction and probed for acetylation (Fig. 4C). Distinct acetylated proteins were identifiable in the region of 11- 16

kDa, corresponding with the predicted masses of histone proteins in *Giardia* (Triana et al., 2001). Importantly, their acetylation level specifically increased in the presence of FR235222. Histone identities of the bands in the 11- 16 kDa region were further confirmed by mass spectrometry analysis (Fig. S1). Collectively, our data provide strong evidence that treatment with the HDAC inhibitor FR235222 induced histone hyper-acetylation in the parasite.

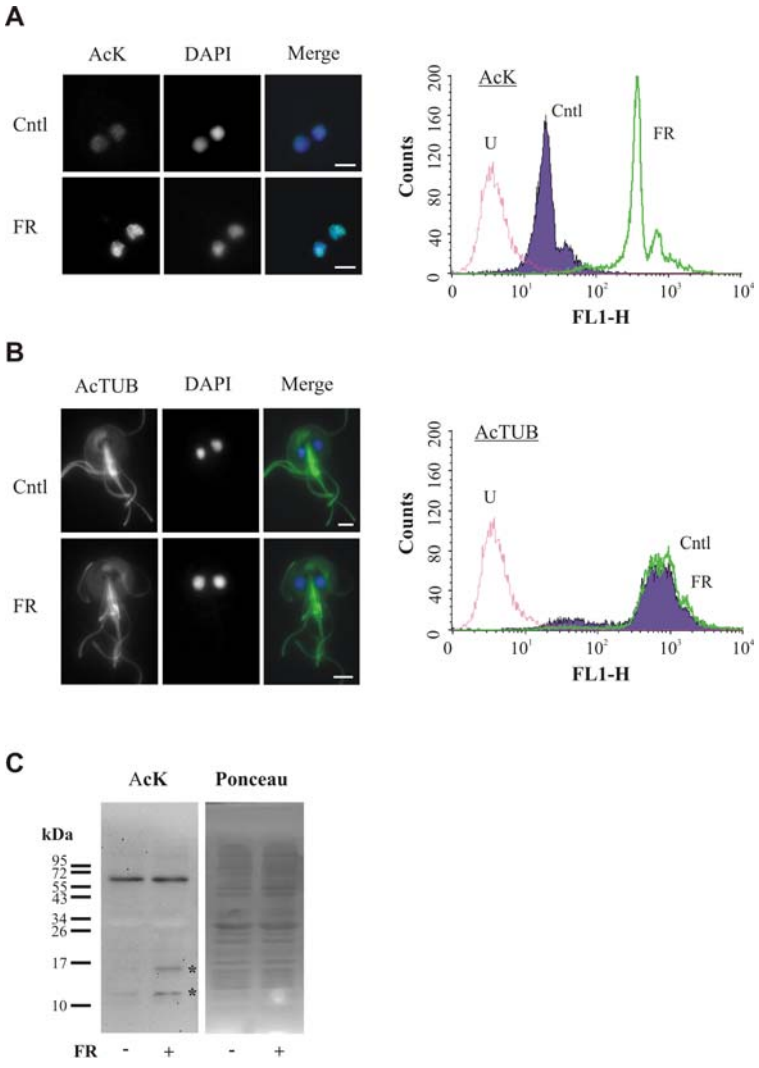

Figure 4: FR235222 treatment increases acetylation levels of encysting cells. A. Encysting parasites were treated with 2 µM FR235222 (FR) or solvent (cntl), as described. Cells were analyzed by immunofluorescence (left panels) after staining with anti-acetylated lysine (AcK) (A) or anti-acetylated tubulin (AcTUB) antibodies (B). DAPI, nuclear staining. Scale bar: 3 µm. The level of AcK and AcTUB upon FR235222 treatment was quantified by flow cytometry (right panels). Overlay histograms showing cells unstained (U), treated with solvent (Cntl) or 2 µM FR235222 (FR). Note the increased AcK signal in presence of the drug. C. Encysting cells were treated with 2 µM FR235222 (FR) or solvent. 16 µg of acid-extracted protein were separated by SDS-PAGE and probed with anti-acetylated lysine antibody. Note the increased acetylation of proteins with the predicted mass of giardial histones (asterisks) in presence of the HDAC inhibitor.

FR235222 inhibits expression of cyst wall proteins in encysting *G. lamblia*. Having shown that FR235222 treatment induces histone hyper-acetylation in *G. lamblia*, we next evaluated whether increased acetylation levels prevented parasite stage conversion to cysts. Induction of encystation results in high levels of expression of the main structural cyst wall proteins (CWPs). Immunofluorescence analysis of CWP1 expression in induced cultures revealed a considerably decreased number of cysts in the inhibitor-treated sample compared with control cells (Fig. 5A). In addition, the few cysts produced in presence of FR235222 were less viable than the control sample (Fig. 5D). To determine whether the low number of cysts was due to a reduced CWP1 expression or a defect of protein secretion and consequent accumulation in the cell interior, we quantified the protein expression in detergent-permeabilized cells. Population-wide analysis by flow cytometry showed that FR235222 severely impaired expression of CWP1 (Fig. 5B). Interestingly, while the maximal inhibition of CWP1 expression was obtained by pre-treating the cells with FR235222 prior to induction of encystation, a substantial decrease of CWP1 protein level was also observed in the absence of drug pre-treatment, indicating a rapid effect of the inhibitor on CWP1 synthesis (Fig. S2).

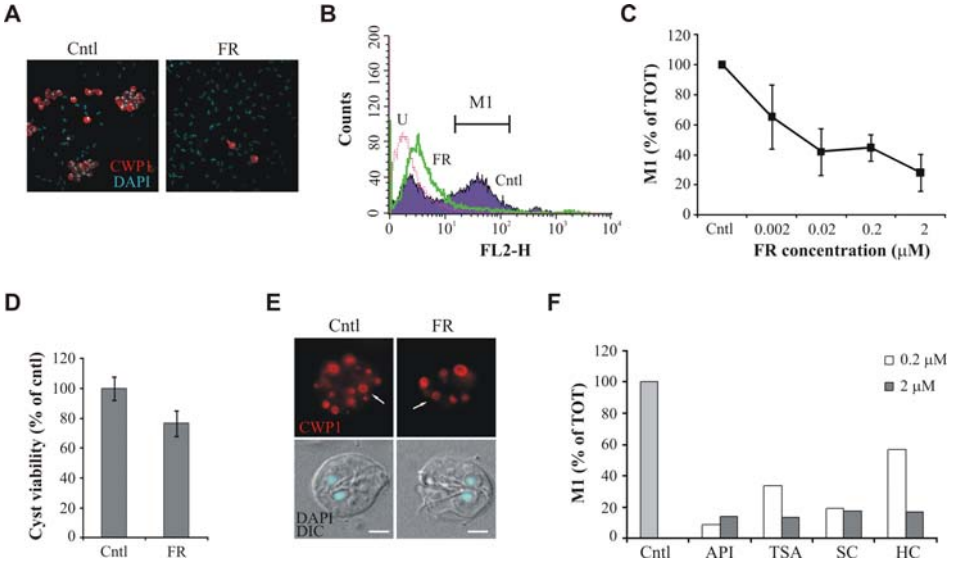

Figure 5: FR235222 treatment inhibits *G. lamblia* encystation. A. Encysting parasites were treated for 24 h with 2 μM FR235222, as described in the experimental procedures section. Cells were stained with anti-cyst wall protein 1 (CWP1) antibody without permeabilization and analyzed by immunofluorescence. Note the decreased number of cysts in the treated sample. DAPI, nuclear staining. B. Encysting parasites were treated as in (A), permeabilized and stained for CWP1 followed by flow cytometry quantification. Overlay histogram showing cells unstained (U), treated with solvent (Cntl) or 2 μM FR235222 (FR). C. Encysting parasites were treated with the indicated concentrations of FR235222 (FR) or solvent (Cntl), stained for CWP1 after permeabilization and analyzed by flow cytometry. The amount of cells with M1 fluorescence is expressed as percentage of total cell number (TOT). Note the dose-dependent decrease in CWP1 expression upon drug treatment. D. Viability of cysts following drug treatment was tested by trypan blue exclusion. Results of a representative experiment are presented as percentage of control ± standard errors (n = 3). E. Immunofluorescence analysis of treated parasites as in (B). Note the normal morphology of encystation-specific vesicles (ESV, arrow) containing CWP1 in both treated and control samples. DAPI, nuclear staining; DIC, differential interference contrast. Scale bar: 3 μm. F. Encysting parasites were treated with the indicated concentrations of HDAC inhibitors apicidin (API), Trichostatin A (TSA), scripaid (SC) and HC-toxin (HC) and CWP1 expression was quantified by flow cytometry after permeabilization. The amount of cells with M1 fluorescence is expressed as percentage of total cell number (TOT). The analysis revealed that all the compounds tested inhibited the expression of CWP1.

Next we performed a dose-response analysis to determine the potency of the FR235222-mediated inhibition of *G. lamblia* encystation. Flow cytometry quantification revealed that FR235222 was effective in inhibiting CWP1 expression already at low nanomolar concentration (Fig. 5C).
In addition, we tested whether FR235222 treatment inhibited not only CWP1 expression, but also altered the protein's intracellular distribution, a phenotype we recently described when parasite encystation was blocked following inhibition of sphingolipid synthesis (Štefanić et al., submitted). Immunofluorescence analysis of encysting parasites showed that both in control cells and in the minor proportion of FR235222-treated cells with detectable CWP1 levels, the protein was mainly localized in ESVs with typical morphology, indicating that formation of these compartments was not compromised (Fig. 5E).
To further confirm that the FR235222 inhibition of *G. lambia* encystation was indeed a specific effect, additional known HDAC inhibitors, i.e., apicidin, TSA, scripaid and HC-toxin, were tested. All the inhibitors were highly effective in reducing CWP1 expression, as assessed by flow cytometry analysis (Fig. 5F) and enumeration of CWP1-expressing parasites by manual counting (Fig. S4). Collectively, our data indicate that exposure of encysting cells to HDAC inhibitors severely compromised the encystation process by preventing induction of CWP expression.

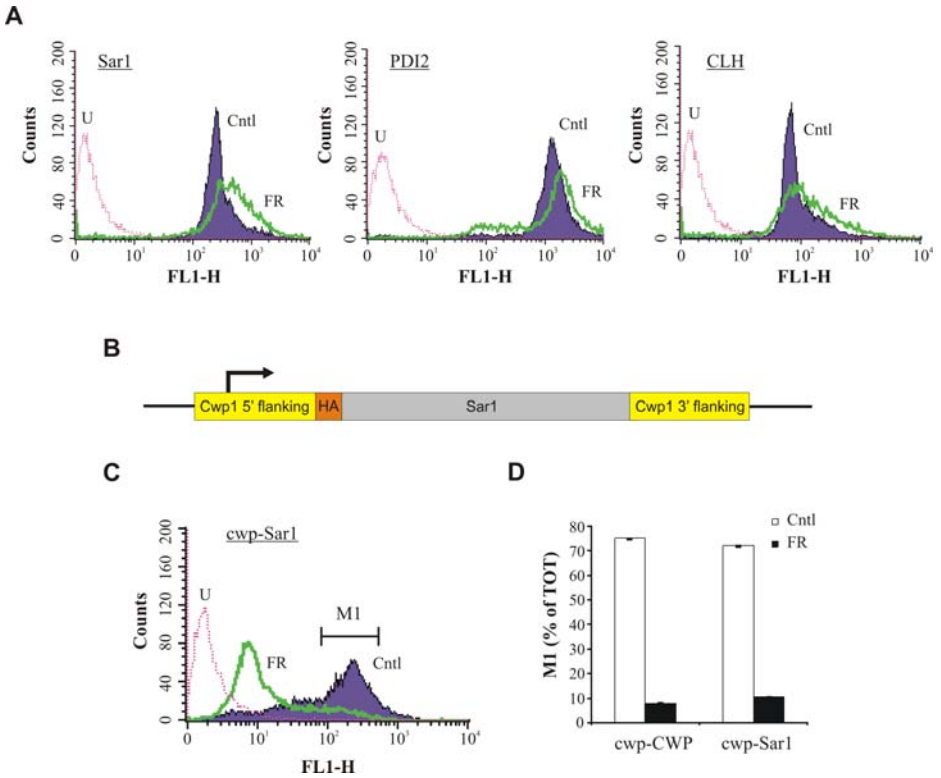

Figure 6: FR235222 treatment does not reduce the expression of constitutive proteins. A. Encysting parasites were treated for 24 h with FR235222, as described. Flow cytometry quantification of Sar1, protein disulfide isomerase 2 (PDI2) and clathrin (CLH) showed that the protein expression did not decrease upon inhibitor treatment. Overlay histograms showing cells unstained (U), treated with solvent (Cntl) or 2 μM FR235222 (FR). B, schematic representation of Sar1-HA construct. C. Engineered parasites expressing Sar1-HA under control of CWP1 promoter were treated as in (A), stained for recombinant Sar1 using an anti-HA antibody and quantified by flow cytometry. Overlay histogram showing cells unstained (U), treated with solvent (Cntl) or 2 μM FR235222 (FR). D. The same engineered parasites were additionally probed for endogenous CWP1 expression. The amount of cells with M1 fluorescence is expressed as percentage of total cell number (TOT). Note the decreased expression of both proteins upon inhibitor treatment.

FR235222 treatment does not down-regulate the expression of constitutively-expressed proteins. Next we asked whether FR235222-mediated down-regulation of protein expression took place at a global level or it was specific for encystation-induced protein. We tested this by quantifying the degree of regulation of constitutively-expressed proteins. The cellular levels of three unrelated endogenous proteins (namely the small GTPase Sar1, the endoplasmic reticulum-resident protein disulfide isomerase 2 (PDI2) and clathrin), which are involved in the secretory transport of CWP protein but whose expression is not stage-regulated, were monitored in encysting cells treated with FR235222. Flow cytometry quantification using antibodies against these three proteins revealed that none of them decreased in presence of the inhibitor (Fig. 6A), indicating that HDAC targeting does not result in a general reduction of protein expression.

We next tested whether the elements responsive to FR235222 regulation were located in the non-coding flanking regions of CWP1. To do this, 120 nucleotides of CWP1 5' untranslated region (UTR) flanking region containing the CWP1 promoter (Hehl et al., 2000) were cloned in front of recombinant Sar1 fused to a N-terminal HA tag as a reporter, followed by 180 nucleotides of 3'sequence flanking the CWP1 ORF, containing the poly A addition site (Fig. 6B). Transgenic parasites were obtained by stable integration of the construct into the parasite genome. Similar to the observed inhibition of endogenous CWP1, FR235222 treatment down-regulated the expression of the Sar1-HA reporter in engineered parasites (Fig. 6C, D). Drug-mediated inhibition of Sar1-HA expression was also observed in parasites transiently transfected with an analogous construct which was maintained episomaly (not shown). These results show that the short regions flanking the CWP1 ORF and containing all elements necessary for stage-regulated expression of CWP1 were sufficient for preventing CWP1 induction in response to FR235222 treatment.

FR235222 does not inhibit *G. lamblia* replication. FR235222 treatment was shown to efficiently block the replication of Apicomplexan parasites with an EC_{50} of 10 nM (Bougdour et al., 2009). Interestingly, when *G. lamblia* were incubated with FR235222 up to 2 μM, no reduction of replication was observed in encysting parasites and only a modest inhibition in trophozoite cultures (Fig. 7A). This result indicates that the increased levels of histone acetylation induced by FR235222 were not caused by toxicity or dying parasites. Next we tested the sensitivity of the parasite to other HDAC inhibitors. Neither treatment with apicidin, nor with scripaid or HC-toxin up to 2 μM affected parasite replication (data not shown). In contrast, treatment with trichostatin A (TSA) severely inhibited replication of both parasite stages at nanomolar concentrations; as TSA is a broad range inhibitor of cellular deacetylases (Blagosklonny et al., 2002), is it conceivable that the block of replication is due to a non-specific activity toward other essential proteins. Taken together, these results show that treatment with HDAC inhibitors which are known to affect replication in other species, often did not have the same inhibitory effect on *G. lamblia* replication.

Given the close association of *Giardia* with the hosts' intestinal epithelial cells, we tested whether FR235222 was detrimental for mammalian cells. Four intestinal and fibroblast cell lines were grown to sub-confluence (Fig. 7B) or confluence (not shown), exposed to the drug, and their metabolic activity was quantified as a measure of cell viability. At both confluencies, 24 h of treatment with 0.02 μM FR235222 (a concentration which blocks *G. lamblia* encystation) did not affect metabolic activity of the intestinal cells and only moderately reduced the activity in the fibroblasts. Higher inhibitor concentrations up to 2 μM induced different responses in different cell types, ranging from no alteration in viability in Caco-2 cells to 50% inhibition in fibroblasts. Moreover, inhibitor-mediated toxicity was not induced during co-culture of intestinal cells with *G. lamblia* (Fig. S3). These results indicate that FR235222 treatment at concentrations inhibitory for *G. lamblia* encystation did not reduce the viability of mammalian intestinal cells.

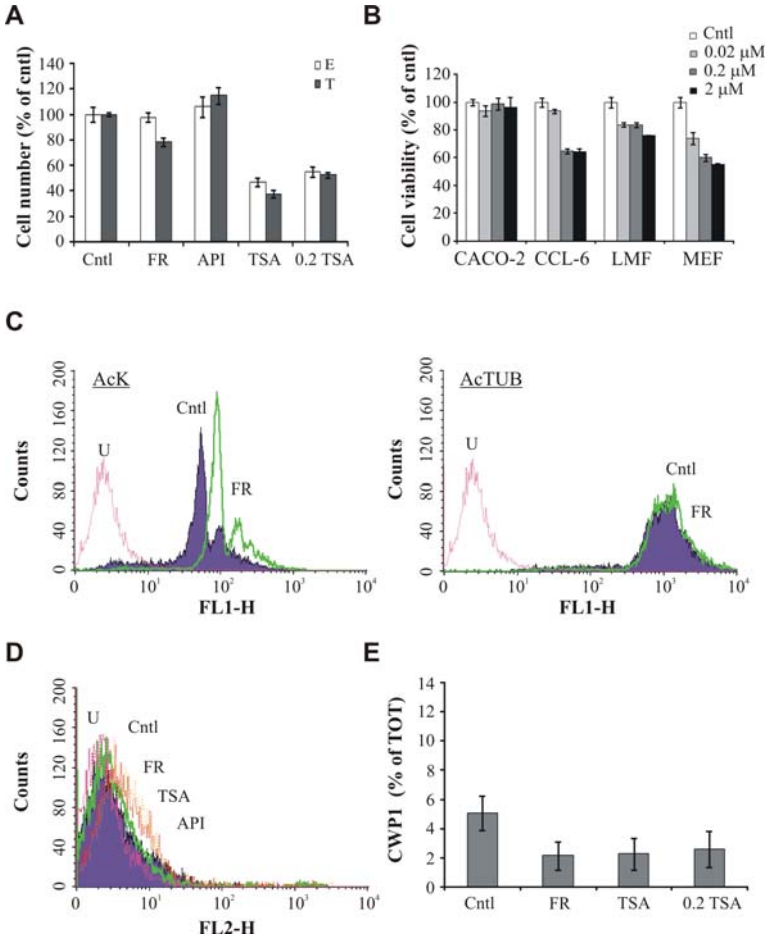

Figure 7: FR235222 treatment of trophozoites does not induce parasite encystation. A. Trophozoites (T) and encysting parasites (E) were treated for 24 h with 2 µM of the HDAC inhibitors FR235222 (FR), apicidin (API), Trichostatin A (TSA), 0.2 µM TSA or solvent (cntl). Parasite numbers are expressed as percentage of untreated samples (cntl). Data are average ± SE (n=9) of a representative experiment done in duplicate. B. Viability of mammalian cells treated for 24 h with solvent (cntl) or FR235222 at the indicated concentrations was assessed by measuring AlamarBlue reduction (Biosource). Results of a representative experiment are presented as percentage of control ± standard errors (n = 3). C. Trophozoites were treated for 24 h with FR235222 and levels of AcK (left panel) and acetylated tubulin (right panel) were quantified by flow cytometry. Overlay histograms showing cells unstained (U), treated with solvent (Cntl) or 2 µM FR235222 (FR). D. Trophozoites were treated for 24 h with 2 µM FR235222 (FR), apicidin (API), Trichostatin A (TSA), or solvent (cntl) and probed for CWP1. Overlay histogram of the treated cells is shown. U, unstained cells. Note the absence of CWP1 induction upon drug treatment. E. Cells were treated for 24 h with 2 µM FR235222 (FR), Trichostatin A (TSA), 0.2 µM TSA or solvent (cntl) and analyzed by immunofluorescence. Number of parasites expressing CWP1 was expressed as percentage of the total number of parasites, assessed by nuclear staining, ± standard errors (n = 6).

FR235222 treatment of trophozoites does not induce stage conversion. Our findings revealed that increasing the levels of histone acetylation with FR235222 treatment during encystation blocked stage differentiation in *G. lamblia*. To further investigate the hypothesis that acetylation must decrease to allow differentiation, we evaluated whether pharmacologically increased acetylation in trophozoites would keep

the cells at the trophozoite stage or induce parasite differentiation. FR235222 incubation increased histone acetylation in trophozoites (Fig. 7C, left panel), although not as potently as in encysting cells (Fig. 4A). Importantly, the degree of tubulin acetylation did not change in the presence of the drug (Fig. 7C, right panel), indicating that FR235222 was effective in specifically modulating the histone acetylation levels in both life stages of the parasite. To test whether HDAC inhibition in trophozoites induced parasite stage differentiation, we quantified the expression of the encystation-induced protein CWP1 in presence of the HDACi FR235222, TSA or apicidin. Flow cytometry analysis (Fig. 7D) and enumeration of CWP1-expressing parasites by manual counting (Fig. 7E and S4) did not reveal any increase in CWP1 expression in presence of the inhibitors tested compared with control cells. In addition, no giardial 14-3-3 re-localization to the parasite nuclei was detected in the presence of FR235222 (Fig. S5), as is typically observed during parasite encystation (Lalle et al., 2006). Collectively, these data indicate that treatment of trophozoites with HDAC inhibitors did not promote but rather decreased the rate of spontaneous encystation.

FR235222 alters gene expression in encysting cells and trophozoites. As changes in histone acetylation are known to modulate gene transcription, we used a genome-wide approach to investigate whether FR235222 treatment modified the expression of a specific range of genes or induced a general modulation of the expression profile in *G. lamblia*. Transcriptomes of both encysting cells and trophozoites cultured in presence or absence of the inhibitor were compared by microarray analysis. cDNA was labeled with either Cy5-dUTP (FR235222-treated) or Cy3-dUTP (control), hybridized to a *G. lamblia* microarray, and genes whose expression varied by a minimum of two fold following inhibitor treatment were considered significantly regulated (p- value <0.01).
Overall, 88 genes in encysting cells and 118 genes in trophozoites were found to be differentially regulated by FR235222 (Fig. S6), corresponding to ~2% of the 4969 currently predicted *Giardia* genes, and to ~1% of the total 9747 genes, including putative deprecated ones. The majority of the genes were up-regulated in both the parasite stages, indicating that HDAC inhibition acted primarily by promoting gene transcription of a selected set of genes. However in encysting cells treated with FR235222, induction of five genes crucial for parasite encystation was blocked, namely the DNA-binding transcription factor Myb2 (Huang et al., 2008; Sun et al., 2002), the three structural proteins forming the protective cyst wall (CWP1-3) and glucosamine-6-phosphate deaminase (GNP, also known as G6PI-B), which is involved in the biosynthesis of the cyst wall polysaccharide (Knodler et al., 1999) (Fig. 8A). These data also confirms that the lack of CWP1 induction in encysting parasites treated with FR235222 is due to reduced mRNA levels.

FR235222 up-regulates the expression of identical genes in the two life stages of the parasite. We then compared the transcriptomes of encysting cells and trophozoites to test whether the transcriptional response to inhibitor treatment was similar in the two stages of the *G. lamblia* life cycle. Using Gene Ontology predictions of the Giardia Genome database, we grouped the FR235222-regulated genes into functional classes. Fig. 8C shows the striking similarity of the gene classes modulated in encysting cells and trophozoites. The family of high cysteine membrane proteins (Davids et al., 2006) was a highly represented class, which also showed the highest level of up-regulation. Other highly represented classes were kinases of the NEK family, proteins annotated as 21.1 and proteins involved in metabolic functions. While many of the regulated genes had gene annotations in the Giardia Genome database, a considerable number of the genes indentified in both experimental conditions (38% in encysting cells and 49% in trophozoites) were hypothetical proteins of unknown function.

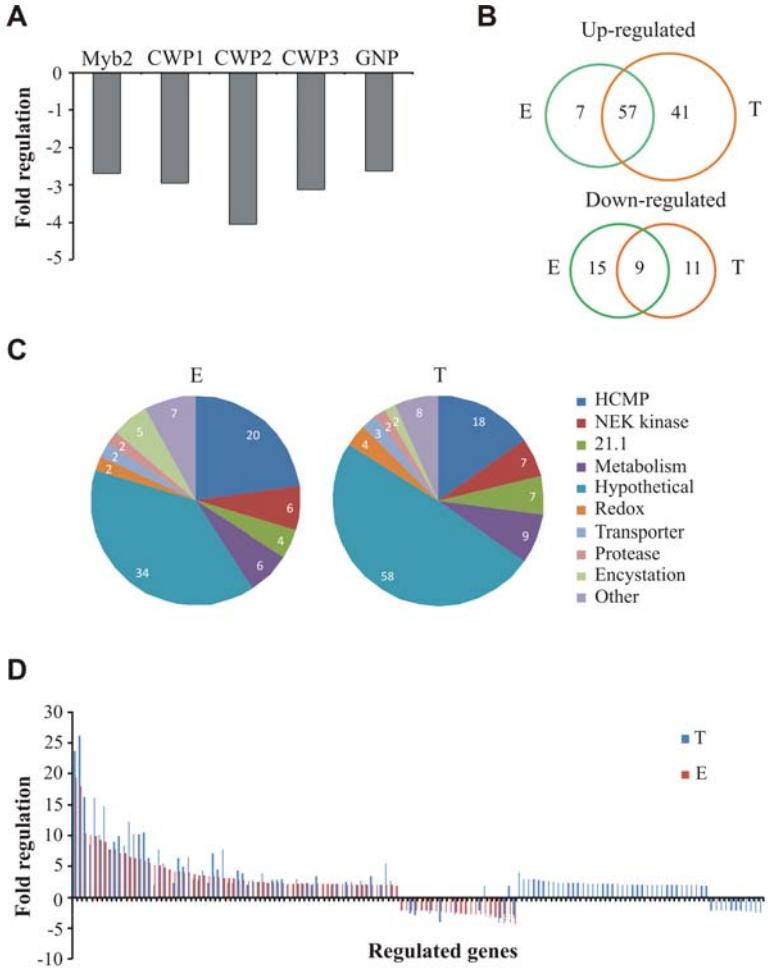

Figure 8: FR235222 treatment modulates gene expression. RNA extracted from encysting cells and trophozoites treated for 15 h with 2 μM FR235222 or solvent were used for dual channel microarray analysis. The comparison of the transcription profiles of treated versus untreated samples are shown. A. Drug treatment of encysting cells down-regulated the expression of known encystation-specific genes. Names and Giardia DB accession numbers are the following: Myb1-like protein, Myb2, (GL50803_8722); cyst wall protein 1, CWP1, (GL50803_5638); cyst wall protein 2, CWP2, (GL50803_5435); cyst wall protein 3, CWP3, (GL50803_2421); glucosamine-6-phosphate deaminase, GNP, (GL50803_8245). B. Venn diagram of genes regulated by FR235222 in encysting cells (E) and trophozoites (T). No prominent overlap of genes regulated by FR235222 was observed in the opposite direction: only two genes down-regulated in encysting cells were up-regulated in trophozoites and none of the genes up-regulated in encysting cells was down-regulated in trophozoites. C. Functional classes defined by Gene Ontology (GO) terms of the FR235222 regulated genes in encysting cells (E) and trophozoites (T). D. Pattern of gene up- and down-regulated following FR235222 treatment of encysting cells (E) and trophozoites (T).

The set of genes modulated by FR235222 not only belonged to similar gene classes but also overlapped considerably in the two experimental conditions (Fig. 8B, D). Of the 64 genes up-regulated in encysting cells, 57 were also found to be up-regulated in trophozoites, while of the 24 down-regulated genes, 9 were in common with the trophozoite gene list. No correlation was found in stage-specific gene regulation: in

encysting cells only two of the down-regulated genes were up-regulated in trophozoites, and none of the up-regulated gene was down-regulated in trophozoites. Interestingly, all of the high cysteine membrane proteins identified in our array were up-regulated in both encysting cells and trophozoites (with one exception in the trophozoites). Similarly, all the NEK kinases and all but one of the 21.1 proteins were up-regulated in both parasite stages.

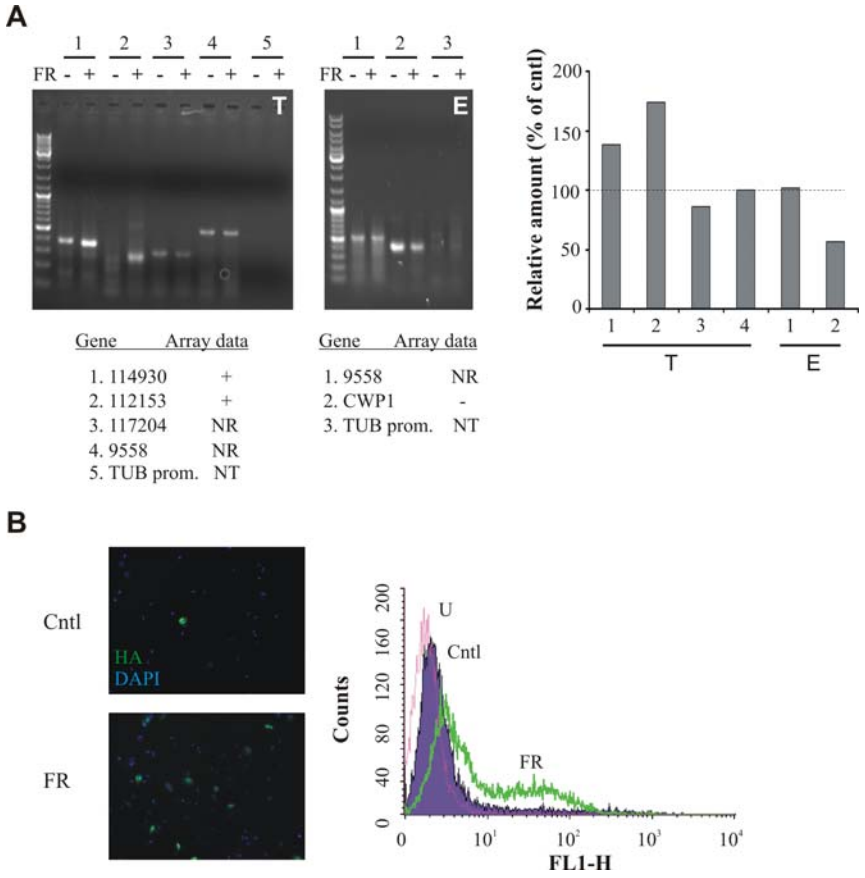

Figure 9: Confirmation of microarray data. A. RNA extracted from trophozoites and encysting cells treated for 15 h with 2 µM FR235222 or solvent were tested by reverse transcriptase (RT)-PCR for the transcription of regulated and not regulated gene products. Primer pairs binding to the tubulin (TUB) promoter were used as negative control. The obtained amplification products confirmed the gene regulation observed by microarray analysis. +, up-regulated; -, down-regulated; NR, not regulated; NT, not transcribed. Right panel, densitometric quantification of the relative amount of the gene products upon FR235222 treatment expressed as percentage of untreated control (cntl). B. The gene product GL50803_17120, whose expression was up-regulated by 2 µM FR235222 in both encysting cells and trophozoites, was HA-tagged and episomaly expressed under control of its endogenous promoter. Encysting parasites were treated with 2 µM FR235222 (FR) or solvent (cntl) and the expression of the recombinant protein monitored by immunofluorescence (left panel) and flow cytometry (right panel) analyses. Note the increased expression of the protein upon drug treatment. DAPI, nuclear staining. U, unstained cells.

In order to determine whether the genomic environment plays a role in the expression of FR235222-regulated genes, we asked whether regulated genes were clustered. All regulated genes were distributed on 17 genomic scaffolds and a positive correlation was found between the number of regulated genes and the number of genes present on a given scaffold (Fig. S7A). Analysis of the gene position in the genomic

scaffolds revealed that the regulated genes were not distributed in tight clusters containing multiple consecutive genes (Fig S7B); in addition, regulated genes belonging to the same gene classes were not located in the same genomic location, indicating that physical proximity is not required for FR235222-induced transcriptional co-regulation. However, statistical approaches based on graphical and numerical computations revealed small groups of potentially co-regulated genes which were distributed non-randomly in scaffolds CH991762 and CH991763 in encysting cells, and in scaffold CH991763 in trophozoites (Fig. S7C, S8). The biological significance of these findings remains to be determined.

Validation of gene expression regulation. To confirm the expression patterns observed by microarray analysis, we performed RT-PCR of selected genes using RNA extracted from FR235222-treated trophozoites and encysting cells. Specifically, in the trophozoite sample we analyzed two genes whose expression was up-regulated upon FR235222 treatment (GL50803_114930 and GL50803_112153), while in the encysting cell sample we assessed the abundance of CWP1 transcript, whose expression was down-regulated upon inhibitor treatment. Analyses of genes which were not regulated by the inhibitor (GL50803_ 117204 and GL50803_ 9558) or not transcribed (tubulin promoter sequence(Elmendorf *et al.*, 2001)) were used as a loading and as a negative control, respectively. In each case, the abundance of transcripts detected by RT-PCR confirmed the microarray data (Fig.9A). Importantly, PCR reactions using the original, non retro-transcribed RNA as template did not give any detectable products, confirming the absence of contamination with genomic DNA (not shown).
In addition, FR235222-induced up-regulation of gene expression was further confirmed at the protein level. A N-terminal HA epitope tagged variant of the gene product, GL50803_17120, whose expression increased in both encysting cells and trophozoites upon inhibitor treatment, was expressed in trophozoites. As seen in the RT-PCR results, immunofluorescence and flow cytometry analyses substantiated the increased expression in presence of the inhibitor (Fig. 9B). Collectively, these results unambiguously validate the microarray data both at the transcriptional and translational level.

DISCUSSION

G. lamblia encystation is critical for both parasite survival outside the host and disease transmission. Despite the considerable amount of information available on *G. lamblia* encystation at the cellular level, the molecular underpinnings of its regulation remain limited. In the present study, we investigated the role of epigenetic chromatin modification in the parasite stage differentiation. We found that exposure of parasites to the HDAC inhibitor FR235222 increased the levels of histone acetylation, altered gene transcription and inhibited *G. lamblia* encystation, thus providing the first evidence that epigenetic mechanisms control stage differentiation in this parasite. Notably, FR235222 treatment effectively inhibited CWP1 expression at low nanomolar concentrations, suggesting that the observed phenotype is a consequence of specific inhibition of giardial HDAC. In addition, the fact that only 1-2% of predicted genes are affected and that clear functional categories are identified, argues against a random off-target effect.

A highly reduced histone deacetylation machinery is present in *G. lamblia*. *G. lamblia* has a compact genome organization and few identified regulatory elements, consistent with significant reductive evolution (Morrison et al., 2007). Thus, this protist is considered an interesting model for investigating minimized cellular systems. Analysis of the parasite genome revealed the occurrence of genes coding for putative chromatin modifying proteins, including histone acetylases, deacetylases and methylases, suggesting that mechanisms for epigenetic regulation of gene expression are present in this parasite. Interestingly, demethylases seem to be absent in *G. lamblia*, *Trichomonas*, *Entameba histolytica* and microsporidians, indicating that demetylase activity is dispensable for these parasites or carried out by unrelated enzymes (Iyer et al., 2008).

Consistent with its reduced cellular machinery, only one classical HDAC homologue is annotated in the *G. lamblia* genome (GL50803_3281) and its nuclear localization further support a deacetylase activity on histone proteins. The presence of a single HDAC is in striking contrast with the size of the HDAC repertoire found not only in metazoan but also in unicellular protozoa, including the apicomplexan *T. gondii* with 5 putative HDACs. It is worth mentioning that a single representative of HDAC I was identified so far in another enteric parasite, *Entamoeba hystolitica*, suggesting that simplified mechanisms for regulating histone acetylation are operational in basal organisms (Ramakrishnan et al., 2004).
Sequence alignments, 3-D modeling and prediction of inhibitor binding mode highlighted the high degree of giardial HDAC conservation, in particular at the catalytic site. Moreover, compared with the five *T. gondii* HDACs, giardial HDAC showed the highest degree of similarity with HDAC3, the target of FR235222, further arguing for a specific interaction of the inhibitor with the giardial enzyme.
Of note, the sequence of giardial HDAC contains a 4 amino acid insertion (position 283-286) not found in other species. While amino acid insertions appear to be common in *G. lamblia* proteins, as exemplified by giardial histone acetyl transferase (Morrison et al., 2007), their size is typically larger (20 amino acids on average). The significance of the extra amino acids in the giardial HDAC is unknown.

Histone acetylation regulates stage-specific gene expression during *G. lamblia* encystation. We obtained three lines of evidence indicating that epigenetic mechanisms are involved in regulating expression of encystation-specific genes. Firstly, we observed that the level of histone acetylation decreased during encystation, which is consistent with the parasites differentiating to a dormant stage. Based on this, we can formulate the hypothesis that the high acetylation levels effectively makes the parasite refractory to entering differentiation after going through the S-G2 transition of the cell cycle (Bernander et al., 2001). Secondly, we tested this hypothesis by actively increasing the acetylation levels during encystation. This reduced the synthesis of a relatively small subset of gene products and specifically blocked induction of all known encystation-specific genes. This reveals an as yet unknown level of stage-specific control of encystation-specific genes in addition to the regulation by transcription factors. Importantly, we showed that short flanking regions of encystation-specific proteins are sufficient for the FR235222-mediated inhibition of gene expression, indicating that no distant regulatory elements are required for modulation of these genes. Thirdly, we demonstrated that histone hyperacetylation altered gene transcription; while the majority of FR235222-responsive genes were up-regulated, the mRNA of encystation-specific genes were down-regulated. Taken together, our data indicate that chromatin acetylation states plays a key role in the regulation of parasite differentiation by controlling the level of gene transcription, possibly by altering the accessibility of the promoter region to Myb2 and other cis-acting factors implicated in regulation of encystation-specific genes.
Although we unambiguously showed that increased histone acetylation repressed the transcription of encystation-specific genes, this repression challenges the classical view where histone hyperacetylation is associated with increased gene transcription. Interestingly, inhibition of stage differentiation in response to selected HDAC inhibitors, TSA and HC-toxin, but not apicidin, has also been reported in *Entamoeba* parasites, but the molecular mechanism still remains to be investigated (Byers et al., 2005).
One plausible explanation is that the repression of encystation-specific gene expression in *G. lamblia* is indirect and occurs via the action of a repressor, which is in turn positively regulated by the increased histone acetylation. The identification of negative cis-active elements in the CWP2 promoter (Davis-Hayman et al., 2003) further supports the presence of a repressor mechanism to maintain low levels of encystation-specific proteins during vegetative growth. Block of up-regulation of the trans-activator transcription factor Myb2 in presence of FR235222 suggests that the putative repressor may act upstream of Myb2 activation.
In other protozoa such as *Toxoplasma gondii* and *Entamoeba histolytica* it has been proposed that HDAC regulation of specific genetic loci is stage-specific, and HDAC inhibition during encystation may de-repress trophozoite-specific genes in *E. histolytica*, thus arresting parasite differentiation (Ehrenkaufer et

al., 2007; Saksouk et al., 2005). However our findings suggest in several ways that *G. lamblia* may possess a simpler HDAC regulation, namely, (i) only one classical HDAC is found in the parasite genome, arguing against the presence of stage-specific differential HDAC expression; (ii) using the HDAC inhibitor FR235222, we found increased acetylation in both trophozoites and encysting cells, suggesting that giardial HDAC is indeed operational in both parasite stages; (iii) contrary to what was observed in *T. gondii* and *E. histolytica* (Bougdour et al., 2009; Ehrenkaufer et al., 2007), HDACi treatment of trophozoites does not trigger parasite stage conversion, suggesting that a trophozoite-specific HDAC engaged in the repression of encystation-specific genes is not present in *G. lamblia*. On the other hand, we showed that the levels of histone acetylation decreased in encysting cells compared with trophozoites. While we cannot exclude that this decrease is due to a reduced activity of histone acetyltransferases, inhibition of HDAC was sufficient to reverse the phenomenon and to block encystation. Hence it is likely that *G. lamblia* does not rely on several stage-specific HDACs but rather on a single HDAC whose activity is differentially modulated in the parasite life stages, possibly by binding with different stage-specific partners via its C-terminal domain (Pflum et al., 2001). In this context, the regulation of histone acetylases and deacetylases in the different stages of *G. lamblia* is worthy of careful characterization.
Finally, in light of ever increasing indications that HDACs also function as activators of transcription in yeast (Kurdistani and Grunstein, 2003), we cannot dismiss the possibility that the FR235222-mediated inhibition of encystation-specific gene expression may be a direct consequence of the blocked HDAC activity. Future analyses to determine the acetylation pattern of encystation-specific genes will help to further our understanding of the epigenetic regulation mechanisms that control stage differentiation in this parasite.

Whole genome transcriptome regulation upon HDAC inhibition. Our microarray data revealed that FR235222 treatment changed gene expression in both encysting cells and trophozoites. The observed gene regulation is likely to result from a selective inhibition of giardial HDAC and not due to drug-induced lethality, as treated parasites were able to replicate normally in presence of the inhibitor. In addition, analysis of microarray evidence available in the Giardia Genome Database revealed that all but three genes regulated by FR235222 treatment were not regulated during stress induction (not shown), indicating that the gene changes of mRNA levels induced by FR235222 do not result from an inhibitor-induced stress response. Finally, the percentage of genes whose expression was changed by FR235222 was quite small (~2%) and of a similar range to what reported for the treatment with the HDACi TCA in mammalian cells (Heller et al., 2008) and *E. histolytica* (Ehrenkaufer et al., 2007).
Analysis of the modulated genes revealed that, in marked contrast with other cyst-forming parasites *T. gondii* and *E. histolytica*, treatment of *G. lamblia* trophozoites with HDACi did not induce the expression of encystation-specific genes, suggesting that repression of such genes during the vegetative trophozoite stage is not likely to be maintained solely by HDAC activity.
Further comparison of gene expression in encysting cells and trophozoites showed that the genes sensitive to FR235222 were strikingly similar in the two stages of the parasite life cycle. This overlap in expression profile emphasizes that the developmental program is accomplished with only very few changes in the global expression pattern. Besides hypothetical proteins, the major class of up-regulated genes were high cysteine membrane proteins (HCMp), a recently described family (Davids et al., 2006) whose function in *G. lamblia* remains enigmatic. While we found that the expression of 26% of the known HCMp genes is modulated by FR235222, only ~1% of the previously mentioned VSP family, also composed of cysteine rich proteins, was affected. The result was quite surprising, as histone acetylation of the upstream region of VSP was proposed to positively regulate the expression of the single VSP variant present on the cell surface at any given time, and thus acting as a master regulator of antigenic variation in *G. lamblia* (Kulakova et al., 2006). The fact that inducing histone hyperacetylation did not result in a general increase in VSP expression suggests that the epigenetic histone modification by the acetylation mark may

not be sufficient to promote VSP transcription, and that additional mechanisms are required to regulate the expression of these proteins. Alternatively, the use of different *G. lamblia* isolates (WB, prototype of Assemblage A in our study, and GS, prototype of Assemblage B in (Kulakova et al., 2006)) might also account for some differences in gene regulation, as the two isolates present different phenotypes *in vitro* and *in vivo* (Franzen et al., 2009; Monis et al., 2009).

The other two protein families whose expression was modulated by FR235222 were cytoskeletal proteins 21.1 and members of the NIMA-related protein kinases (NEK) (Morrison et al., 2007). The latter are widely represented in eukaryotes, but their role remains poorly characterized. Interestingly, the NEK family shows a significant expansion in *G. lamblia*, where it constitutes the majority of the parasite kinome (Morrison et al., 2007). The significance of this expansion is currently unknown.

Finally, genes of the proteins and protein families significantly affected by FR235222 treatment were scattered in different scaffolds of the parasite genome, indicating that HDAC inhibition can modulate the expression of functionally related genes independent of their genomic location. It is worth noting that statistical approaches identified three examples of non-randomly distributed gene sets in both encysting cell and trophozoite transcriptomes. Interestingly, the cluster found in trophozoites contained the CWP1 gene surrounded by four up-regulated genes. As CWP1 mRNA was found to be slightly up-regulated in our trophozoite array without detecting parasite stage differentiation, it is possible that the CWP1 genomic surrounding may have influenced CWP1 transcription without activation of the complete encystation program.

In conclusion, we showed for the first time that HDAC inhibition increased histone acetylation and induced transcriptional changes in *G. lamblia*, substantiating the presence of an evolutionarily conserved mechanism for epigenetic regulation of gene expression in this early divergent parasite. In addition, we provided evidence that the HDAC repertoire is highly reduced and the phenotypic and transcriptional responses following HDAC inhibition are simpler in *G. lamblia* than in other cyst-forming parasites, indicative of the minimized cellular processes typical of this parasite. Lastly, we discovered that HDAC inhibition, while not affecting parasite replication, potently blocked *G. lamblia* encystation and that short flanking regions of encystation-specific proteins were sufficient for the drug-mediated repression of gene expression. Collectively, these results reveal that the transcriptional changes during stage-differentiation are under the control of epigenetic regulation, and further illuminate the poorly understood mechanisms of gene regulation in this parasite. Additionally, our findings clearly demonstrate that HDAC activity is a promising target for pharmacological agents aiming to effectively block the production of *G. lamblia* cysts and thus reduce disease transmission.

EXPERIMENTAL PROCEDURES

Biochemical reagents. Unless otherwise stated, all chemicals were purchased from Sigma and cell culture reagents from Gibco-BRL. Inhibitor stock solutions were prepared at the following concentrations: 179 mM FR235222, 1.6 mM apicidin, 1 mM Trichostatin A (TSA), 2.29 mM HC-toxin, 3.06 mM scripaid. Inhibitors were freshly diluted to the concentrations required for the individual experiment.

Parasite and tissue culture. Trophozoites of the *Giardia lamblia* strain WBC6 (ATCC catalog number 50803) were grown axenically as described (Sonda et al., 2008). Harvested parasites were counted using the improved Neubauer chamber. New subcultures were obtained by inoculating $5x10^4$ trophozoites from confluent cultures into new 11 mL culture tubes. Two-step encystation was induced as described previously (Gillin et al., 1989) by cultivating the cells for ~44 h in medium without bile (pre-encysting medium) and subsequently in medium with higher pH and porcine bile (encysting medium).

Drug treatment of trophozoites was performed by incubating sub-confluent cultures for 24 h with the inhibitors at the concentrations indicated in the figure legend of the individual experiments. Drug treatment of encysting cells was performed in two steps: 8 h drug incubation in pre-encysting medium and

additional 16 h incubation in encysting medium. Viability of cysts following drug treatment was tested by trypan blue exclusion (Aley *et al.*, 1994).
Mammalian cells used in this study were: Caco-2 (human colon adenocarcinoma, ATCC HTB 37), Intestine 407 (human embryonic jejunoileum, ATCC CCL-6), primary lung fibroblasts isolated from 6- to 8-week old mice kindly provided by E. Gulbins (University of Duisburg-Essen, Essen, Germany) and mouse embryonic fibroblasts (MEF) kindly provided by A. Schinkel (The Netherlands Cancer Institute, Amsterdam, The Nederlands). Cells were routinely cultured in Dulbecco's modified Eagle medium (DMEM) or Minimum Essential Media supplemented with non essential amino acids and sodium pyruvate, in case of primary fibroblasts. All media were supplemented with 10% fetal calf serum, 2 mM glutamine, 50 U of penicillin/mL, and 50 µg of streptomycin/mL. Cultures were maintained at 37°C with 5% CO_2 in tissue culture flasks and trypsinized at least once a week.

Expression vector construction and transfection. The plasmid for episomal expression of hemagglutinin (HA)-tagged GlHDAC (GL50803_3281) under control of CWP1 promoter was based on the expression cassette C1-CWP (Hehl et al., 2000). The plasmid for stable expression of HA-tagged Sar1 under control of CWP1 promoter was engineered as described (Stefanic et al., 2009). The plasmid for the episomal expression of HA-tagged GL50803_17120 was based on the expression cassette C1-CWP where the CWP1 promoter was replaced by the endogenous promoter. Oligonucleotides (5'-3' orientation) used for the construct were the following: for GL50803_3281, *PstI*-s CGCTGCAGATGCCGCCTTCAAAACCCTC and HA-*PacI*-as CGTTAATTAACTACGC GTAGTCTGGGACATCGTATGGGTAGTTCTCATCTAACCCCGCTTC; for GL50803_17120, *XbaI*-s CGTCTAGACTACTATGGATGAAGCCGAG and HA-*NsiI*-as CGATGCATCGCGTAGTCTGGGACATCGTATGGGTAAATCGTGATGTTGTTAGTTAAAC encoding the HA epitope tag for the amplification of 200 bp upstream the starting codon containing the endogenous promoter followed by the protein leader sequence; 17120-*NsiI*-s CGATGCATGGTGTCCGCGAAGGAAAATATG and 17120-*PacI*-as CGTTAATTAACTAGCTATAAATGGCTGCAATG for the amplification of the GL50803_17120 coding sequence. 15 µg of plasmid vector DNA was electroporated (350V, 960µF, 800Ω) into trophozoites. For stable genome integration, the plasmid DNA was linearized using *SwaI* restriction enzyme before electroporation. Linearized plasmid targets the *G. lamblia* triose phosphate isomerase locus (GL50803_93938) and integration occurs by homologous recombination under selective pressure with the antibiotic puromycin (Jimenez-Garcia et al., 2008).
Gene expression analysis. Trophozoites were treated for 15 h with 2 µM FR235222 or solvent; encysting cells were similarly treated in two steps: 8 h drug incubation in pre-encysting medium and additional 7 h incubation in encysting medium. RNA was isolated using an RNAeasy kit (Qiagen, Stanford, CA) following the "Animal Cells Spin" protocol. Residual genomic DNA was removed with DNase 1 digestion according to the manufacturer's protocol. The integrity of the RNA was analyzed in a Bioanalyser (Agilent Technologies Inc., Palo Alto, CA) with "Eukaryote Total RNA Nano Series II" settings.
For dual channel microarray analysis, extracted total RNA was processed using the Amino Allyl MessageAmp™II a RNA Amplification Kit (Ambion, Austin, TX) and labelled with N-hydroxysuccinimidyl ester-derivatized reactive dyes Cy™3 or Cy™5, according to the manufacturer's protocol. After purification, 2 µg each of Cy3 or Cy5 labelled aRNA were denatured, added to SlideHyb™ Buffer I (Ambion), and hybridized to *G. lamblia* microarrays version 2 (TIGR) in a Tecan HybStation at the Functional Genomics Centre Zurich, Switzerland. The arrays are aminosilane surface coated glass slides with 9115 oligonucleotides (70mers) designed to cover the whole *G. lamblia* WBC6 strain genome.

Prior to hybridization, slides were hydrated and blocked with 150 µl BSA-Buffer (0.1mg/ml BSA, 0.1%SDS in 3xSSC-Buffer) for 1h at 42°C. After washing, samples were injected and hybridized for 16 h at 42°C. Slides were scanned in an Agilent Scanner G2565AA, using laser lines 543 nm and 633 nm for excitation of Cy3 and Cy5, respectively**.** Spatial scanning resolution was 10 µm, single pass. The scanner output files were quantified using the Genespotter Software (MicroDiscovery GmbH, Berlin, Germany) with default settings and 2.5 µm radius. The median spot intensities were evaluated with the Web application MAGMA (Rehrauer et al., 2007) and normalized using the print-tip-wise loess correction of the *limma* package (Smith, 2005). Potential gene-specific dye-effects were estimated from self-self hybridizations. Differential expression of genes during FR235222 treatment is reported as the $\log_2$ of the drug-induced fold-change compared with control treated samples, as well as the p-value for differential expression as estimated by the empirical Bayes model implemented in *limma*. All reactions were performed in triplicate.

Semi-quantitative reverse transcriptase polymerase chain reaction (RT-PCR). 300 ng of the isolated RNA described above were mixed with 10 µM k-anchorV primer and cDNA was synthesized using the Quiagen Omniscript Kit (Qiagen, Stanford, CA) according to the manufacturer's protocol. Fifty-fold dilutions of cDNA were used as template for PCR amplification using 0.4 µM each of gene-specific forward primers and a k-adaptor reverse primer. PCR products were separated on 1.5% agarose gels, visualized with ethidium bromide, and images recorded in a MultiImage™ Light Cabinet with AlphaEase®FC software (Alpha Innotech, San Leonardo, CA, USA). Primers used in the study are: k-anchorV, CCGGAATTCGGTACCTCTAGA(T18)V; k-adaptor, CCGGAATTCGGTACCTCTAGA; Tubulin, ATTTAGAATTCAAATCAGCAAATTC; 114930, GCCAGGGCCTCATCGAAC; 117204, ATACGTGGGGGTGGAGAAC; 112135, CGTCCTCTGCTACTCCTTTG; 9558, CGGACCATTACTTCTACGTACT; CWP1, CTGGTACATGAGTGACAACGCT.

Fluorescence microscopy and flow cytometry analysis. For immunolabeling, harvested cells were washed twice in ice-cold PBS, and fixed 3% formaldehyde solution in PBS. Fixed cells were and blocked, with or without previous permeabilization with 0.2% Triton X-100 in PBS for 20 min, and incubated with primary antibodies for 1 h. The primary antibodies used in this study were: anti-acetyl lysine rabbit antiserum (Abcam, Cambridge, MA), 1:500 dilution; anti-acetylated tubulin (Sigma), 1:500 dilution; Cy3-conjugated anti-cyst wall protein 1 (CWP1) mouse monoclonal antibody (Waterborne, New Orleans, LA), 1:60 dilution; anti-clathrin heavy chain (CLH) mouse antiserum (Marti et al., 2003), 1:2000 dilution; anti-protein disulfide isomerase 2 (PDI2) mouse antiserum, 1:1000 dilution; anti-Sar1 mouse antiserum (Stefanic et al., 2009), 1:300 dilution; Alexa488-conjugated anti-HA mouse monoclonal antibody (Roche Diagnostics GmbH, Manheim, Germany) 1:30 dilution; anti-giardial 14-3-3 (Lalle et al., 2006) 1:50 dilution, kindly provided by M. Lalle (Istituto Superiore di Sanita', Rome, Italy). Fluorophore-conjugated secondary antibodies were purchased from Invitrogen (Basel, Switzerland.) and used at 1: 200 dilution. Microscopy analyses were performed on a Leica DM IRBE fluorescence microscope (Leica Microsystems,Wetzlar, Germany) using the appropriate settings. Single cell quantification of fluorescence was performed using a FACSCalibur flow cytometer (Becton & Dickinson, Basel, Switzerland).

Mammalian cells metabolic assay. The metabolic activity of mammalian cells was tested by using the AlamarBlue® assay (Biosource, Camarillo, CA). Briefly, mammalian cells were grown to confluence or semi-confluence in 96-well plates, incubated for 24 h with FR235222 at the concentrations indicated in the figure legend, and processed according to the manufacturer instructions. For co-culture experiments, cells were seeded in 96-well plates at in 96-well plates at $3x10^4$ cells/well and incubated for 24 h to confluence. Harvested *G.lamblia* trophozoites were added to the cell monolayers at $6x10^4$ parasites/well, followed by 24 h incubation with 2 µM FR235222 and viability assay.

Western blot analysis of nuclear proteins. Encysting cells were treated with 2 µM FR235222 as described before. Nuclear extracts were prepared by mild detergent lysis as described (Bougdour et al., 2009). Briefly, $6x10^7$ cells were collected, washed in ice-cold PBS and resuspended in 700 µL lysis buffer (10 mM HEPES, 10 mM KCl, 1.5 mM $MgCl_2$, 0.5 mM dithiothreitol (DTT), 0.5 % NP-40, 1 mM PMSF and protease inhibitor cocktail). The nuclear pellet was collected by centrifugation at 10000×*g* for 10 min at 4°C and acid extracted for 2 h by adding 200µL each of 5 M $MgCl_2$ and 0.8 M HCl. Insoluble material was removed by centrifuging at 13000×*g* for 10 min at 4°C and soluble proteins containing basic histones were precipitated with 25% TCA. Precipitated proteins were washed twice with ice-cold acetone and resuspended in 100µL H_2O. Aliquots corresponding to 16 µg of proteins were analyzed by SDS-PAGE on a 15% gel followed by Coomassie blue staining and probed, following western blotting, using the previously described anti-acetyl lysine rabbit antiserum (Abcam) at 1:2000 dilution. Immunoreactive bands were visualized with horseradish peroxidase-conjugated secondary antibodies and enhanced chemiluminescence (ECL).

Determination of protein concentration. Protein content was determined using the Bio-Rad Protein Assay according to the instructions provided by the manufacturer. Bovine serum albumin was used for the standard curve.

Mass spectrometry identification of histones. Trophozoites were treated with 2 µM FR235222 for 24 h, harvested, washed in ice-cold PBS. $3x10^7$ cells were then resuspended in 500 µL lysis buffer (10 mM HEPES, 10 mM KCl, 1.5 mM $MgCl_2$, 0.5 mM dithiothreitol (DTT), 0.5 % NP-40, 1 mM PMSF and protease inhibitor cocktail) , incubated for 30 min at 4°C and the nuclear pellet was collected by centrifugation at 10000×*g* for 10 min at 4°C. The pellet was resuspended in 5 mL IP buffer (10 mM HEPES, 10% glycerol, 5 mM EDTA, 1 % NP-40, 1 mM PMSF), sonicated and incubated with 5 µL anti-acetyl lysine rabbit antiserum overnight at 4°C, followed by addition of protein-A conjugated beads. After incubation at 4°C under rotary agitation for 5 h, the beads were washed, resuspended in 30 µL sample buffer, boiled and treated with 3.3 µL iodoacetamide (0.5 M in 1 M Tris-HCl pH 8.0) for 15 min at room temperature. Proteins were separated on a 15 % gel, stained using the mass spectrometry-compatible SilverQuest™ silver staining Kit (Invitrogen) and the excised bands analyzed by peptide mass fingerprint using LC/MS/MS.

Protein structure prediction. The SWISS-MODEL web service (Arnold *et al.*, 2006; Guex and Peitsch, 1997; Schwede *et al.*, 2003) was used to build 3-D models of GlHDAC and HsHDAC8. Docking of FR235222 in the catalytic site of GlHDAC was performed using the program WITNOTP (Armin Widmer, Novartis Pharma, Basel). Alignments were performed with Multalin (http://bioinfo.genopoletoulouse.prd.fr/multalin/) and sequence comparisons were performed using Blast2.

Bioinformatic analyses. For visual identification of cluster candidates, we defined for each scaffold a metric M_f based on a potential function f analogous to the gravitational potential of mass points. In addition to a constant threshold, we used a linear combination $\mu_{pot}+\lambda \cdot s_{pot}^{+}$, based on mean μ_{pot} and conditional standard deviation s_{pot}^{+} of all potential fields generated by all permutations of gene distributions. The metric M_f was used to calculate the cluster hierarchy on all levels by complete linkage. All clusters were ranked according to the calculated probability $p_{cluster}$, based on hypergeometric distributions. For the identification of statistically evident clusters, we defined approximate permutation tests based on the Null-hypothesis H_0 of random and uniform distribution of regulated genes within the scaffolds, and the three following test statistics: mean deviation X_1 and standard deviation X_2 of the number of not-regulated genes between two regulated genes, and maximum number of consecutive short intervals ($\leq$ k) of non-regulated genes $X_{3,k}$ to account for the cluster size. The distributions of these test

statistics were approximated by Monte Carlo sampling 100‘000 random permutations for each scaffold. The functions used in this study were: $f(x)_{x\neq xi} := \sum_{(i=1,\ldots,n)} 1/(x-x_i)$, $f(x_i) := c << 0$; $M_f(x,y) := \max_{z \in [x,y]}(|f(x)-f(z)|)$; $f_{\mathbf{b}}(x)_{bx\neq 1} := \sum_{(i=1,\ldots,d)} b_i/(x-i)$, $f_{\mathbf{b}}(x)_{bx=1} := c << 0$; $\mu_{pot}(x) := (\sum_{\mathbf{p} \in \boldsymbol{P}} f_{\mathbf{p}}(x))/|\boldsymbol{P}|$; $(s_{pot}^{+})^2 := (\sum_{\boldsymbol{Q}=\{\mathbf{p}|\mathbf{p} \in \boldsymbol{P} \wedge f_{\mathbf{p}}(x)>0\}} (f_{\mathbf{p}}(x)-\mu_{pot}(x))^2)/|\boldsymbol{Q}|$; $p_{Cluster\ Ca,b,r} := \Pr\{Y_{b-a-2,n,d}=r-2\}\cdot\Pr\{Y_{2,2,n-(b-a-2)}=2\}$, where d = number of genes of a scaffold, n = number of regulated genes in a scaffold, $x_1<x_2<\ldots<x_n$, $1 \le x_i \le d$ the positions (consecutive numbers) of the regulated genes, $\mathbf{b} = (b_1, b_2, \ldots, b_d)$, $b_i = if(i \neq x_i, 0, 1)$, $\boldsymbol{P}$ = set of all permutations of $\mathbf{b}$, $Y_{m,s,t}$ a hypergeometric random variable as m draws without replacement from a population of t genes, thereof s regulated, $C_{a,b,r}$ a cluster $\{a=x_1<\ldots<b=x_r\}$ with r elements.

AKNOWLEDGMENTS

We thank Astellas Pharma Inc. for their kind gift of FR235222 compound, M. Lalle for kindly providing the anti-14-3-3 antibodies, Armin Widmer (Novartis Pharma, Basel) for the program WITNOTP and Therese Michel for technical assistance.

G. lamblia microarrays (version 2) were kindly offered through NIAID’s Pathogen Functional Genomics Resource Centre, managed and funded by Division of Microbiology and Infectious Diseases, NIAID, NIH, DHHS and operated by the J. Craig Venter Institute. The Functional Genomics Centre Zurich, Switzerland (www.fgcz.uzh.ch) is a joint facility of the ETH Zurich and the University of Zurich.

This work was supported by grants of the Marie Heim-Vögtlin Foundation and Fondation Pierre Mercier pour la Science to SS, of the Swiss National Science Foundation (Grant nr. 3100A0-112327) to ABH, CNRS (ATIP+), Agence National de la Recherche (ANR-MIME program), and INSERM (Contrat d’Interface) to MAH.

ABBREVIATIONS

CWP, cyst wall protein; ESVs, encystation-specific vesicles; HDAC, histone deacetylase; HAT, histone acetylase; HDACi, HDAC inhibitor; TSA, trichostatin A.

REFERENCES

Adam, R.D. (2001) Biology of Giardia lamblia. *Clin Microbiol Rev* **14**: 447-475.

Aley, S.B., Zimmerman, M., Hetsko, M., Selsted, M.E., and Gillin, F.D. (1994) Killing of Giardia lamblia by cryptdins and cationic neutrophil peptides. *Infect Immun* **62**: 5397-5403.

Arnold, K., Bordoli, L., Kopp, J., and Schwede, T. (2006) The SWISS-MODEL workspace: a web-based environment for protein structure homology modelling. *Bioinformatics* **22**: 195-201.

Bazan-Tejeda, M.L., Arguello-Garcia, R., Bermudez-Cruz, R.M., Robles-Flores, M., and Ortega-Pierres, G. (2007) Protein kinase C isoforms from Giardia duodenalis: identification and functional characterization of a beta-like molecule during encystment. *Arch Microbiol* **187**: 55-66.

Bernander, R., Palm, J.E., and Svard, S.G. (2001) Genome ploidy in different stages of the Giardia lamblia life cycle. *Cell Microbiol* **3**: 55-62.

Blagosklonny, M.V., Robey, R., Sackett, D.L., Du, L., Traganos, F., Darzynkiewicz, Z., Fojo, T., and Bates, S.E. (2002) Histone deacetylase inhibitors all induce p21 but differentially cause tubulin acetylation, mitotic arrest, and cytotoxicity. *Mol Cancer Ther* **1**: 937-941.

Bolden, J.E., Peart, M.J., and Johnstone, R.W. (2006) Anticancer activities of histone deacetylase inhibitors. *Nat Rev Drug Discov* **5**: 769-784.

Bougdour, A., Maubon, D., Baldacci, P., Ortet, P., Bastien, O., Bouillon, A., Barale, J.C., Pelloux, H., Menard, R., and Hakimi, M.A. (2009) Drug inhibition of HDAC3 and epigenetic control of differentiation in Apicomplexa parasites. *J Exp Med* **206**: 953-966.

Byers, J., Faigle, W., and Eichinger, D. (2005) Colonic short-chain fatty acids inhibit encystation of Entamoeba invadens. *Cell Microbiol* **7**: 269-279.

Chen, Y.H., Su, L.H., Huang, Y.C., Wang, Y.T., Kao, Y.Y., and Sun, C.H. (2008) UPF1, a conserved nonsense-mediated mRNA decay factor, regulates cyst wall protein transcripts in Giardia lamblia. *PLoS One* **3**: e3609.

Clark, M., III, R.D.C., and Opdenbosch, N.V. (1989) Validation of the general purpose tripos 5.2 force field. *Journal of Computational Chemistry* **10**: 982-1012.

Davids, B.J., Reiner, D.S., Birkeland, S.R., Preheim, S.P., Cipriano, M.J., McArthur, A.G., and Gillin, F.D. (2006) A new family of giardial cysteine-rich non-VSP protein genes and a novel cyst protein. *PLoS One* **1**: e44.

Davis-Hayman, S.R., Hayman, J.R., and Nash, T.E. (2003) Encystation-specific regulation of the cyst wall protein 2 gene in Giardia lamblia by multiple cis-acting elements. *Int J Parasitol* **33**: 1005-1012.

Dawson, S.C., Sagolla, M.S., and Cande, W.Z. (2007) The cenH3 histone variant defines centromeres in Giardia intestinalis. *Chromosoma* **116**: 175-184.

Dowling, D.P., Gantt, S.L., Gattis, S.G., Fierke, C.A., and Christianson, D.W. (2008) Structural studies of human histone deacetylase 8 and its site-specific variants complexed with substrate and inhibitors. *Biochemistry* **47**: 13554-13563.

Ehrenkaufer, G.M., Eichinger, D.J., and Singh, U. (2007) Trichostatin A effects on gene expression in the protozoan parasite Entamoeba histolytica. *BMC Genomics* **8**: 216.

Ellis, J.G., Davila, M., and Chakrabarti, R. (2003) Potential involvement of extracellular signal-regulated kinase 1 and 2 in encystation of a primitive eukaryote, Giardia lamblia. Stage-specific activation and intracellular localization. *J Biol Chem* **278**: 1936-1945.

Elmendorf, H.G., Singer, S.M., Pierce, J., Cowan, J., and Nash, T.E. (2001) Initiator and upstream elements in the alpha2-tubulin promoter of Giardia lamblia. *Mol Biochem Parasitol* **113**: 157-169.

Finnin, M.S., Donigian, J.R., Cohen, A., Richon, V.M., Rifkind, R.A., Marks, P.A., Breslow, R., and Pavletich, N.P. (1999) Structures of a histone deacetylase homologue bound to the TSA and SAHA inhibitors. *Nature* **401**: 188-193.

Franzen, O., Jerlstrom-Hultqvist, J., Castro, E., Sherwood, E., Ankarklev, J., Reiner, D.S., Palm, D., Andersson, J.O., Andersson, B., and Svard, S.G. (2009) Draft genome sequencing of giardia intestinalis assemblage B isolate GS: is human giardiasis caused by two different species? *PLoS Pathog* **5**: e1000560.

Gerwig, G.J., van Kuik, J.A., Leeflang, B.R., Kamerling, J.P., Vliegenthart, J.F., Karr, C.D., and Jarroll, E.L. (2002) The Giardia intestinalis filamentous cyst wall contains a novel beta(1-3)-N-acetyl-D-galactosamine polymer: a structural and conformational study. *Glycobiology* **12**: 499-505.

Gillin, F.D., Boucher, S.E., Rossi, S.S., and Reiner, D.S. (1989) Giardia lamblia: the roles of bile, lactic acid, and pH in the completion of the life cycle in vitro. *Exp Parasitol* **69**: 164-174.

Glozak, M.A., and Seto, E. (2007) Histone deacetylases and cancer. *Oncogene* **26**: 5420-5432.

Guex, N., and Peitsch, M.C. (1997) SWISS-MODEL and the Swiss-PdbViewer: an environment for comparative protein modeling. *Electrophoresis* **18**: 2714-2723.

Haumaitre, C., Lenoir, O., and Scharfmann, R. (2009) Directing cell differentiation with small-molecule histone deacetylase inhibitors: the example of promoting pancreatic endocrine cells. *Cell Cycle* **8**: 536-544.

Hehl, A.B., Marti, M., and Kohler, P. (2000) Stage-specific expression and targeting of cyst wall protein-green fluorescent protein chimeras in Giardia. *Mol Biol Cell* **11**: 1789-1800.

Hehl, A.B., and Marti, M. (2004) Secretory protein trafficking in Giardia intestinalis. *Mol Microbiol* **53**: 19-28.

Heller, G., Schmidt, W.M., Ziegler, B., Holzer, S., Mullauer, L., Bilban, M., Zielinski, C.C., Drach, J., and Zochbauer-Muller, S. (2008) Genome-wide transcriptional response to 5-aza-2'-deoxycytidine and trichostatin a in multiple myeloma cells. *Cancer Res* **68**: 44-54.

Huang, Y.C., Su, L.H., Lee, G.A., Chiu, P.W., Cho, C.C., Wu, J.Y., and Sun, C.H. (2008) Regulation of cyst wall protein promoters by Myb2 in Giardia lamblia. *J Biol Chem* **283**: 31021-31029.

Iyer, L.M., Anantharaman, V., Wolf, M.Y., and Aravind, L. (2008) Comparative genomics of transcription factors and chromatin proteins in parasitic protists and other eukaryotes. *Int J Parasitol* **38**: 1-31.

Jenuwein, T., and Allis, C.D. (2001) Translating the histone code. *Science* **293**: 1074-1080.

Jimenez-Garcia, L.F., Zavala, G., Chavez-Munguia, B., Ramos-Godinez Mdel, P., Lopez-Velazquez, G., Segura-Valdez Mde, L., Montanez, C., Hehl, A.B., Arguello-Garcia, R., and Ortega-Pierres, G. (2008) Identification of nucleoli in the early branching protist Giardia duodenalis. *Int J Parasitol* **38**: 1297-1304.

Knodler, L.A., Svard, S.G., Silberman, J.D., Davids, B.J., and Gillin, F.D. (1999) Developmental gene regulation in Giardia lamblia: first evidence for an encystation-specific promoter and differential 5' mRNA processing. *Mol Microbiol* **34**: 327-340.

Kouzarides, T. (2007) Chromatin modifications and their function. *Cell* **128**: 693-705.

Kulakova, L., Singer, S.M., Conrad, J., and Nash, T.E. (2006) Epigenetic mechanisms are involved in the control of Giardia lamblia antigenic variation. *Mol Microbiol* **61**: 1533-1542.

Kurdistani, S.K., and Grunstein, M. (2003) Histone acetylation and deacetylation in yeast. *Nat Rev Mol Cell Biol* **4**: 276-284.

Lalle, M., Salzano, A.M., Crescenzi, M., and Pozio, E. (2006) The Giardia duodenalis 14-3-3 protein is post-translationally modified by phosphorylation and polyglycylation of the C-terminal tail. *J Biol Chem* **281**: 5137-5148.

Lauwaet, T., Davids, B.J., Torres-Escobar, A., Birkeland, S.R., Cipriano, M.J., Preheim, S.P., Palm, D., Svard, S.G., McArthur, A.G., and Gillin, F.D. (2007) Protein phosphatase 2A plays a crucial role in Giardia lamblia differentiation. *Mol Biochem Parasitol* **152**: 80-89.

Lujan, H.D., Mowatt, M.R., and Nash, T.E. (1998) The Molecular Mechanisms of Giardia Encystation. *Parasitol Today* **14**: 446-450.

Margueron, R., Trojer, P., and Reinberg, D. (2005) The key to development: interpreting the histone code? *Curr Opin Genet Dev* **15**: 163-176.

Marti, M., and Hehl, A.B. (2003) Encystation-specific vesicles in Giardia: a primordial Golgi or just another secretory compartment? *Trends Parasitol* **19**: 440-446.

Marti, M., Li, Y., Schraner, E.M., Wild, P., Kohler, P., and Hehl, A.B. (2003) The secretory apparatus of an ancient eukaryote: protein sorting to separate export pathways occurs before formation of transient Golgi-like compartments. *Mol Biol Cell* **14**: 1433-1447.

Monis, P.T., Caccio, S.M., and Thompson, R.C. (2009) Variation in Giardia: towards a taxonomic revision of the genus. *Trends Parasitol* **25**: 93-100.

Mori, H., Urano, Y., Abe, F., Furukawa, S., Tsurumi, Y., Sakamoto, K., Hashimoto, M., Takase, S., Hino, M., and Fujii, T. (2003) FR235222, a fungal metabolite, is a novel immunosuppressant that inhibits mammalian histone deacetylase (HDAC). I. Taxonomy, fermentation, isolation and biological activities. *J Antibiot (Tokyo)* **56**: 72-79.

Morrison, H.G., McArthur, A.G., Gillin, F.D., Aley, S.B., Adam, R.D., Olsen, G.J., Best, A.A., Cande, W.Z., Chen, F., Cipriano, M.J., Davids, B.J., Dawson, S.C., Elmendorf, H.G., Hehl, A.B., Holder,

M.E., Huse, S.M., Kim, U.U., Lasek-Nesselquist, E., Manning, G., Nigam, A., Nixon, J.E., Palm, D., Passamaneck, N.E., Prabhu, A., Reich, C.I., Reiner, D.S., Samuelson, J., Svard, S.G., and Sogin, M.L. (2007) Genomic minimalism in the early diverging intestinal parasite Giardia lamblia. *Science* **317**: 1921-1926.

Pan, Y.J., Cho, C.C., Kao, Y.Y., and Sun, C.H. (2009) A Novel WRKY-like Protein Involved in Transcriptional Activation of Cyst Wall Protein Genes in Giardia lamblia. *J Biol Chem* **284**: 17975-17988.

Pflum, M.K., Tong, J.K., Lane, W.S., and Schreiber, S.L. (2001) Histone deacetylase 1 phosphorylation promotes enzymatic activity and complex formation. *J Biol Chem* **276**: 47733-47741.

Ramakrishnan, G., Gilchrist, C.A., Musa, H., Torok, M.S., Grant, P.A., Mann, B.J., and Petri, W.A., Jr. (2004) Histone acetyltransferases and deacetylase in Entamoeba histolytica. *Mol Biochem Parasitol* **138**: 205-216.

Rehrauer, H., Zoller, S., and Schlapbach, R. (2007) MAGMA: analysis of two-channel microarrays made easy. *Nucleic Acids Res* **35**: W86-90.

Rodriquez, M., Terracciano, S., Cini, E., Settembrini, G., Bruno, I., Bifulco, G., Taddei, M., and Gomez-Paloma, L. (2006) Total synthesis, NMR solution structure, and binding model of the potent histone deacetylase inhibitor FR235222. *Angew Chem Int Ed Engl* **45**: 423-427.

Saksouk, N., Bhatti, M.M., Kieffer, S., Smith, A.T., Musset, K., Garin, J., Sullivan, W.J., Jr., Cesbron-Delauw, M.F., and Hakimi, M.A. (2005) Histone-modifying complexes regulate gene expression pertinent to the differentiation of the protozoan parasite Toxoplasma gondii. *Mol Cell Biol* **25**: 10301-10314.

Schemies, J., Sippl, W., and Jung, M. (2009) Histone deacetylase inhibitors that target tubulin. *Cancer Lett* **280**: 222-232.

Schwede, T., Kopp, J., Guex, N., and Peitsch, M.C. (2003) SWISS-MODEL: An automated protein homology-modeling server. *Nucleic Acids Res* **31**: 3381-3385.

Smith, G.K. (2005) *Limma: linear models for microarray data.* New York: Springer.

Sonda, S., Stefanic, S., and Hehl, A.B. (2008) A sphingolipid inhibitor induces a cytokinesis arrest and blocks stage differentiation in Giardia lamblia. *Antimicrob Agents Chemother* **52**: 563-569.

Stefanic, S., Morf, L., Kulangara, C., Regos, A., Sonda, S., Schraner, E., Spycher, C., Wild, P., and Hehl, A.B. (2009) Neogenesis and maturation of transient Golgi-like cisternae in a simple eukaryote. *J Cell Sci*.

Sun, C.H., Palm, D., McArthur, A.G., Svard, S.G., and Gillin, F.D. (2002) A novel Myb-related protein involved in transcriptional activation of encystation genes in Giardia lamblia. *Mol Microbiol* **46**: 971-984.

Sun, C.H., Su, L.H., and Gillin, F.D. (2006) Novel plant-GARP-like transcription factors in Giardia lamblia. *Mol Biochem Parasitol* **146**: 45-57.

Touz, M.C., Nores, M.J., Slavin, I., Carmona, C., Conrad, J.T., Mowatt, M.R., Nash, T.E., Coronel, C.E., and Lujan, H.D. (2002a) The activity of a developmentally regulated cysteine proteinase is required for cyst wall formation in the primitive eukaryote Giardia lamblia. *J Biol Chem* **277**: 8474-8481.

Touz, M.C., Nores, M.J., Slavin, I., Piacenza, L., Acosta, D., Carmona, C., and Lujan, H.D. (2002b) Membrane-associated dipeptidyl peptidase IV is involved in encystation-specific gene expression during Giardia differentiation. *Biochem J* **364**: 703-710.

Touz, M.C., Ropolo, A.S., Rivero, M.R., Vranych, C.V., Conrad, J.T., Svard, S.G., and Nash, T.E. (2008) Arginine deiminase has multiple regulatory roles in the biology of Giardia lamblia. *J Cell Sci* **121**: 2930-2938.

Triana, O., Galanti, N., Olea, N., Hellman, U., Wernstedt, C., Lujan, H., Medina, C., and Toro, G.C. (2001) Chromatin and histones from Giardia lamblia: a new puzzle in primitive eukaryotes. *J Cell Biochem* **82**: 573-582.

Vannini, A., Volpari, C., Filocamo, G., Casavola, E.C., Brunetti, M., Renzoni, D., Chakravarty, P., Paolini, C., De Francesco, R., Gallinari, P., Steinkuhler, C., and Di Marco, S. (2004) Crystal structure of a eukaryotic zinc-dependent histone deacetylase, human HDAC8, complexed with a hydroxamic acid inhibitor. *Proc Natl Acad Sci U S A* **101**: 15064-15069.

Vannini, A., Volpari, C., Gallinari, P., Jones, P., Mattu, M., Carfi, A., De Francesco, R., Steinkuhler, C., and Di Marco, S. (2007) Substrate binding to histone deacetylases as shown by the crystal structure of the HDAC8-substrate complex. *EMBO Rep* **8**: 879-884.

Wang, C.H., Su, L.H., and Sun, C.H. (2007) A novel ARID/Bright-like protein involved in transcriptional activation of cyst wall protein 1 gene in Giardia lamblia. *J Biol Chem* **282**: 8905-8914.

SUPPLEMENTAL ONLINE MATERIAL

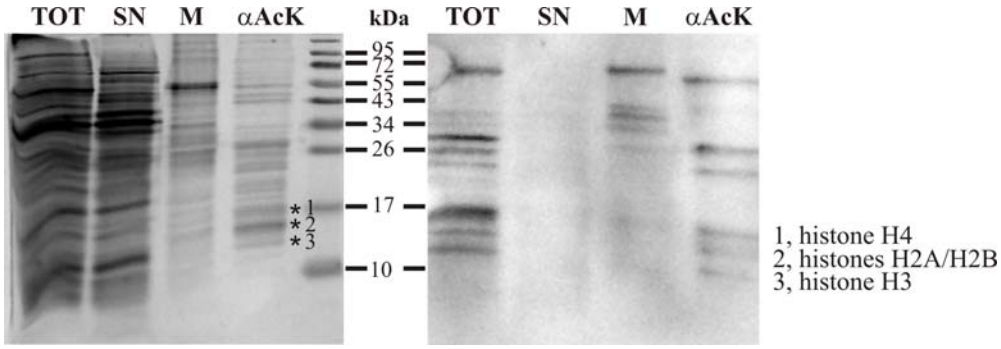

Figure S1: Mass spectrometry analysis of histones. Trophozoites were treated with 2 μM FR235222 for 24 h and histones immunoprecipitated as described in the experimental procedures section. Protein were separated by SDS-PAGE, silver stained (left panel) or probed with anti-acetylated lysine antibody (right panel). Asterisks indicate the bands excised and analysed by LC/MS/MS. TOT, total extract; SN, supernatant after nuclear pellet isolation; M, mock IP; αAcK, IP with anti-acetyl lysine rabbit antiserum.

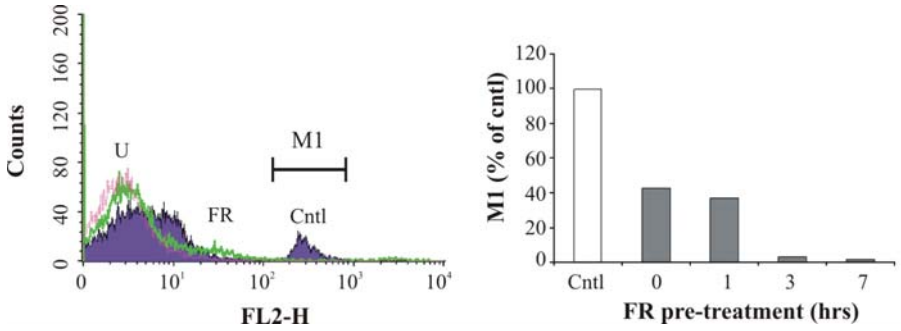

Figure S2: Time course of FR235222 inhibition of encystation. The effect of 2 μM FR235222 on encystation was monitored by adding the inhibitor in pre-encysting medium at 0, 1, 3, 7 h before inducing encystation for 16 h in presence of 2 μM FR235222. Parasites were stained for CWP1 and analyzed by flow cytometry. Left panel, overlay histogram showing cells unstained (U), solvent treated (Cntl) and pre-treated for 7 h with 2 μM FR235222 (FR). Right panel, the amount of cells with M1 fluorescence is expressed as percentage of total cell number (TOT).

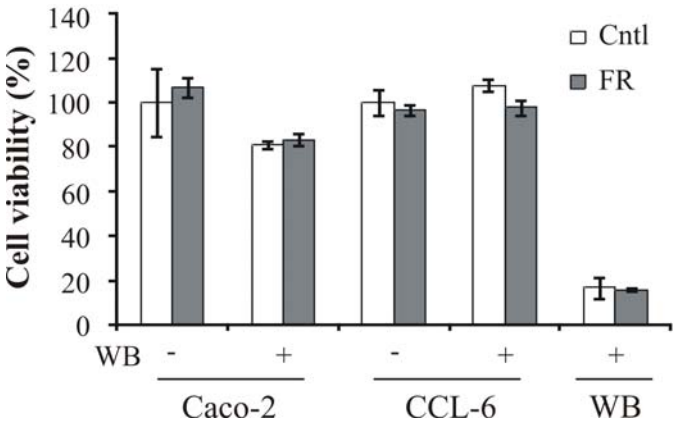

Figure S3: Viability of FR235222 treated intestinal cells co-cultured with *G. lamblia*. Caco-2 and CCL-6 cells were cultured with or without *G. lamblia* trophozoites of the WBC6 strain (WB) for 24 h in presence of solvent (cntl) or FR235222 at concentrations not affecting the viability of the cells (2 and 0.02 μM, respectively). Viability was assessed by measuring AlamarBlue reduction (Biosource). Results of a representative experiment are presented as percentage of control treated cells cultured in absence of *G. lamblia* (± standard errors, $n = 3$). WB bars, *G. lamblia* trophozoites cultured without intestinal cells.

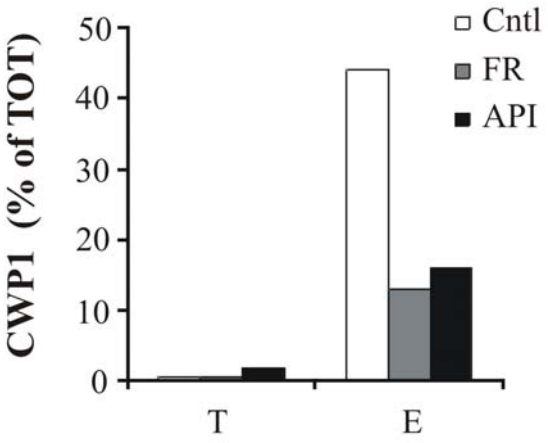

Figure S4: CWP1 expression upon FR235222 treatment. Trophozoites (T) and encysting cells (E) were treated for 24 h with 2 μM FR235222 (FR), apicidin (API), or solvent (cntl) and analyzed by immunofluorescence. Number of parasites expressing CWP1 was expressed as percentage of the total number of parasites (TOT), assessed by nuclear staining, ± standard errors ($n = 6$).

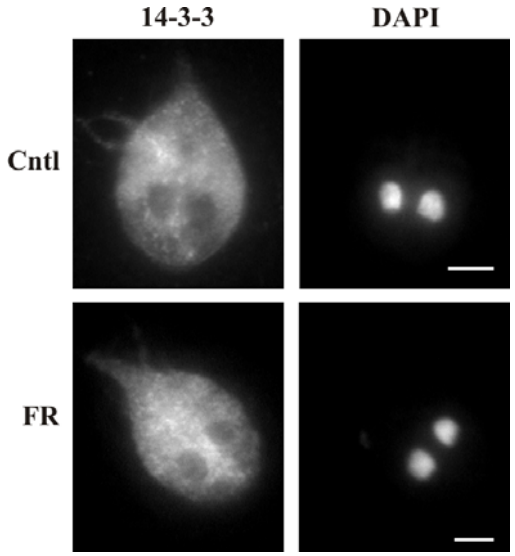

Figure S5: FR235222 treatment of trophozoites does not induce nuclear translocation of 14-3-3. Trophozoites were treated for 24 h with 2 μM FR235222 (FR) or solvent (cntl), stained with anti-giardial 14-3-3 antibody and analyzed by immunofluorescence. DAPI, nuclear staining. Scale bar: 3 μm.

Gene ID	Description	T Fold regulation	E Fold regulation
114930	high cysteine membrane protein Group 4	26.21	18.05
112673	high cysteine membrane protein VSP-like	23.83	19.40
102575	Hypothetical Protein	16.40	10.48
3269	Hypothetical Protein	16.25	9.93
112135	high cysteine membrane protein VSP-like	14.88	8.99
14259	Glucose 6-phosphate N-acetyltransferase	12.35	6.63
8505	Hypothetical Protein	10.70	5.89
118710	Hypothetical Protein	10.27	6.33
112135	high cysteine membrane protein VSP-like	10.26	6.37
112305	high cysteine membrane protein VSP-like	10.10	9.36
6175	Nitroreductase family protein	10.06	7.24
14247	TM efflux prot	9.11	7.83
9548	Cathepsin L precursor	8.60	10.23
31886	Hypothetical Protein	8.40	7.19
92983	Protein 21.1	7.88	5.21
36351	Hypothetical Protein	7.83	3.21
113512	high cysteine membrane protein Group 6	7.78	7.90
114215	Hypothetical Protein	7.17	3.41
32453	Hypothetical Protein	6.58	4.04
91707	high cysteine membrane protein Group 1	6.44	4.25
9338	Hypothetical Protein	6.44	5.63
17120	CEGP1 protein	5.54	2.04
115066	high cysteine membrane protein VSP-like	5.43	4.96
10659	high cysteine membrane protein Group 1	4.97	4.16
37605	Hypothetical Protein	4.52	3.27
20020	Hypothetical Protein	4.49	3.61
117655	Hypothetical Protein	4.44	2.83
32578	Hypothetical Protein	4.10	
17476	CXC-rich protein	3.93	2.49
100877	blasthit 2e-12 variant-specific surface protein AS7	3.90	2.81
34163	Hypothetical Protein	3.48	2.24
121724	Hypothetical Protein	3.42	2.11
112008	blasthit 1e-08 HUMANHypothetical protein KIAA1223	3.07	2.29
3855	Hypothetical Protein	3.03	
4313	vsp with INR	3.03	3.85
22217	Hypothetical Protein	3.02	
10829	Glucosamine-6-phosphate deaminase	3.00	
8377	Hypothetical Protein	2.96	2.43
120906	Hypothetical Protein	2.93	2.45
32139	Hypothetical Protein	2.90	2.44
11040	kinase, NEK	2.89	2.62
114470	high cysteine membrane protein Group 6	2.88	3.68
37595	Hypothetical Protein	2.81	
8585	Hypothetical Protein	2.76	2.03
3279	ribonuclease	2.75	2.14
4507	CTP synthase/UTP-ammonia lyasen	2.69	
36327	Hypothetical Protein	2.64	
113030	kinase, NEK	2.62	2.61
114210	blasthit 4e-12 LRP1	2.59	2.16
11976	Hypothetical Protein	2.56	
98867	Hypothetical Protein	2.51	2.15
37897	Hypothetical Protein	2.48	
25816	high cysteine membrane protein Group 1	2.47	3.15
102542	kinase, NEK	2.46	2.25

Gene ID	Description	T Fold regulation	E Fold regulation
9605	predicted protein	2.44	
114779	Hypothetical Protein	2.44	2.28
11930	retinoic acid induced 17; PIAS-like protein hZimp10	2.43	
113512	high cysteine membrane protein Group 6	2.41	3.48
113741	blasthit 3e-05 putative integral membrane protein	2.41	4.31
6492	blasthit 2e-12 hypothetical protein AN0137.2	2.38	
6291	Hypothetical Protein	2.36	2.45
7244	Hypothetical Protein	2.34	
17604	blasthit 2e-08 HUMANHypothetical protein KIAA1223	2.34	
6639	Protein 21.1	2.32	
101451	Hypothetical Protein	2.27	
4846	Protein 21.1	2.23	
15030	Protein 21.1	2.22	
112937	blasthit 8e-05 HUMANHypothetical protein KIAA1223	2.21	2.18
35352	Hypothetical Protein	2.21	
9051	Hypothetical Protein	2.20	
21924	kinase, NEK	2.19	
39824	Hypothetical Protein	2.17	2.11
8960	blasthit 2e-08 unnamed protein product	2.17	2.19
127181	Hypothetical Protein	2.16	
92919	Hypothetical Protein	2.15	
114210	blasthit 4e-12 LRP1	2.13	
13272	blasthit 3e-11 LOC402865 protein	2.13	
17012	Hypothetical Protein	2.12	
137726	ABC transporter ABCA.1	2.12	
8048	Hypothetical Protein	2.12	2.06
36776	Hypothetical Protein	2.12	2.15
16519	AstB/chuR-related protein	2.11	
3546	kinase, NEK	2.11	
32701	high cysteine protein (HCp)	2.11	2.31
15125	Hypothetical Protein	2.10	
16283	amino acid transporter family	2.08	
102180	high cysteine protein	2.07	2.25
38584	Hypothetical Protein	2.07	
117437	blasthit 6e-11 HUMANSerine/threonine-protein kinase RIPK4	2.06	
14331	variant-specific surface protein AS1	2.06	5.37
12229	Hypothetical Protein	2.05	
13922	blasthit 2e-08 Large exoproteins	2.03	2.72
13412	60S acidic ribosomal protein P0	2.03	
9210	Hypothetical Protein	2.02	
7260	Aldose reductase	2.02	
5435	cyst wall protein 2	2.01	-4.04
5638	cyst wall protein 1	2.01	-2.96
14863	Hypothetical Protein	2.01	
14759	6-phosphogluconate dehydrogenase, decarboxylating	2.00	
3593	Alcohol dehydrogenase	-2.04	
17198	Leucine-rich repeat protein	-2.05	-2.78
11448	Phosphomannomutase-2	-2.10	
8958	Hypothetical Protein	-2.11	
16111	Elongation factor 1-alpha	-2.13	
37109	Hypothetical Protein	-2.13	
9620	high cysteine membrane protein Group 2	-2.15	
9008	Aldose reductase	-2.17	
31956	Hypothetical Protein	-2.21	

Gene ID	Description	T Fold regulation	E Fold regulation
103829	Hypothetical Protein	-2.25	
16670	Hypothetical Protein	-2.36	
9099	blasthit 0.0002 Probable COP9 signalosome complex subunit 7	-2.41	
36663	Hypothetical Protein	-2.50	-2.12
112359	Hypothetical Protein	-2.51	-2.09
11209	Cathepsin L precursor	-2.81	-2.10
20781	Hypothetical Protein	-2.88	-2.42
14200	Molybdenum cofactor sulfurase	-3.30	-4.25
11449	Predicted ATPase of the PP-loop superfamily	-4.02	-2.23
7421	Casein kinase II beta chain	-4.08	-3.36
114474	Hypothetical Protein	-4.08	-3.60
3470	ABC transporter family protein		2.18
8227	ATP-binding cassette protein 5		2.22
103709	blasthit 0.0004 unnamed protein product		2.09
12082	blasthit 1e-10 Biotin-(acetyl-CoA carboxylase) ligase		-2.11
10552	blasthit 4e-10 HUMANThyroglobulin precursor		-2.34
2421	Cyst wall protein 3		-3.13
8245	Glucosamine-6-phosphate deaminase		-2.64
15250	high cysteine membrane protein Group 6		2.31
135231	Histone H3		-2.05
33672	Hypothetical Protein		-2.38
32657	Hypothetical Protein		-2.75
17188	kinase, NEK		2.19
11436	Molybdopterin biosynthesis MoeB protein		-2.55
8722	Myb 1-like protein (gMyb2)		-2.70
14626	Oxidoreductase, short chain dehydrogenase/reductase family		-2.21
102444	Protein 21.1		-2.03
115831	S4:AY14125; vsp with INR		4.63
23015	Serine palmitoyltransferase 1		-2.12
9046	Sugar transport family protein		-3.16
137740	vsp with INR		2.00

Figure S6: List of FR235222 regulated genes. Microarray analysis was performed on encysting cells (E) and trophozoites (T) treated with 2 µM FR235222, as described in the Experimental procedures section. Genes whose regulation reached the significance threshold are shown. Orange, up-regulation; blue, down-regulation.

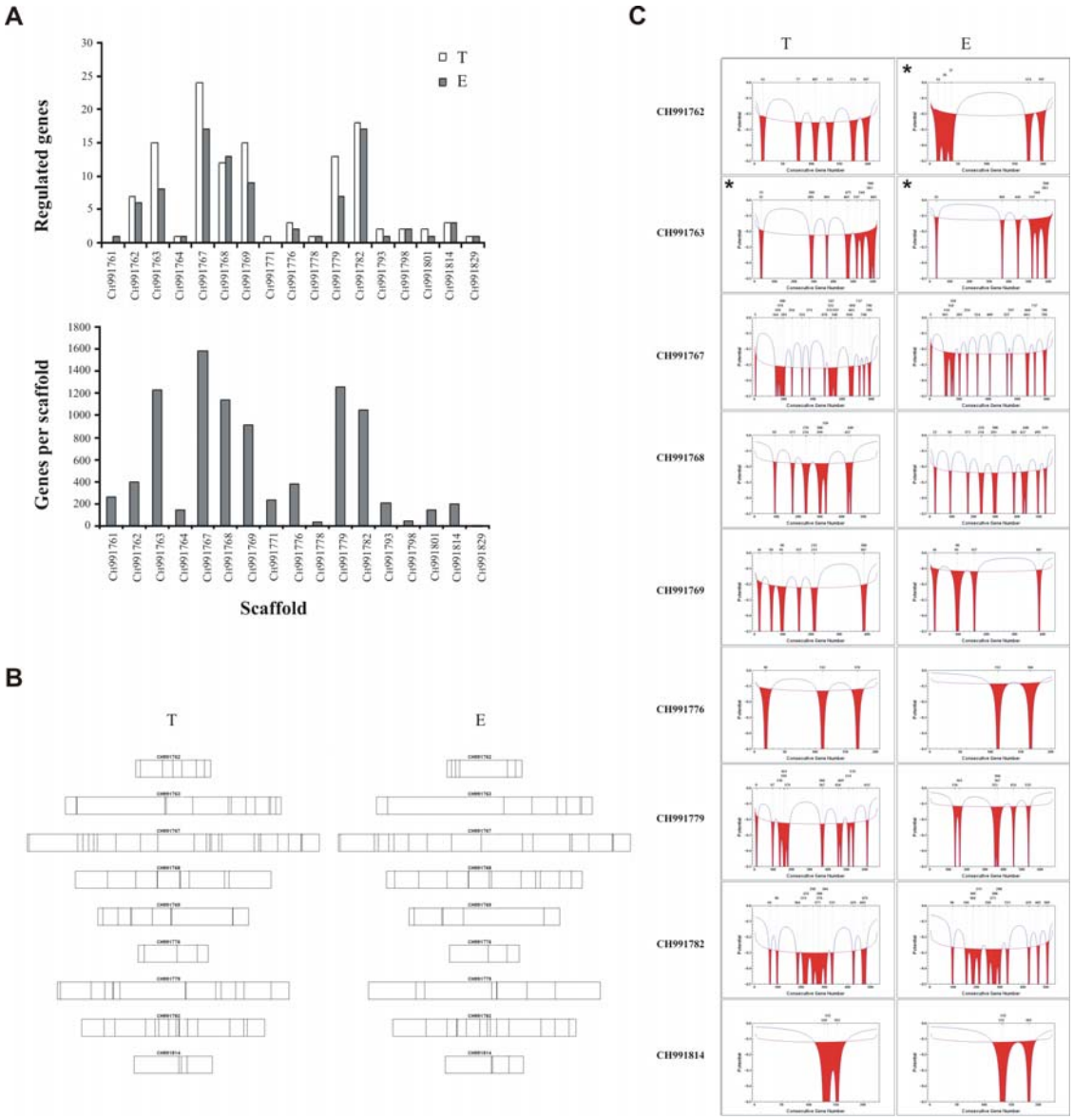

Figure S7: Analysis of regulated gene location in genomic scaffolds. Microarray analysis was performed on encysting cells (E) and trophozoites (T) treated with 2 μM FR235222, as described in the Experimental procedures section. A. Correlation between the number of regulated genes and the number of genes present in the indicated genomic scaffolds. B. Distribution of regulated genes over 9 genomic scaffolds. Scaffolds containing less than three regulated genes were not included in the analysis. C. Potential plots for regulated genes with threshold $\mu_{pot}+\lambda \cdot s_{pot}^{+}$ with $\lambda=1$. Asterisks indicate the scaffolds with non-randomly distributed co-regulated genes (tested on a significance level $\alpha=0.05$).

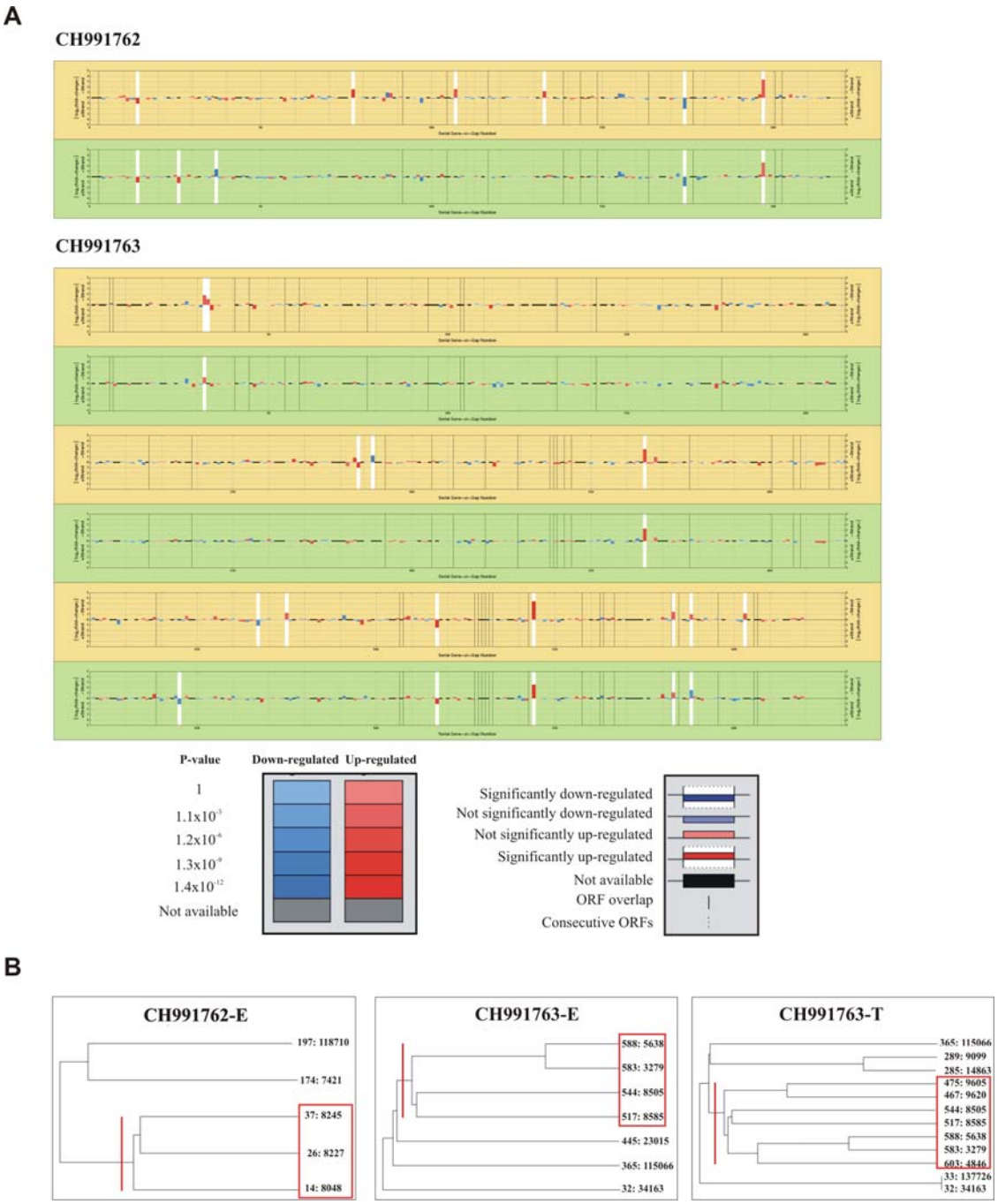

Figure S8: Cluster analysis of regulated genes. Microarray analysis was performed on encysting cells (E) and trophozoites (T) treated with 2 µM FR235222, as described in the Experimental procedures section. A. Expression profiles of scaffolds CH991762 and CH991763 containing non-randomly distributed co-regulated genes. Yellow, trophozoite profiles; Green, encysting cell profiles. B. Dendrograms of regulated genes in scaffolds CH991762 and CH991763 based on the potential-induced metric M_f. Cluster candidates are boxed in red (tested on a significance level α=0.05).

1 The role of P-glycoprotein in host-parasite interaction

P-gp is an exceptional membrane transporter because of its ability to carry a large variety of compounds across the plasma membrane. This ability to transport a broad range of substrates makes P-gp a key mediator of multidrug resistance, a phenomenon which is found in a variety of cell types, from pathogenic prokaryotic microorganisms to human cancer cells. P-gp is often over-expressed in multidrug resistant cells upon therapeutic treatment. In addition, the protein is also expressed at basal levels in non-resistant cells, but its role in the biology of normal cells has not been completely elucidated. Proposed functions for P-gp include a broad range of important cellular processes range from roles in immunological processes to membrane lipid remodelling. In this context, there is a great interest to understand the physiological functions of P-gp in absence of drug pressure.

In my studies I investigated whether P-gp has a role in host-pathogen interaction. As a model pathogen we used the human intracellular parasite *T. gondii*, which causes toxoplasmosis, a potentially life-threatening disease in immunocompomized individuals. Our project had two goals:

1) To define the role of host cell P-gp in host-parasite interaction. To this end, we compared three cell lines of mouse embryonic fibroblasts expressing different levels of P-gp, namely wild type (WT), P-gp knockout (P-gp KO) and P-gp KO complemented with human P-gp (P-gp KO/P-gp). Using these host cells, we analysed the role of host P-gp in parasite replication and cholesterol transport, processes that are crucial for successful *T. gondii* propagation and survival.

2) To characterise P-gp in the parasite and elucidate its function in host-parasite interaction. We pharmacologically inhibited *T. gondii* P-gp (TgP-gp) with the specific P-gp inhibitor GF120918 (GF) and we used P-gp KO as host cells to avoid the effects derived from host P-gp inhibition. Using this model system, we analysed the role of TgP-gp in parasite invasion, replication and lipid metabolism.

In my thesis work I show for the first time that both host cell and parasite P-gp play an important role in host-parasite interaction.

1.1 HOST P-gp

Host P-gp is essential for *T. gondii* replication.

Parasite replication inside a host cell is a crucial element in *T. gondii* pathogenesis, as it results in host cell lysis. Previous studies showed that parasite replication could be inhibited by P-gp modulators (1,2). However, given the ubiquitous presence of P-gp, the contribution of host versus parasite P-gp in the observed inhibition could not be resolved. To overcome this limitation, we used three cell types with different P-gp expression to exclusively analyse the role of host P-gp during *T. gondii* infection. Our analyses revealed a positive correlation between the levels of P-gp expression in the host cell and intracellular parasite burden, proving the essential role of host P-gp in *T. gondii* replication.

P-gp is localized mainly in the plasma membrane, which is the first barrier that pathogens need to cross to infect the host cell and a role of host P-gp in host cell invasion has been shown recently for the bacterial pathogen *Listeria monocytogenes* (3). We therefore analysed whether host cell P-gp is required for *T. gondii* invasion. Our results showed that parasite invasion was not affected in absence of host P-gp, indicating that the decreased parasite burden in P-gp KO cells did not derive from reduced parasite invasion.

Host P-gp is required for cholesterol transport from the host to the parasite.

Our analysis showed that *T. gondii* replication significantly decreased in the absence of host P-gp. In order to elucidate the molecular mechanism of decreased parasite replication we focused our analysis on cholesterol transport from the host cell to the parasite, a key process to guarantee *T. gondii* replication due to cholesterol auxotrophy in the parasite (4). To scavenge host cholesterol, the parasite forms a unique system of tubular structures (H.O.S.T.), which sequester cholesterol-containing endo-lysosomes from the host cytoplasm into the parasitophorous vacuole (PV) (5). Importantly, interference with cholesterol trafficking, including cholesterol translocation from lysosomes, blocks the delivery of cholesterol to the PV and significantly reduces parasite replication (4).

Previous studies using drug-selected cell lines over-expressing P-gp suggested that P-gp may play a role in modulating the intracellular trafficking of cholesterol (6,7). Thus, we hypothesized that host P-gp is involved in the transport of host cholesterol to the parasite and that its absence will limit the cholesterol delivery to the PV and consequently reduce parasite replication. To test this hypothesis we compared the transport of host cholesterol to the PV in host cells expressing different levels of the protein. By using biochemistry and microscopy-based approaches, we found that the transport of host cholesterol to the parasite correlated with the levels of P-gp expression in host cells. In addition, we confirmed that the limiting factor for parasite replication in P-gp KO cells was indeed limiting availability of host cholesterol. Importantly, we observed that P-gp KO host cells accumulated free cholesterol in the endo-lysosomes associated to the PV, suggesting that cholesterol mobilization from endo-lysosomes to the PV is reduced in absence of host P-gp.

To further understand how P-gp modulates cholesterol transport to the PV, we localized the protein in *T. gondii* infected host cells. Host P-gp was present predominantly in the plasma membrane; however, it was also associated with the PV. This localization in the PV proximity suggests two possible options: i) P-gp is present in organelles closely associated with the PV or/and ii) P-gp localizes in the parasitophorous vacuole membrane (PVM). We favour the first option as P-gp was shown to partially localize in early endosomes and lysosomes (8), organelles which are also associated with the PV. On the other hand, it is possible that host P-gp is incorporated in the PVM, as this membrane derives from the invagination of the host plasma membrane, where P-gp is located. However, the PVM is devoid of most of host-derived transmembrane proteins (9). Thus a direct incorporation of host P-gp in the PVM seems less likely but cannot be excluded as host-derived, raft-associated transmembrane proteins were found to be inserted within the PVM (10).

Based on the data presented here, we propose that host P-gp localizes in endo-lysosomes associates with the PV and contributes to the mobilization the cholesterol from these compartments to the parasite, an essential process for *T. gondii* replication.

P-gp modulates cholesterol trafficking from endo-lysosomes to the plasma membrane in fibroblasts.

We showed that host P-gp is required for cholesterol transport from the host endo-lysosomes to the parasite. This observation suggests that P-gp may promote cholesterol transport not only to the PV but also to other cellular locations. So far, the studies addressing the role of P-gp in cholesterol trafficking produced different results. P-gp was proposed to redistribute cholesterol in the plasma membrane via flipping it from the inner to the outer leaflet, thus making it more accessible to cholesterol acceptors (11). In addition, P-gp over-expression was also shown to

increase the uptake of cholesterol-containing micelles (12) and to modulate cholesterol biosynthesis (13). Moreover, P-gp over-expression was reported to increase cholesterol esterification (6,14). However, another study concluded that P-gp expression does not play a major role in cholesterol homeostasis (15). A limiting factor in these previous studies investigating the role of P-gp in cholesterol homeostasis was the use of unspecific P-gp inhibitors or drug-selected multidrug resistant cell lines, as both approaches have the potential of drug-induced side effects.

For these studies we were able to use host cells deficient for and complemented with P-gp, which allowed us to avoid possible off-target effects of drug treatment. To analyze P-gp's involvement in cholesterol homeostasis, we quantified several parameters of cholesterol trafficking, including exogenous cholesterol trafficking to the ER followed by esterification, cholesterol content in the plasma membrane and cholesterol efflux to extracellular acceptors. We found that free and esterified cholesterol accumulated in endo-lysosomes and intracellular lipid droplets, respectively, while free cholesterol levels decreased in the plasma membrane of P-gp KO cells. Importantly, these perturbations of cholesterol trafficking observed in absence of host P-gp were reversed upon P-gp complementation.

Based on our data, we propose that P-gp mediates cholesterol trafficking from endo-lysosomes to the plasma membrane but not from plasma membrane to ER, where cholesterol esterification takes place. These changes in cholesterol trafficking in the absence of P-gp did not reduce the viability or proliferation of the P-gp KO cells, suggesting the presence of possible compensatory mechanisms. However, the cholesterol auxotrophy of *T. gondii* made the parasite very sensitive to these changes, which resulted in inhibition of replication. Thus, the infection of these cells by *T. gondii* really made the effects of the perturbed host cholesterol trafficking resulting from P-gp absence visible and, therefore, *T. gondii* could be regarded as a bio-indicator of altered cholesterol homeostasis in the host cell.

1.2 PARASITE P-gp

Inhibition of *T. gondii* P-gp strongly decreases parasite replication.

In the first part of our project we showed that host P-gp is essential for parasite replication because it is required for cholesterol transport from the host to the parasite (16). Based on this essential role of host P-gp, we analysed if also *T. gondii* P-gp (TgP-gp) played a role in parasite replication. Indeed, we found that parasite replication was strongly reduced when we inhibited TgP-gp using the P-gp specific inhibitor GF on the host cell background of P-gp KO cells. Given that host P-gp plays a role in cholesterol transport, we hypothesized that TgP-gp may also be involved in the transport of either parasite-derived lipids and/or host-derived lipids scavenged by *T. gondii*, including long-chain fatty acids and phospholipids (17). In support of a P-gp mediated transport of cellular lipids, P-gp was shown to flip not only short-chain fluorescent analogues of different phospho- and sphingolipids but also the natural lipid platelet-activating factors (PAFs) (18-20). In addition, P-gp flipping activity in both directions across the plasma membrane was further supported by the recently resolved crystal structure of the protein, which revealed a substrate-binding internal cavity open to both the cytoplasm and the plasma membrane inner leaflet (21). To test whether TgP-gp has a role in lipid transport we inhibited P-gp activity in extracellular parasites and analysed the lipid synthesis using metabolic labelling. We found that inhibition of TgP-gp reduced lipid synthesis and incorporation of the precursor palmitic acid. These results suggest that functional TgP-gp is important for palmitic

acid transport and subsequent lipid synthesis in *T. gondii*. Importantly, using immuno-EM we showed that TgP-gp is localized not only in the plasma membrane of the parasite but also in the PV tubular network. This network connects the parasite with the lumen and the membrane of the PV and it is suggested to function as a reticulum to increase the surface area for transfer of nutrients from the host cell cytoplasm (22). Thus, it is possible that the flipping activity of TgP-gp contributes to the transport of host-derived lipids across the tubular network membranes. However, further analyses are required to elucidate the precise mechanism of host lipid uptake by the parasite.

Inhibition of *T. gondii* P-gp strongly decreases parasite invasion.

As *T. gondii* is an obligate intracellular parasite, it has to actively enter the host cell to ensure its propagation and survival. Host cell invasion is a complex process which includes initial attachment of the parasite to the host, parasite re-orientation to position its apical end in contact with the host cell, formation a moving junction between the parasite and host cell membranes mediated by secreted parasite proteins, including microneme proteins (MICs) (23,24) and, finally, host cell penetration using gliding motility (25,26). The invasion process depends on calcium (Ca^{2+}) homeostasis regulation but the precise mechanism of this regulation is not defined yet.

In our study we showed that treatment with the P-gp inhibitor GF decreased the ability of the parasite to invade host cells. The GF-mediated inhibition of parasite invasion was likely due to *T. gondii* P-gp inhibition, as we previously showed that host cell P-gp is not involved in the invasion process (16). As the first step of parasite invasion is attachment to the host cell, we analysed whether the decreased rate of *T. gondii* invasion upon GF treatment was due to the parasite's reduced ability to attach to the host. We found that treatment with GF decreased parasite attachment to the host cell, while, surprisingly, increasing the secretion of the microneme adhesin MIC2 and motility. Attachment, micronemal adhesins secretion, and motility are important steps in the invasion process. The relationship between these steps is complex and suggests the existence of different regulatory pathways (27). For instance, sustained microneme secretion inhibits parasite invasion due to the exhaustion of micronemal adhesins required for host cell attachment (28). It was also shown that Ca^{2+} homeostasis regulates the different invasion steps (29-31), however, the precise mechanisms of Ca^{2+} regulation has not been characterised yet.

In our study we showed that P-gp inhibitor treatment uncoupled parasite microneme secretion and motility from attachment and invasion. Importantly, we also found that TgP-gp localized in *T. gondii* acidocalcisomes. Acidocalcisomes are the largest Ca^{2+} storage compartments in *T. gondii* and the most acidic compartments in the parasite (32-34). Acidocalcisomes contain the Ca^{2+}-antiporter ATPase TgA1 which is responsible for Ca^{2+} uptake in exchange for H^+ (33). In addition, acidocalcisome membrane includes the proton pumps H^+-ATPase and H^+-pyrophosphatase, which contribute to the acidification of these organelles and to the regulation of intracellular pH homeostasis (33,35). The modality of Ca^{2+} release from acidocalcisomes is not characterised in detail, but H^+ transport to the acidocalcisomes is regarded as a key regulator of this process (32).

Based on our results, we propose that decreased parasite attachment and invasion observed during GF treatment were caused by altered regulation of Ca^{2+} homeostasis due to inhibition of TgP-gp in acidocalcisome membranes. In support of a role for TgP-gp in Ca^{2+} homeostasis, possibly via regulation of H^+ transport, several studies showed that tumour cell lines with over-expressed P-gp contained higher intracellular

level of Ca^{2+} compared with control cells (36-38). Whether the changes in Ca^{2+} homeostasis are mediated directly or indirectly by P-gp is not clarified yet. However, it is possible that the protein affects cellular Ca^{2+} regulation by acting on H^+ transport, a P-gp- mediated process previously identified using single-cell photometry of human P-gp transfectants or analysis of the P-gp bacterial homologue LmrA (39-41). In summary, our study revealed that TgP-gp plays an essential role in the Ca^{2+} -dependent invasion process and pointed out the interesting possibility that acidocalcisome-localized TgP-gp is involved in regulating Ca^{2+} fluxes in these organelles, likely by modulating H^+ transport.

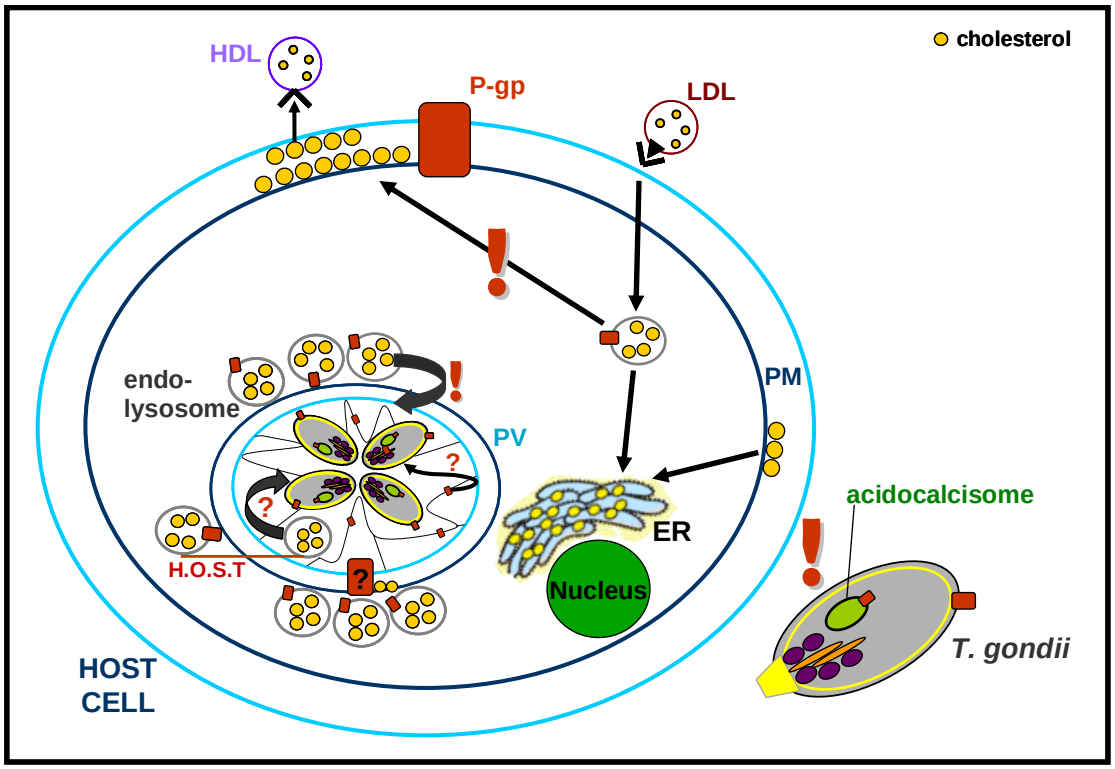

Proposed model: **Host P-gp** is localized in endo-lysosomes and is promoting cholesterol trafficking from these organelles to the plasma membrane (PM) and to the *T. gondii* parasitophorous vacuole (PV). P-gp mediated cholesterol transport to the PV is crucial for parasite replication. **Parasite P-gp** is localized in the *T. gondii* PM, PV tubular network (lines inside the PV) and in acidocalcisomes, the main parasite Ca^{2+} storage. This protein is important for *T. gondii* replication possibly due to its role in parasite lipid transport. Parasite P-gp is also important for *T. gondii* attachment to and invasion of host cells. Exclamation marks indicate the processes modulated by P-gp (cholesterol trafficking inside the host cell and parasite invasion outside the host cell). Low density lipoprotein (LDL), high density lipoprotein (HDL).

2 Epigenetic regulation of stage conversion in *G. lamblia*

The intestinal human pathogen *G. lamblia*, a worldwide cause of diarrhoea, has a simple life cycle with two developmental stages: motile, asexually replicating trophozoites and infective, environmentally resistant cysts. Stage conversion from trophozoites to cysts is essential for survival and transmission of this pathogen. Despite the importance of this process, the molecular mechanisms of its regulation remain poorly understood.

Here, we showed for the first time that inhibition of *G. lamblia* histone deacetylase with the potent HDAC inhibitor FR235222 blocked the formation of

infective cysts and induced transcriptional changes in both *G. lamblia* developmental stages.

Histone acetylation levels regulate *G. lamblia* stage conversion

Histone acetylases (HAT) and histone deacetylases (HDACs) play a major role in controlling gene expression by modulating the levels of chromatin acetylation. Histone hyperacetylation is usually linked to chromatin decondensation and subsequent activation of gene transcription, while histone hypoacetylation is linked to chromatin condensation and transcriptional repression (42). We investigated whether epigenetic mechanisms dependent on histone acetylation are involved in the stage conversion of *G. lamblia*, a process which is regulated at the transcriptional level and results in high levels of transcription of encystation-specific genes during the first 7-9 h post induction. Our analysis showed that levels of histone acetylation decreased in encysting cells compared to trophozoites. Thus we hypothesized that modulation of histone acetylation levels is an important element in the regulation of parasite stage conversion. To test this hypothesis, we analysed whether increasing the levels of histone acetylation by inhibiting HDAC activity with FR235222, could prevent parasite encystation. We found that FR235222 treatment of *G. lamblia* during encystation increased the levels of histone acetylation globally, potently prevented the expression of encystation–specific genes and blocked the formation of cysts. FR235222 treatment of trophozoites increased histone acetylation but did not induce stage conversion, further supporting the hypothesis that high acetylation levels effectively prevent the parasite to enter differentiation. Collectively, our data reveal that modulation of histone acetylation levels by HDAC plays a major role in regulating the encystation process in *G. lamblia*. HDAC-dependent regulation of stage conversion has been proposed also in other protozoan parasites such as intracellular *T. gondii* and *Entamoeba histolytica*, another intestinal extracellular parasite (43,44). However, these studies revealed major differences in HDAC-mediated regulation amongst different parasites. For instance, *G. lamblia* contains only one gene homologue of the classical HDAC family while *T. gondii* contains five putative HDAC (45). More importantly, functional differences, such as the induction of tachyzoite to bradyzoite differentiation by inhibition of HDAC points to a polyphyletic origin of mechanisms which control stage-differentiation processes in these protozoa.

FR235222 up-regulates the expression of identical genes in the two life stages of *G. lamblia*.

As changes in the levels of histone acetylation are known to modulate gene transcription, we analysed whether the general pattern of gene expression was modified in different life stages of *G. lamblia* upon HDAC inhibition. Using a genome-wide microarray analysis we showed that FR235222 treatment changed the mRNA profiles in both trophozoites and encysting cells in a very similar manner. An important exception was the inhibition of up-regulation of encystation-specific genes. At first sight this apparently challenges the classical view of histone hyperacetylation associated with increased gene transcription. More likely, however, failure to induce encystation-specific genes following HDAC inhibition is indirect. A possible scenario is that a repressor which binds to the promoter of encystation-specific genes in trophozoites (46) is down-regulated upon induction of encystation as a consequence of the observed histone deacetylation after induction of differentiation.

All together, our data suggest that control of *G. lamblia* stage conversion is under the control of epigenetic regulation and dependent on chromatin remodeling by histone acetylation. In addition, the block of cyst formation observed upon HDAC inhibition reveals that HDAC is a promising target for developing novel anti-Giardia drugs with the potential to reduce the transmission of the disease.

3 References

1. Silverman, J. A., Hayes, M. L., Luft, B. J., and Joiner, K. A. (1997) *Antimicrobial agents and chemotherapy* **41**(9), 1859-1866
2. Sauvage, V., Aubert, D., Bonhomme, A., Pinon, J. M., and Millot, J. M. (2004) *Molecular and biochemical parasitology* **134**(1), 89-95
3. Neudeck, B. L., Loeb, J. M., Faith, N. G., and Czuprynski, C. J. (2004) *Infection and immunity* **72**(7), 3849-3854
4. Coppens, I., Sinai, A. P., and Joiner, K. A. (2000) *The Journal of cell biology* **149**(1), 167-180
5. Coppens, I., Dunn, J. D., Romano, J. D., Pypaert, M., Zhang, H., Boothroyd, J. C., and Joiner, K. A. (2006) *Cell* **125**(2), 261-274
6. Luker, G. D., Nilsson, K. R., Covey, D. F., and Piwnica-Worms, D. (1999) *The Journal of biological chemistry* **274**(11), 6979-6991
7. Debry, P., Nash, E. A., Neklason, D. W., and Metherall, J. E. (1997) *The Journal of biological chemistry* **272**(2), 1026-1031
8. Fu, D., and Roufogalis, B. D. (2007) *American journal of physiology* **292**(4), C1543-1552
9. Mordue, D. G., Desai, N., Dustin, M., and Sibley, L. D. (1999) *The Journal of experimental medicine* **190**(12), 1783-1792
10. Charron, A. J., and Sibley, L. D. (2004) *Traffic (Copenhagen, Denmark)* **5**(11), 855-867
11. Garrigues, A., Escargueil, A. E., and Orlowski, S. (2002) *Proceedings of the National Academy of Sciences of the United States of America* **99**(16), 10347-10352
12. Tessner, T. G., and Stenson, W. F. (2000) *Biochemical and biophysical research communications* **267**(2), 565-571
13. Metherall, J. E., Li, H., and Waugh, K. (1996) *The Journal of biological chemistry* **271**(5), 2634-2640
14. Santini, M. T., Romano, R., Rainaldi, G., Filippini, P., Bravo, E., Porcu, L., Motta, A., Calcabrini, A., Meschini, S., Indovina, P. L., and Arancia, G. (2001) *Biochimica et biophysica acta* **1531**(1-2), 111-131
15. Le Goff, W., Settle, M., Greene, D. J., Morton, R. E., and Smith, J. D. (2006) *Journal of lipid research* **47**(1), 51-58
16. Bottova, I., Hehl, A. B., Stefanic, S., Fabrias, G., Casas, J., Schraner, E., Pieters, J., and Sonda, S. (2009) *The Journal of biological chemistry* **284**(26), 17438-17448
17. Charron, A. J., and Sibley, L. D. (2002) *Journal of cell science* **115**(Pt 15), 3049-3059
18. Bosch, I., Dunussi-Joannopoulos, K., Wu, R. L., Furlong, S. T., and Croop, J. (1997) *Biochemistry* **36**(19), 5685-5694
19. van Helvoort, A., Smith, A. J., Sprong, H., Fritzsche, I., Schinkel, A. H., Borst, P., and van Meer, G. (1996) *Cell* **87**(3), 507-517

20. Eckford, P. D., and Sharom, F. J. (2006) *Biochemistry and cell biology = Biochimie et biologie cellulaire* **84**(6), 1022-1033
21. Aller, S. G., Yu, J., Ward, A., Weng, Y., Chittaboina, S., Zhuo, R., Harrell, P. M., Trinh, Y. T., Zhang, Q., Urbatsch, I. L., and Chang, G. (2009) *Science (New York, N.Y* **323**(5922), 1718-1722
22. Sibley, L. D., Niesman, I. R., Parmley, S. F., and Cesbron-Delauw, M. F. (1995) *Journal of cell science* **108 (Pt 4)**, 1669-1677
23. Nichols, B. A., and O'Connor, G. R. (1981) *Laboratory investigation; a journal of technical methods and pathology* **44**(4), 324-335
24. Aikawa, M., Komata, Y., Asai, T., and Midorikawa, O. (1977) *The American journal of pathology* **87**(2), 285-296
25. Dobrowolski, J. M., and Sibley, L. D. (1996) *Cell* **84**(6), 933-939
26. Dobrowolski, J. M., Carruthers, V. B., and Sibley, L. D. (1997) *Molecular microbiology* **26**(1), 163-173
27. Carey, K. L., Westwood, N. J., Mitchison, T. J., and Ward, G. E. (2004) *Proceedings of the National Academy of Sciences of the United States of America* **101**(19), 7433-7438
28. Mondragon, R., and Frixione, E. (1996) *The Journal of eukaryotic microbiology* **43**(2), 120-127
29. Wetzel, D. M., Chen, L. A., Ruiz, F. A., Moreno, S. N., and Sibley, L. D. (2004) *Journal of cell science* **117**(Pt 24), 5739-5748
30. Carruthers, V. B., Giddings, O. K., and Sibley, L. D. (1999) *Cellular microbiology* **1**(3), 225-235
31. Luo, S., Ruiz, F. A., and Moreno, S. N. (2005) *Molecular microbiology* **55**(4), 1034-1045
32. Moreno, S. N., and Zhong, L. (1996) *The Biochemical journal* **313 (Pt 2)**, 655-659
33. Luo, S., Vieira, M., Graves, J., Zhong, L., and Moreno, S. N. (2001) *The EMBO journal* **20**(1-2), 55-64
34. Bouchot, A., Zierold, K., Bonhomme, A., Kilian, L., Belloni, A., Balossier, G., Pinon, J. M., and Bonhomme, P. (1999) *Parasitology research* **85**(10), 809-818
35. Moreno, S. N., Zhong, L., Lu, H. G., Souza, W. D., and Benchimol, M. (1998) *The Biochemical journal* **330 (Pt 2)**, 853-860
36. Wagner-Souza, K., Echevarria-Lima, J., Rodrigues, L. A., Reis, M., and Rumjanek, V. M. (2003) *Molecular and cellular biochemistry* **252**(1-2), 109-116
37. Chen, J. S., Agarwal, N., and Mehta, K. (2002) *Breast cancer research and treatment* **71**(3), 237-247
38. Mestdagh, N., Vandewalle, B., Hornez, L., and Henichart, J. P. (1994) *Biochemical pharmacology* **48**(4), 709-716
39. Velamakanni, S., Lau, C. H., Gutmann, D. A., Venter, H., Barrera, N. P., Seeger, M. A., Woebking, B., Matak-Vinkovic, D., Balakrishnan, L., Yao, Y., U, E. C., Shilling, R. A., Robinson, C. V., Thorn, P., and van Veen, H. W. (2009) *PloS one* **4**(7), e6137
40. van Veen, H. W., Callaghan, R., Soceneantu, L., Sardini, A., Konings, W. N., and Higgins, C. F. (1998) *Nature* **391**(6664), 291-295
41. Hoffman, M. M., and Roepe, P. D. (1997) *Biochemistry* **36**(37), 11153-11168
42. Kouzarides, T. (2007) *Cell* **128**(4), 693-705

43. Bougdour, A., Maubon, D., Baldacci, P., Ortet, P., Bastien, O., Bouillon, A., Barale, J. C., Pelloux, H., Menard, R., and Hakimi, M. A. (2009) *The Journal of experimental medicine* **206**(4), 953-966
44. Ehrenkaufer, G. M., Eichinger, D. J., and Singh, U. (2007) *BMC genomics* **8**, 216
45. Saksouk, N., Bhatti, M. M., Kieffer, S., Smith, A. T., Musset, K., Garin, J., Sullivan, W. J., Jr., Cesbron-Delauw, M. F., and Hakimi, M. A. (2005) *Molecular and cellular biology* **25**(23), 10301-10314
46. Davis-Hayman, S. R., Hayman, J. R., and Nash, T. E. (2003) *International journal for parasitology* **33**(10), 1005-1012

Significance of the research

P-glycoprotein (P-gp) has been extensively studied in the context of the multidrug-resistance (MDR) phenotype, both in tumour cells and in pathogenic organisms, including parasites. Our study using *Toxoplasma gondii* as a model intracellular parasite provided the first evidence that P-gp plays an important role in host-parasite interactions which is different from drug resistance. Specifically, we discovered that host cell P-gp modulates the intracellular trafficking of cholesterol, thus providing new insights into the role of P-gp in cellular lipid metabolism. Moreover, we identified P-gp-mediated *T. gondii* specific processes which are crucial for the parasite survival, thus providing new targets for drug development against this clinically significant pathogen.

Finally, our study investigating stage-differentiation of the enteric parasite *Giardia lamblia* revealed that parasite encystation is under the control of epigenetic regulation, and further illuminated the poorly understood mechanisms of gene regulation in this parasite. Additionally, our findings clearly demonstrate that histone deacetylase activity is a promising target for pharmacological agents aiming to effectively block the production of *G. lamblia* cysts and thus reduce disease transmission.

Perspectives

Our study showed that host cell P-gp mediates cholesterol trafficking from endo-lysosomes to the plasma membrane and to the *Toxoplasma gondii*-containing vacuole. However the precise mechanism of cholesterol trafficking mediated by P-gp has to be further elucidated. To this aim, it is important to analyse intracellular P-gp distribution and trafficking using life-cell microscopy. In addition, it is crucial to determine the effect of P-gp on the expression and localization of other proteins that are known to be involved in cholesterol transport not only in host cells but also in the parasite. Moreover, we showed that *T. gondii* homologue of P-gp is localized in the parasitophorous vacuole network which was suggested to mediate transport of host derived nutrients possibly also lipids to the parasite, thus it would be interesting to analyse whether *T. gondii* P-gp is also involved in cholesterol trafficking.

Moreover, our study showed that treatment with the P-gp-specific inhibitor GF strongly decreased *T. gondii* replication, adhesion and invasion of host cells. Our data on *T. gondii* P-gp functionality, expression and localization strongly argue for a crucial role of P-gp in the parasite biology. However, we cannot exclude the presence of off-target effects induced by the inhibitor. Thus additional investigations using genetic approaches are required to further our understanding of the function of P-gp and possibly other ABC transporters in the biology of *T. gondii*.

Finally, our study on stage conversion of the enteric parasite *Giardia lamblia* clearly indicated that parasite encystation is under control of epigenetic regulation. Specifically, we showed that modulation of histone acetylation levels by histone deacetylase activity is a key factor in the regulation of parasite stage conversion. However the precise molecular mechanism of this regulation remains to be elucidated. Important experiments to address this question include the extensive characterization and regulation of giardial histone acetylation modifying enzymes, and the analysis of acetylation marks in individual promoters using chromatin immunoprecipitation. Finally, future experiment will focus on identifying additional effector molecules, in particular putative repressor(s) which most likely contribute to down-regulate the expression encystation-specific genes during vegetative stage.

Acknowledgments

My greatest thanks belongs to my supervisor Dr. Sabrina Sonda, on the first place for giving me the opportunity to work on such an interesting projects and for the guidance thought the world of science. I am very grateful for her motivation, great support and for her friendship.
I would also like to thank to Prof. Adrian B. Hehl for the nice experience to do my PhD project in his group and for his motivating guidance.
Many thanks go to all members of Hehl group, to Dr. Cornelia Spycher for nice discussions and her Peruvian chairs, to Laura Morf for sweating together not only in sauna and for great hikes in beautiful Swiss mountains, to Dr. Cristian Conrad and Therese Michel for help with German and to Dr. Sasa Stefanic not only for my bike.

I would like to thank to all colleagues from Institute of Parasitology and especially to Prof. Peter Deplazes and Isabelle Tanner.

My very special thanks go to my great friends from our “International hiking adventures club” to Silja, Giovanna, Claudia C., Patricia, Claudia R., Joeska, Erlin, Hsiang-Chun, Ilaria and Ivy and to my Slovak friends Ludmila and Boris for making my time here in Zurich so great!

Last, but not least I would like to thank to my family for never ending support and love. V neposlednom rade, dakujem mojej rodine za bezhranicnu podporu a lasku.

BOTTOVA Iveta, MSc.

Institute of Parasitology
University of Zurich
Winterthurerstrasse 266a
CH-8057 Zurich
Switzerland
Tel.: +41 44 63 58 527
Fax: +41 44 63 58 907
Email: ivabott@gmail.com

Nationality: Slovak

Place of birth: Komarno, Slovakia

Languagues: Slovak (native), English (fluent), French (very good), German (basic), Spanish (basic)

EDUCATION

January 2007- 2010: Ph.D. study, Faculty of Mathematics and Natural Sciences, University of Zurich**,** Ph.D. program: Life Science Zurich Graduate School, Microbiology and Immunology Ph.D. program, Supervisor: Sabrina Sonda, Ph.D. and Prof. Adrian Hehl. *Topic:* Role of P-glycoprotein in host-pathogen interactions with a model pathogen *Toxoplasma gondii*.

2003-2006: Master of Biochemistry, Faculty of Natural Sciences, Comenius University in Bratislava, Slovakia. *Diploma thesis:* The Studies of the Function of the Mycobacterial gene Rv3786c, Supervisor: Katarina Mikusova, Ph.D.

2000-2003: Bachelor of Chemistry, Faculty of Natural Sciences, Comenius University in Bratislava, Slovakia.

1996-2000: Matura, Gymnasium Metodova, Bratislava, Slovakia

FURTHER EDUCATION

2009: Swiss National Foundation post-doc fellowship for young researchers.

2009: FEBS Advanced Course, Ortona, Italy. Youth travel fund award. *Topic:* Lipid signalling and disease.

2008: SKMB course at the Bioimaging Platform, University of Geneva. *Topic:* Confocal microscopy and imiging.

2008: Molecular Microbial Ecology course, Piora, Switzerland.

2006: Slovak academy of Sciences, Bratislava, Slovakia. Supervisor: Martin Valachovic, Ph.D. *Topic:* Sterol uptake in yeast.

2003-2004: Marie Curie EU fellowship, Department of Genetics of Mycobacterium, Institute Pasteur in Paris, France. Supervisor: Mary Jackson, Ph.D. and Prof. Brigitte Gicquel, *Project:* Characterization of putative LAM-deficient mutants of *Mycobacterium tuberculosis.*

INTERNATIONAL CONFERENCES

2009: 10th International Congress on Toxoplasmosis, Kerkrade, The Netherlands. Oral presentation.

2008: COST Action 857, 5th Annual Workshop, Crete, Greece. Apicomplexan Biology in the post genomic era. Oral presentation.

2007: Living together, Physiopathology of Intracellular Parasitic Diseases Strasbourg, France. Poster presentation.

MEMBERSHIP OF PROFESSIONAL ORGANIZATIONS

Swiss Society for Biochemistry
Swiss Society of Tropical Medicine and Parasitology

TEACHING

2009: Assistance to biochemistry laboratory course for undergraduade students. University of Zurich, Switzerland.

LIST OF PUBLICATIONS

Bottova I, Olivieri V, Sauder U, Hehl AB, Sonda S: The P-glycoprotein inhibitor GF120918 modulates Ca^{2+}-dependent processes and lipid metabolism in *Toxoplasma gondii.* 2009. Submitted.

Sonda S, Morf L, **Bottova I**, Hakimi A, Hehl AB: Epigenetic mechanisms control stage differentiation in *Giardia lamblia*. 2009. Submitted.

Bottova I, Hehl AB, Stefanic SA, Fabriàs G, Casas J, Schraner E, Pieters J, Sonda S.: Host cell P-glycoprotein is essential for cholesterol uptake and replication of *Toxoplasma gondii*. *J Biol Chem*. 2009 Jun 26; 284(26):17438-48.

Stadthagen G, Jackson M, Charles P, Boudou F, Barilone N, Huerre M, Constant P, Liav A, **Bottova I**, Nigou J, Brando T, Puzo G, Daffe M, Benjamin P, Coade S, Buxton RS, Tascon RE, Rae A, Robertson BD, Lowrie DB, Young DB, Gicquel B, Griffin R.: Comparative investigation of the pathogenicity of three Mycobacterium tuberculosis mutants defective in the synthesis of p-hydroxybenzoic acid derivatives. *Microbes Infect.* 2006 Jul; 8(8): 2245-53.

Stadthagen G, Kordulakova J, Griffin R, Constant P, **Bottova I**, Barilone N, Gicquel B, Daffe M, Jackson M.: p-Hydroxybenzoic acid synthesis in *Mycobacterium tuberculosis*. *J Biol Chem*. 2005 Dec 9; 280(49): 40699-706.